

Analysis of the Higgs Boson Masses at One-Loop Level in the Complex NMSSM

Diplomarbeit
von

Anne-Kathrin Ender

An der Fakultät für Physik
Institut für Theoretische Physik

Referent: Prof. Dr. M. Mühlleitner
Korreferent: Prof. Dr. D. Zeppenfeld

Dezember 2011

Ich versichere, dass ich diese Arbeit selbstständig verfasst und ausschließlich die angegebenen Hilfsmittel verwendet habe.

Anne-Kathrin Ender
Karlsruhe, den 09. Dezember 2011

Als Diplomarbeit anerkannt.

Prof. Dr. M. Mühlleitner
Karlsruhe, den 09. Dezember 2011

Das Forschungsgebiet der Teilchenphysik beschäftigt sich mit der Welt der Elementarteilchen und den fundamentalen Wechselwirkungen zwischen diesen. Im Bestreben eine Theorie zu finden, die dies alles beschreibt, gab es im Laufe der 1960er und 70er Jahre große Fortschritte, welche schlussendlich zu dem Modell führten, das heute als Standardmodell (SM) der Teilchenphysik bekannt ist. Seit der Entwicklung des Standardmodells wurden enorme experimentelle Anstrengungen unternommen, um dessen Vorhersagen möglichst genau zu bestätigen.

Riesige Teilchenbeschleuniger wurden gebaut, um die Erforschung der Natur bei immer größeren Energien zu ermöglichen. Einer der ersten wirklich großen Beschleuniger war das Tevatron am Fermilab. Hier wurden Proton-Anti-Proton Paare mit einer Strahlenergie von bis zu 1 TeV zur Kollision gebracht. Das Tevatron, welches seinen Namen von seiner Strahlenergie ableitet, nahm bereits 1983 den Betrieb auf. Bis auf einige Unterbrechungen zur technischen Aufrüstung war das Tevatron bis zu diesem Jahr in Betrieb. Während dieses langen Zeitraums wurden selbstverständlich viele Entdeckungen gemacht, wobei die bedeutendste sicher die Entdeckung des Top-Quarks 1995 war. Präzisionsmessungen der Masse des Top-Quarks folgten. Der „Large Electron-Positron Collider“ (LEP) am CERN war von 1989 bis 2000 in Betrieb, als er dann Platz für den LHC machen musste. Eine der größten Errungenschaften am LEP war die Präzisionsmessung der Massen der Z - und W -Bosonen. Schließlich hat nun der „Large Hadron Collider“ (LHC) im ehemaligen LEP Tunnel am CERN letztes Jahr mit der Datennahme begonnen. Mit einer vorgesehenen Strahlenergie von 7 TeV ist der LHC der leistungsfähigste Teilchenbeschleuniger, der jemals gebaut wurde. Zwar arbeitet er im Moment nur mit der Hälfte der vollen Strahlenergie, ab 2014 soll er allerdings mit der vollen Energie beschleunigen. Eine der großen Hoffnungen der Teilchenphysiker ist es, das fehlende Puzzleteil des Standardmodells, das Higgs-Boson, am LHC zu finden.

Das Higgs-Boson spielt eine wichtige Rolle im Rahmen des Standardmodells, da der sogenannte Higgs-Mechanismus eine Erklärung dafür bietet, wie die Vektor-Bosonen eine Masse ungleich Null erhalten ohne dass dabei die Eichinvarianz des SMs verletzt wird. Dabei liegt dem Higgs-Mechanismus das Konzept der spontanen Brechung der elektroschwachen Symmetrie zu Grunde. Das eigentliche Higgs-Boson, ein Spin-0 Teilchen, bleibt als Überbleibsel dieser Symmetriebrechung zurück. Bis jetzt hat sich das Higgs-Boson allerdings der experimentellen Entdeckung entzogen. Dennoch haben die Experimente bereits Einschränkungen für die Masse des Higgs-Bosons hervorgebracht.

Es gibt jedoch Hinweise darauf, dass das Standardmodell nicht vollständig ist, oder vielleicht nur ein Grenzfall einer komplexeren grundlegenden Theorie. Es gibt mehrere mögliche Erweiterungen, mit denen sich die Theoretiker beschäftigen. Eine davon ist das Konzept der Supersymmetrie, welches es ermöglicht, durch die Einführung von Superpartnern für die Teilchen des Standardmodells einige der Probleme des Standardmodells zu umgehen. Auch die Erweiterung, die in dieser Diplomarbeit näher betrachtet wird, ist eine supersymmetrische Erweiterung. Andere mögliche Theorien sind zum Beispiel Theorien mit extra Dimensionen oder die String Theorie, welche sogar den Anspruch stellt irgendwann eine „Theory of Everything“ zu liefern. Selbstverständlich müssen all diese neuen Theorien die experimentell so beeindruckend bestätigten Vorhersagen des Standardmodells reproduzieren. Zusätzlich liefern diese Theorien allerdings auch neue Vorhersagen, die sich von denen des Standardmodells unterscheiden. Bei der Interpretation der experimentellen Daten ist es sehr wichtig diese neuen Vorhersagen mit in die Analyse einzubeziehen.

In dieser Diplomarbeit wird der Higgs-Sektor des komplexen „nächst-minimalen supersymmetrischen Standardmodells“¹ (NMSSM) untersucht. Genauer gesagt wird die Berechnung der vollständigen Einschleifenkorrekturen zu den Massen der Higgs-Bosonen in der diagrammatischen Methode durchgeführt. Da die Einschleifenkorrekturen zu den Massen der Higgs-Bosonen mit divergenten Integralen einhergehen, muss ein Renormierungsverfahren für den Higgs-Sektor durchgeführt werden.

Als Einführung wird allerdings zunächst an die wichtigsten Eigenschaften des Standardmodells erinnert und seine Unzulänglichkeiten werden aufgezeigt. Supersymmetrie ist eine mögliche Erweiterung des Standardmodells, die in der Lage ist einige der Probleme zu lösen. So wird zum Beispiel das Hierarchieproblem des SMs durch die Einführung von Superpartnern, deren Spin sich um $1/2$ von dem des jeweils zugehörigen SM Teilchens unterscheidet, gelöst. Außerdem bieten supersymmetrische Theorien mögliche Kandidaten für die Dunkle Materie und im Rahmen des MSSMs kommt es zu einer Vereinigung der Kopplungskonstanten an der GUT-Skala.

Das NMSSM ist eine Erweiterung des MSSMs (Minimales Supersymmetrisches Standardmodell), welches die minimal nötige Anzahl an Superpartnern aufweist. Im MSSM erhält jedes Teilchen des Standardmodells einen Superpartner: die SM-Fermionen erhalten skalare Superpartner, die Sfermionen, und die Eichbosonen (gauge bosons) des SMs erhalten fermionische Superpartner, die sogenannten Gauginos. Um sowohl den up-artigen wie auch den down-artigen Fermionen eine Masse geben zu können, werden zwei komplexe Higgs-Doublets benötigt. Dadurch ist die Theorie automatisch frei von Anomalien. Zusätzlich zu diesem minimalen Teilcheninhalt weist der Higgs-Sektor des NMSSM noch ein komplexes Singulett-Feld auf. Einer der Hauptgründe für die Einführungen dieses zusätzlichen Singulett-Felds ist, dass so das μ -Problem des MSSM gelöst werden kann. Der Parameter μ wird dynamisch generiert, wenn das Singulett-Feld seinen Vakuumerwartungswert annimmt und muss damit nicht mehr per Hand auf die Größenordnung der elektroschwachen Skala gesetzt werden, wie es im MSSM nötig ist.

Da sich diese Arbeit insbesondere mit dem Higgs-Sektor des NMSSM beschäftigt, wird dieser detailliert diskutiert. Der NMSSM Higgs-Sektor besteht aus insgesamt sieben Higgs-Bosonen: fünf neutralen und zwei geladenen. Im Spezialfall des reellen NMSSM gilt CP-Erhaltung und den neutralen Higgs-Bosonen kann eine CP-Quantenzahl zugewiesen werden. In diesem Fall gibt es zwei CP-ungerade und drei CP-gerade Higgs-Bosonen. Die Higgs-Massenmatrix in der Basis der Wechselwirkungseigenzustände kann vom Higgs-Potential abgeleitet werden. Auf

¹Englisch: „Next-to minimal Supersymmetric Extension of the Standard Model“

Born-Niveau kann eine Entkopplung des Goldstone-Bosons mit Hilfe einer Rotation erreicht werden. Um zu einem neuen Satz von Ausgangsparametern zu gelangen, werden sowohl die Tadpol-Bedingungen wie auch die Masse des geladenen Higgs-Bosons ausgenutzt, um andere Parameter zu eliminieren. Während der gesamten Diskussion wird dabei im CP-verletzenden NMSSM gearbeitet. Das heißt per se werden alle Parameter als komplex angenommen. Die Superpartner der Higgs-Bosonen, die Higgsions, mischen mit den Gauginos zu den Neutralinos und Charginos. Diese beiden Sektoren werden explizit behandelt.

Für die Berechnung der Massen der Higgs-Bosonen auf Einschleifen-Niveau muss der Higgs-Sektor renormiert werden. Die Renormierung wird mit Hilfe des Counterterm Formalismus durchgeführt. Wobei zunächst nur der Spezialfall des reellen NMSSM betrachtet wird und erst später der allgemeinere Fall des komplexen NMSSM. Als Hauptschema wird ein Renormierungsschema verwendet, welches On-Shell und $\overline{\text{DR}}$ -Renormierungsbedingungen mischt. Für das reelle NMSSM wurde zusätzlich noch ein reines $\overline{\text{DR}}$ und ein reines On-Shell Schema implementiert. Um einen nicht-trivialen Cross-Check zu ermöglichen, werden sowohl Renormierungsbedingungen aus dem Higgs- als auch aus dem Neutralino- und Chargino-Sektor verwendet.

Für die eigentliche Berechnung der Higgs-Boson Massen auf Einschleifen-Niveau geht man von der renormierten Zwei-Punkt-Vertex-Funktion aus. Aus dieser können, wenn die Counterterme und Selbstenergien des Higgs-Sektors bekannt sind, mit Hilfe eines Iterationsverfahrens die Massen der Higgs-Bosonen berechnet werden. Die Einschleifendiagramme, die zur Berechnung der Selbstenergien nötig sind, wurden zunächst analytisch berechnet und später dann numerisch ausgewertet.

Für einige Beispiel-Szenarien wurde eine numerische Analyse durchgeführt. Für den Spezialfall des reellen NMSSM wurden die Ergebnisse der unterschiedlichen Renormierungsschemata miteinander verglichen. Die Ergebnisse unterschieden sich um höchstens 10%. Als Anhaltspunkt für die Stärke, mit welcher das Higgs-Boson an die Teilchen des SMs koppelt, wurde im Fall des reellen NMSSMs der Singulett-Anteil des entsprechenden Higgs-Bosons betrachtet. Da die Kopplung des Higgs-Bosons an die Teilchen des SMs mit zunehmendem Singulett-Anteil abnimmt, kann ein Higgs-Boson mit großem Singulett-Anteil der experimentellen Entdeckung entgehen, selbst wenn das SM Higgs-Boson der entsprechenden Masse bereits ausgeschlossen ist. Daher ist der Singulett-Anteil eine nützliche Größe, die es erlaubt Rückschlüsse auf die Eigenschaften des entsprechenden Higgs-Bosons zu ziehen. Die Untersuchung der Abhängigkeit der Higgs-Boson Massen von der Masse des Top-Quarks zeigte, dass der Großteil der Korrekturen zum leichten MSSM-artigen CP-geraden Higgs-Boson vom Top-Sektor herrührt. Durch die Variation der Renormierungsskala, welche in den Einschleifenkorrekturen auftaucht, können die fehlenden Korrekturen höherer Ordnung auf $\mathcal{O}(10\%)$ abgeschätzt werden. Im Gegensatz zum MSSM sind im NMSSM Higgs-Bosonen-Massen größer als die Masse des Z-Bosons bereits auf Born-Niveau möglich. Dennoch sind die Einschleifenkorrekturen sehr wichtig, da sie die Masse des leichtesten CP-geraden Higgs-Bosons über die untere LEP-Schranke für die Higgs-Bosonen-Masse heben. Besonders für Higgs-Bosonen mit kleiner Masse können die Einschleifenkorrekturen sehr groß sein, so dass sie an einigen Parameterpunkten die Masse des Higgs-Bosons sogar mehr als verdreifachen können. Wie die Diskussion der experimentellen Ausschlussgrenzen zeigt, bietet das NMSSM phänomenologisch zulässige Szenarien, die bei der Higgssuche in Betracht gezogen werden sollten, da sie Higgs-Bosonen vorhersagen, deren Eigenschaften sich von denen des MSSMs und SMs unterscheiden.

Um den allgemeineren Fall des CP-verletzenden NMSSMs, d.h. das komplexe NMSSM, behandeln zu können, müssen nur zwei zusätzliche Counterterme im Vergleich zum reellen NMSSM

eingeführt werden. Wie gezeigt wurde, tritt CP-Verletzung bereits auf Born-Niveau auf, wenn man einen endlichen Wert für eine der im Higgs-Sektor vorkommenden Phasen annimmt. Als Anhaltspunkt für das Ausmaß der CP-Verletzung wurde untersucht, zu welchem Anteil die Higgs-Bosonen aus den CP-geraden Wechselwirkungseigenzuständen bestehen. Im CP-erhaltenen Fall ist dieser CP-gerade Anteil entweder Null oder Eins. Die Abweichung von diesen beiden Werten kann daher als Maß für die CP-Verletzung betrachtet werden. Die maximale Abweichung in den betrachteten Beispiel-Szenarien betrug 2.3%. Das Mischen der CP-geraden und CP-ungeraden Wechselwirkungseigenzustände kann die Kopplung des jeweiligen Higgs-Bosons noch weiter unterdrücken. Außerdem wurde ein Szenario untersucht, in welchem CP-Verletzung erst auf Einschleifen-Niveau im Higgs-Sektor auftritt. Es zeigte sich, dass obwohl diese Phasen nur durch die Einschleifenkorrekturen Einfluss auf die Rechnung nehmen, eine Variation dieser Phasen zu Effekten von einigen GeV in der Masse der Higgs-Bosonen auf Einschleifen-Niveau führen kann.

Alles zusammen genommen trägt diese Arbeit zu dem Bestreben bei, phänomenologische Vorhersagen für den Higgs-Sektor des NMSSMs zu machen, welche einen neuen Blickwinkel auf die derzeitige Higgs-Suche am LHC ermöglichen könnten. Die Berechnung der Einschleifenkorrekturen zu den Massen der Higgs-Bosonen ist hierbei allerdings nur ein erster Schritt. Um ein vollständiges Bild zu erhalten, wird es unter anderem nötig sein, Korrekturen höherer Ordnung zu den Massen der Higgs-Bosonen zu berechnen. Es existieren bereits erste Rechnungen für die dominanten Beiträge der Zweischleifenkorrekturen in der Literatur. Des Weiteren wäre es wünschenswert, die auf Einschleifen-Niveau korrigierten Vertizes zur Verfügung zu haben. All diese Teile zusammengenommen erlauben es, phänomenologische Vorhersagen für den Higgs-Sektor des NMSSMs zu machen, die es ermöglichen sollten diesen von den Higgs-Sektoren des MSSMs oder des SMs zu unterscheiden.

1	Introduction	1
2	Standard Model of Particle Physics and Supersymmetry as its Extension	5
2.1	The Standard Model of Particle Physics	5
2.1.1	Problems of the Standard Model	6
2.1.2	The Hierarchy Problem	7
2.2	Supersymmetry	9
3	The Next-to-Minimal Supersymmetric Extension of the Standard Model	11
3.1	Particle Content	11
3.2	The NMSSM Lagrangian	12
3.3	Motivation for the NMSSM	14
3.4	The Higgs Sector at Tree-Level	15
3.4.1	The Higgs Potential	15
3.4.2	The Tadpole Conditions	16
3.4.3	The Mass Matrices for the Neutral Higgs States	17
3.4.4	The Charged Higgs Boson	19
3.4.5	Parameters of the Higgs Sector	20
3.5	The Neutralino and Chargino Sectors at Tree-Level	21
4	Renormalization and Calculation of the One-Loop Higgs Boson Masses	23
4.1	General Remarks on Renormalization	23
4.1.1	Counterterm Formalism	24
4.1.2	Renormalization Conditions	25
4.2	Counterterms in the NMSSM Higgs Sector	28
4.3	One-Loop Higgs Masses in the Real NMSSM	29
4.4	Mixing Matrix Elements at One-Loop in the Real Higgs Sector	32
4.5	Mixing with the Goldstone Boson at One-Loop	34
4.6	Renormalization Schemes for the Real Higgs Sector	36
4.6.1	Mixed Renormalization Scheme	36
4.6.2	$\overline{\text{DR}}$ Renormalization Scheme	41
4.6.3	On-Shell Renormalization Scheme	42

4.7	One-Loop Higgs Masses in the Complex NMSSM	43
4.8	Mixing Matrix Elements at One-Loop in the Complex Higgs Sector	44
4.9	Renormalization of the Complex Higgs Sector	44
4.9.1	Remark on the Counterterms of the Phases	47
5	Numerical Analysis	49
5.1	Input Parameters	50
5.2	Real Higgs Sector	51
5.2.1	Variation of λ	52
5.2.2	Variation of T_κ	56
5.2.3	Variation of M_{H^\pm}	57
5.2.4	Exclusion Limits	59
5.3	Complex Higgs Sector	62
5.3.1	CP-Violation at Tree-Level	63
5.3.2	CP-Violation Induced at One-Loop Level	68
6	Summary and Conclusion	71
A	The Supersymmetric Lagrangian	73
B	Loop Functions	75
C	Running Top and Bottom Quark Masses	77
D	Counterterm Mass Matrix of the Higgs Sector	79
E	Chargino and Neutralino Counterterm Mass Matrices	89
	Acknowledgments	91
	References	93

The field of particle physics concerns itself with understanding elementary particles and fundamental interactions. The breakthrough in finding a theory that describes the world of elementary particles happened during the 1960s and 70s, when the Standard Model of Particle Physics (SM) [1–3], as we know it today, took form. Since then tremendous experimental efforts have been undertaken to confirm the SM predictions.

Huge particle colliders were built to probe nature at ever higher energies. One of the first really big collider experiments was the proton-antiproton collider at Fermilab, the Tevatron. The name Tevatron refers to its beam energy of up to 1 TeV. It began operation in 1983 and ran – with intermissions due to upgrades – until this year. During this long period of data taking many discoveries were made, with the most important one certainly being the discovery of the top quark in 1995. Precision measurements of the top quark mass followed. The Large Electron-Positron collider (LEP) at CERN was in operation from 1989 until 2000, when it had to make room for the LHC. One of the major achievements at LEP was the precision measurement of the Z and W -boson masses. Finally, the Large Hadron Collider (LHC) in the former LEP tunnel at CERN started taking data last year. With a design energy of 7 TeV per beam the LHC is the most powerful collider ever built. At the moment it runs at only half the potential beam energy, but it is scheduled to achieve full beam energy in 2014. One of the big hopes is that the last missing piece of the SM, the Higgs boson, will finally be found at the LHC.

The Higgs boson plays a crucial role in the framework of the SM, since the Higgs mechanism [4] provides an explanation of how vector bosons can acquire a nonzero mass without violating the gauge invariance of the SM model. The Higgs mechanism relies on the concept of spontaneous electroweak symmetry breaking. As a relic of this mechanism a scalar particle, the Higgs boson, emerges. Up to now, however, the Higgs boson has eluded discovery at the collider experiments. Nevertheless, the experiments have set bounds on the mass of the SM Higgs boson.

However, there are hints that the SM is not complete or might just be the limit of a more complex underlying theory. There are several possible extensions that are considered by theorists. One of them is supersymmetry [5], which introduces superpartners to the SM particles

and thereby resolves some of the insufficiencies of the SM. In fact, this thesis concerns itself with a supersymmetric extension of the SM. Other examples for theories beyond the SM are theories with extra dimensions or string theory, which even aspires to provide a theory of everything someday. Of course, all these new theories have to reproduce the well-established SM results. But they also make new predictions which differ from those of the SM. Therefore, it is essential to take these new predictions into consideration when interpreting the experimental data.

In this thesis the Higgs sector of the complex Next-to-Minimal Supersymmetric extension of the Standard Model (NMSSM) [6, 7] is studied. To be more precise, the full one-loop calculation of the Higgs bosons masses in the complex NMSSM applying a diagrammatic approach is presented. As the one-loop corrections to the Higgs boson masses involve divergent contributions, we need to perform a renormalization procedure. To this end, we employ a renormalization scheme that mixes on-shell and $\overline{\text{DR}}$ renormalization conditions. In the special case of the real NMSSM, a pure on-shell and a pure $\overline{\text{DR}}$ scheme were implemented as well. The accurate calculation of the loop-corrected masses is an important contribution to the phenomenological predictions for the NMSSM Higgs sector. If the LHC finds a Higgs signal, it will be especially crucial to have precise predictions from the various models to determine what “kind” of Higgs was actually discovered.

The Higgs sector of the NMSSM is much more complicated than that of the SM. The SM Higgs sector consists of one complex Higgs doublet field. When going to a supersymmetric theory one needs at least two complex doublet fields. This minimal extension is called the Minimal Supersymmetric Standard Model (MSSM) and features five Higgs bosons: two charged Higgs bosons and three neutral Higgs bosons. In the CP-conserving case two of the neutral Higgs bosons are CP-even and one is CP-odd. In comparison to the MSSM, the NMSSM is extended by one additional complex singlet field. This results in a total of seven Higgs bosons in the NMSSM: two charged Higgs bosons and five neutral Higgs bosons. In the CP-conserving case three of the neutral Higgs bosons are CP-even and two of them are CP-odd. In the NMSSM there can be additional decay channels, such as a light CP-even Higgs boson decaying into a pair of even lighter CP-odd Higgs bosons. Such additional decay channels might lead to the light CP-even Higgs boson escaping detection. Therefore, it is important to incorporate such new possibilities into the analysis of the experimental data.

Furthermore, the number of Higgs bosons is not the only thing that increases when going from the SM to supersymmetric models. In the SM the Higgs mass is the only free parameter of the Higgs sector. However, in the NMSSM there are at least twelve parameters, some of which can be complex. The enlarged parameter set can lead to new effects in the phenomenology of the Higgs sector. Therefore, it is instructive to study the dependence of the Higgs boson masses on these different parameters by means of some example scenarios.

The thesis is structured as follows. Chapter 2 consists of two main parts. In the first part (Section 2.1), a brief overview of the key features of the SM is given. Its insufficiencies are also brought to the readers attention. One of them, the hierarchy problem, is considered in more detail and supersymmetry is offered as a solution. Hence, the second part of Chapter 2 (Section 2.2) presents the core ideas and concepts of supersymmetry.

In Chapter 3 the NMSSM is introduced. After establishing the theoretical background of the NMSSM by presenting the particle content (Section 3.1) and commenting on the NMSSM Lagrangian, which can be derived from the superpotential (Section 3.2), we motivate the NMSSM in Section 3.3 by explaining its advantages, especially in comparison to the MSSM. Section 3.4 is devoted to the NMSSM Higgs sector at tree-level. In a detailed discussion

the Higgs mass matrix is derived from the Higgs potential using the tadpole conditions to simplify the mass matrix. If not stated otherwise, the more general case of the complex NMSSM is considered, although the simplifications which occur when restricting oneself to real parameters are always mentioned explicitly. At the end of this section an overview of the parameters of the Higgs sector is given. Section 3.5 deals with the neutralino and chargino sectors of the NMSSM at tree-level. They are presented explicitly, since we make use of renormalization conditions from these sectors in our renormalization schemes.

Chapter 4 describes the renormalization procedure and the calculation of the one-loop Higgs boson masses. It begins with some general remarks on renormalization, introduces the counterterm formalism and states the typical renormalization conditions for the masses of scalars, fermions and vector bosons. Section 4.2 lists all counterterms necessary to renormalize the NMSSM Higgs sector. From then on we separate the real and the complex NMSSM strictly. Since the real NMSSM is less complicated, the whole renormalization procedure for the Higgs sector is at first only described in this restricted model and the complex NMSSM is considered later on. Section 4.3 presents different methods for the calculation of the one-loop Higgs boson masses in the real NMSSM. The calculation of the mixing matrix elements of the Higgs sector in the real NMSSM at one-loop is described in Section 4.4. Section 4.5 comments on the mixing of the Higgs bosons with the Goldstone boson at one-loop. Finally, the different renormalization schemes used for the real NMSSM are discussed in Section 4.6. Then we move on to the complex NMSSM. Once again the calculation of the one-loop Higgs boson masses and the mixing matrix elements at one-loop is explained. Finally, Section 4.9 deals with the renormalization scheme chosen for the complex NMSSM.

Chapter 5 contains the numerical analysis. After defining the necessary input parameters in Section 5.1, a few scenarios that exemplify some of the typical higher order effects are investigated, both in the real NMSSM (Section 5.2) and in the complex NMSSM (Section 5.3). For the real NMSSM we also apply the experimental exclusion limits. For the analysis of the complex NMSSM we consider scenarios that display CP-violation in the Higgs sector already at tree-level, as well as one scenario where CP-violation is induced at one-loop level.

Standard Model of Particle Physics and Supersymmetry as its Extension

This chapter very briefly summarizes the key features of the Standard Model of Particle Physics. After mentioning some of the insufficiencies of the Standard Model, supersymmetry is offered as a possible solution to some of the problem of the Standard Model.

2.1 The Standard Model of Particle Physics

The Standard Model of Particle Physics (SM) [1–3] describes the world of elementary particles and the fundamental interactions¹. So far, the phenomenology predicted by the SM is in remarkable agreement with the precision measurements at the collider experiments such as LEP and Tevatron or at present the LHC. These experiments did not only lead to the discovery of all particles predicted by the SM except for the Higgs boson, but also tested the theory at a precision level of 10^{-3} .

The SM is a renormalizable non-abelian gauge theory based on the group represented by the direct product $SU(3)_C \otimes SU(2)_L \otimes U(1)_Y$, with the gauge symmetry $SU(2)_L \otimes U(1)_Y$ being spontaneously broken to $U(1)_{\text{em}}$. The $SU(3)_C$ gauge group describes the strong interaction. The corresponding gauge boson is the gluon. The $SU(2)_L \otimes U(1)_Y$ gauge symmetry describes the electroweak interaction. After electroweak symmetry breaking the corresponding gauge bosons are the photon, which mediates the electromagnetic interaction, and the vector bosons W^\pm and Z^0 , which mediate the weak interaction. The particles of the SM can be arranged according to their transformation properties under the different gauge groups (see Table 2.1).

Firstly, there are the fermionic spin 1/2 particles, the leptons and the quarks. These are often referred to as matter particles since they are the constituents of matter. The leptons and quarks are divided into three generations. The 2nd and 3rd generation are basically heavier copies of the first. In the case of the leptons these generations combine a lepton with electric charge $Q = -1$ and a neutral lepton (the neutrino). The leptons are: the electron,

¹Strictly speaking only the interactions relevant at the subatomic level are included. Hence, gravity is not incorporated in the SM.

name	field	$(SU(3)_C \otimes SU(2)_L \otimes U(1)_Y)$
leptons	$L = (\nu_L, e_L)^T$	$(\mathbf{1}, \mathbf{2}, -1/2)$
	e_R^\dagger	$(\mathbf{1}, \mathbf{1}, 1)$
quarks	$Q = (u_L, d_L)^T$	$(\mathbf{3}, \mathbf{2}, 1/6)$
	u_R^\dagger	$(\bar{\mathbf{3}}, \mathbf{1}, -2/3)$
	d_R^\dagger	$(\bar{\mathbf{3}}, \mathbf{1}, 1/3)$
Higgs	$\phi = (\phi^+, \phi^0)^T$	$(\mathbf{1}, \mathbf{2}, 1/2)$

Table 2.1: Matter particles and Higgs doublet in the SM and their corresponding quantum numbers. The generation indices on the quark and lepton fields, as well as the color indices on the quark fields were omitted.

the muon, the tau and the corresponding neutrinos. The left-handed components of the leptons transform as a doublet under the $SU(2)_L$ transformation, whereas the right-handed components transform as singlets. Up to now there is only indirect evidence of right-handed neutrinos, provided by the neutrino oscillation experiments. Additionally, these experiments set the upper bound on the mass of the neutrinos at very small values. As a consequence right-handed neutrinos are not included in the SM and the left-handed neutrinos are assumed to be massless. The different quarks are: the up-type quarks (up, charm, top) and the down-type quarks (down, strange, bottom). The up-type quarks carry an electric charge of $Q = 2/3$ and the down-type quarks carry an electric charge of $Q = -1/3$. Just as for the leptons the left-handed components of the quarks transform as a doublet under the $SU(2)_L$ transformation and the right-handed components as a singlet. In contrast to the leptons the quarks also carry a color charge (red, blue, green) and therefore also interact via the strong interaction.

Furthermore, there are the spin 1 vector bosons, as mentioned above, which mediate the interactions. In a theory with exact gauge symmetry all gauge bosons are massless by construction. But since the W - and Z -bosons are known to be massive, gauge symmetry breaking has to take place. To avoid explicit symmetry breaking, the $SU(2)_L \otimes U(1)_Y$ is spontaneously broken via the Higgs mechanism [4]. In the Higgs mechanism a complex doublet ϕ of spin zero fields is introduced (see Table 2.1). When the neutral component of the doublet acquires a vacuum expectation value (VEV) the electroweak symmetry is spontaneously broken and the W - and Z -bosons, as well as all particles coupling directly to the Higgs field, acquire a mass. A relic of this mechanism is one physical spin zero particle, the Higgs boson. This is the only SM particle not yet discovered. The Higgs search is one of the major goals of the LHC.

2.1.1 Problems of the Standard Model

Despite the tremendous success of the SM, it displays some insufficiencies. The obvious shortcomings are certainly that the SM fails to explain several experimental results.

- Neutrino oscillation experiments have shown that neutrinos do have mass [8]. Of course, this also implies that right-handed neutrinos have to exist. But in the SM the neutrinos are assumed to be massless and the right-handed neutrinos are not included at all.

- Cosmological measurements have established that about 25% of the matter and energy density of the universe consists of so-called cold dark matter. The SM, however, does not offer an adequate dark matter candidate.
- The CP-violation inherent in the SM is not large enough to explain the imbalance of matter and anti-matter observed in the universe.
- Gravity is not included in the SM.

Aside from these experimental arguments there are also some theoretical arguments. For example, the SM features many parameters (e.g. particle masses, mixing matrix elements and couplings) whose values need to be adjusted according to the experimental results, since their values cannot be predicted within the SM. Furthermore, the Higgs mechanism for electroweak symmetric breaking is put in by hand. There is no dynamical explanation where it comes from. It would be desirable to have some more fundamental theory, which reduces the number of parameters and explains the Higgs mechanism. Also, if the SM was a low-energy limit of some yet unknown fundamental theory, one would expect that the values of the gauge coupling constants unify in the high energy-limit. In the SM this kind of unification does not occur. Such a fundamental theory, which is often referred to as “Grand Unified Theory” (GUT), should also include gravity, which becomes important at the elementary particle level for very high energies. Another theoretical argument against the SM is the so-called hierarchy problem [9], which will be considered in more detail in the following section.

2.1.2 The Hierarchy Problem

On the one hand the scale at which electroweak symmetry breaking occurs is experimentally known to be approximately $v \approx 246$ GeV, while on the other hand the SM is expected to be valid up to the Planck scale $M_{Pl} \approx 2.4 \cdot 10^{18}$ GeV, at which point new physics is expected to enter². The huge difference in these scales turns out to be problematic when considering the radiative corrections to the Higgs boson mass.

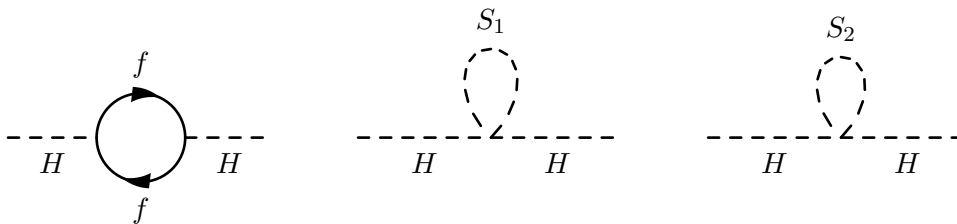


Figure 2.1: Radiative corrections to the Higgs boson mass.

Let us assume a theory in which the Higgs field couples to a fermion f and two complex scalars S_1 and S_2 in the following way

$$\mathcal{L} = \dots - \lambda_f H \bar{f} f - \lambda_S^2 |H|^2 (|S_1|^2 + |S_2|^2). \quad (2.1)$$

The Feynman diagrams contributing to the corrections to the Higgs boson mass are shown in Fig. 2.1. The diagram with the fermion loop (left diagram of Fig. 2.1) yields the radiative

²Gravity should become important at this scale.

correction

$$\Delta m_H^2 \Big|_{\text{fermion-loop}} = -\frac{\lambda_f^2}{8\pi^2} \cdot \Lambda^2 + \dots \quad (2.2)$$

with Λ being the cutoff introduced to regularize the loop integral. The ellipsis stand for additional terms logarithmic in Λ which are not of interest here. Under the assumption that new physics enters at M_{Pl} , the cutoff should be $\Lambda \approx M_{Pl}$. Since the radiative corrections are quadratic in the cutoff³, these corrections are roughly 30 orders of magnitude larger than the value of $m_H^2 \approx (100 \text{ GeV})^2$ required by electroweak symmetry breaking. Of course the bare Higgs mass can be adjusted to just cancel the radiative corrections in the right way, but such extreme fine-tuning seems unnatural.

Hence, new theories that avoid the hierarchy problem are constructed. One possible solution is supersymmetry. As will be discussed in detail in the following chapter, supersymmetry relates bosons to fermions. In fact, the theory we wrote down in Eq. (2.1) takes the first step to do so, since it contains the same number of bosonic as of fermionic degrees of freedom. So let us consider the contribution from the scalars (last two diagrams in Fig. 2.1),

$$\Delta m_H^2 \Big|_{\text{scalar-loops}} = +2 \cdot \frac{\lambda_S^2}{16\pi^2} \cdot \Lambda^2 + \dots \quad (2.3)$$

It is quite obvious, that if the fermionic and scalar coupling were equal, $\lambda_f = \lambda_S$, then the two contributions would cancel one another and render fine tuning unnecessary. This is exactly what happens in supersymmetric theories.

³These quadratic divergences occur only for scalar particles as the masses of fermions and vector bosons are protected from them by chiral symmetry and gauge invariance, respectively.

2.2 Supersymmetry

Supersymmetry (SUSY) [5] is a spacetime symmetry relating bosons to fermions and vice versa. For detailed introductions to SUSY and reviews see for example [10–12]. Coleman and Mandula formulated a theorem [13] which states that the maximal set of spacetime symmetry transformations compatible with relativistic quantum field theory is given by the Poincaré group. However, in their analysis they only considered Lie algebras. Haag, Lopuszanski and Sohnius found that if an extended Lie algebra, which also incorporates anticommuting relations for the symmetry generators⁴, is used the spacetime symmetry group can be enlarged by including supersymmetry [14]. The generator of supersymmetry is a fermionic operator Q that transforms a bosonic into a fermionic state and vice versa:

$$Q |\text{Boson}\rangle = |\text{Fermion}\rangle \quad \text{and} \quad Q |\text{Fermion}\rangle = |\text{Boson}\rangle. \quad (2.4)$$

Hence, one specific fermionic single particle state is always related to one specific bosonic single particle state. They are called each others “superpartners”. The superpartners can be arranged in a supermultiplet. This supermultiplet contains the same number of fermionic and bosonic degrees of freedom and the particles in the supermultiplet have the same gauge transformation properties; i.e. they have the same hypercharge, weak isospin and color charge. There are two types of supermultiplets in SUSY: the chiral supermultiplet and the vector supermultiplet. The chiral supermultiplet consists of a two-component Weyl fermion and a complex scalar field. It is sometimes also referred to as “matter supermultiplet”, because the matter particles of the SM, i.e. quarks and leptons, and their scalar superpartners can be arranged in such a multiplet. The gauge bosons of the SM and their fermionic superpartners can be arranged in vector supermultiplets.

Considering this supermultiplet structure, it is apparent that going from the SM to a supersymmetric theory at least doubles the particle content. The supersymmetric theory with the same gauge structure as the SM and the minimal particle content is called the Minimal Supersymmetric Standard Model (MSSM). In the MSSM the SM fermions receive spin-0 superpartners, which are named by adding an “s” in front of the fermion’s name and denoted with a tilde over the SM abbreviation. So, for example the superpartner of the left-handed top (denoted by t_L) is the left-handed⁵ stop (denoted by \tilde{t}_L), the superpartner of the right-handed electron (denoted by e_R) is the right-handed selectron (denoted by \tilde{e}_R), etc. The gauge bosons before electroweak symmetry breaking, the W^+ , W^- , W^0 and B^0 receive spin-1/2 superpartners, the winos and bino denoted as \tilde{W}^+ , \tilde{W}^- , \tilde{W}^0 and \tilde{B}^0 . In order to give masses to up- and down-type quarks and to circumvent anomalies one needs two complex Higgs doublets. After electroweak symmetry breaking and gauge fixing this results in three neutral Higgs bosons (one CP-odd and two CP-even ones in the CP-conserving MSSM) and two charged Higgs bosons. The superpartners of the Higgs bosons are called Higgsinos. It is important to note that the superpartners are not necessarily mass eigenstates. For example, the left- and the right-handed sfermions \tilde{f}_L and \tilde{f}_R usually mix to form the mass eigenstates \tilde{f}_1 and \tilde{f}_2 . Furthermore, the neutral wino and the bino mix with the neutral Higgsinos to yield the neutralinos, while the charged winos and the charged Higgsinos mix to form the charginos. In the MSSM there are four neutralinos and two charginos.

One problem that arises when going to a supersymmetric model like the MSSM is that if an unbroken supersymmetry was assumed, there had to be superpartners of the same mass as

⁴This is the so-called graduated Lie algebra.

⁵Since the stop is a scalar “left-handed” does not refer to chirality in this case.

the corresponding SM particle. Of course, no such particles have been discovered yet and therefore SUSY has to be broken. Unfortunately, it is not yet known how this supersymmetry breaking works. Thus “soft breaking” terms are added to the Lagrangian by hand. These soft breaking terms provide a mass splitting between the SM particles and their superpartners, making the latter heavier without spoiling the relation between the fermionic and bosonic couplings to the Higgs boson which led to the cancellations solving the hierarchy problem.

After this short explanation of the core concept of supersymmetry the question arises whether it is really worth it to introduce so many new particles and parameters. In fact, SUSY offers solutions to several of the SM problems:

- SUSY solves the hierarchy problem by relating bosons to fermions.
- If R-parity conservation is assumed, SUSY offers a cold dark matter candidate. R-parity is a multiplicative quantum number. SM particles are assigned R-parity $R = +1$ and their superpartners have R-parity $R = -1$. If R-parity conservation holds, SUSY particles can only be created in pairs in SM particle collisions. Also, the lightest supersymmetric particle (LSP) is stable, since it cannot decay any further. The LSP is typically the lightest neutralino and a possible dark matter candidate.
- In the framework of the MSSM gauge coupling unification can be achieved at the GUT-scale [15].
- In the electromagnetic theory local gauge invariance leads to a massless spin-1 vector boson, the photon. Likewise, local supersymmetry leads to a massless spin-2 particle, the graviton. This graviton would then be the gauge boson mediating gravitation. The only drawback is that these supersymmetric theories are not renormalizable. But this can nevertheless be seen as a hint that SUSY might somehow be connected to finding a quantum theory of gravity.

The Next-to-Minimal Supersymmetric Extension of the Standard Model

The Next-to-Minimal Supersymmetric Extension of the Standard Model (NMSSM) [6, 7] is, as the name suggests, a supersymmetric extension of the SM. It is referred to as “next-to-minimal” since its particle content is extended by one complex singlet field compared to the minimal possible particle content of any supersymmetric theory with the same gauge structure as the Standard Model. This chapter will first introduce the NMSSM by presenting the particle content and the Lagrangian. A short motivation as to why the NMSSM is worth consideration will be followed by a detailed discussion of the Higgs sector, and of the neutralino and the chargino sectors. For reviews of the NMSSM see for example [16] or [17].

3.1 Particle Content

The particle content of the NMSSM is given in Table 3.1. The only difference compared to the MSSM particle content, which was described in the previous chapter, is the addition of a complex Higgs singlet field S . The first part of the table lists all the chiral supermultiplets while the second part lists the gauge supermultiplets. The first column gives the name of the superfield, which is always denoted by a hat. The second column gives the superpartners which form the supermultiplet. Since the NMSSM is supposed to be a supersymmetric extension of the SM, there are of course the quarks and the leptons, as well as their corresponding superpartners the squarks and the sleptons. For simplicity only the first generations of the quarks/squarks and leptons/sleptons are included in the table. The other generations obviously have the same gauge transformation properties as the first ones. To cover the quark/squark sector three superfields are needed. The left-handed up- and down-type quarks and squarks can be combined into the doublets \hat{Q} and $\hat{\tilde{Q}}$, which make up the superfield \hat{Q} . The right-handed up- and down-type quarks and squarks, however, have to be considered separately and can be arranged into the two superfields \hat{u} and \hat{d} . It is common to use the conjugate right-handed fields so that they transform as left-handed fields. The arrangement in the lepton/slepton sector is quite similar. The left-handed electron and neutrino fields are combined in the superfield \hat{L} , while the right-handed electron fields are included in \hat{e} .

chiral supermultiplets		spin-0	spin-1/2	$(SU(3)_C \otimes SU(2)_L \otimes U(1)_Y)$
quark/squark	\hat{Q}	$\tilde{Q} = (\tilde{u}_L, \tilde{d}_L)^T$	$Q = (u_L, d_L)^T$	$(\mathbf{3}, \mathbf{2}, 1/6)$
	\hat{u}	\tilde{u}_R^*	u_R^\dagger	$(\bar{\mathbf{3}}, \mathbf{1}, -2/3)$
	\hat{d}	\tilde{d}_R^*	d_R^\dagger	$(\bar{\mathbf{3}}, \mathbf{1}, 1/3)$
lepton/slepton	\hat{L}	$\tilde{L} = (\tilde{\nu}_e, \tilde{e}_L)^T$	$L = (\nu_e, e_L)^T$	$(\mathbf{1}, \mathbf{2}, -1/2)$
	\hat{e}	\tilde{e}_R^*	e_R^\dagger	$(\mathbf{1}, \mathbf{1}, 1)$
Higgs/Higgsino	\hat{H}_u	$H_u = (H_u^+, H_u^0)^T$	$\tilde{H}_u = (\tilde{H}_u^+, \tilde{H}_u^0)^T$	$(\mathbf{1}, \mathbf{2}, 1/2)$
	\hat{H}_d	$H_d = (H_d^0, H_d^-)^T$	$\tilde{H}_d = (\tilde{H}_d^0, \tilde{H}_d^-)^T$	$(\mathbf{1}, \mathbf{2}, -1/2)$
	\hat{S}	S	\tilde{S}	$(\mathbf{1}, \mathbf{1}, 0)$
gauge supermultiplets		spin-1/2	spin-1	$(SU(3)_C \otimes SU(2)_L \otimes U(1)_Y)$
gluon/gluino		\tilde{g}	g	$(\mathbf{8}, \mathbf{1}, 0)$
W-boson/wino		$\tilde{W}^\pm, \tilde{W}^0$	W^\pm, W^0	$(\mathbf{1}, \mathbf{3}, 0)$
B-boson/bino		\tilde{B}^0	B^0	$(\mathbf{1}, \mathbf{1}, 0)$

Table 3.1: Particle content of the NMSSM. The upper table lists the matter particles that can be arranged in chiral supermultiplets. The lower table displays the gauge particles in gauge supermultiplets. For readability the generation indices on the quark and lepton fields, as well as the color indices on the quark fields, were omitted. For the hypercharge Y the convention $Q = I_W^3 + Y$, with Q being the electric charge and I_W^3 the third component of the weak isospin, is used.

In the Higgs sector we have the two Higgs doublets necessary to generate masses for both up- and down-type quarks and to avoid anomalies. They are denoted by \hat{H}_u and \hat{H}_d . When acquiring a vacuum expectation value, the neutral component of the scalar superpartner of the superfield \hat{H}_u , namely H_u^0 , gives masses to the up-type quarks. Likewise H_d^0 generates the masses for the down-type quarks and the charged leptons. In addition to these, there is a complex singlet field \hat{S} . The addition of this singlet field results in slightly more complicated Higgs and neutralino sectors. Instead of three neutral Higgs bosons, as in the MSSM, there are now five neutral Higgs bosons after gauge fixing. So including the two charged Higgs bosons, there are a total of seven Higgs bosons in the NMSSM, compared to only five in the MSSM. As mentioned earlier, the superpartners of the Higgs, the Higgsinos, mix with the gauginos to form the neutralinos and charginos. The number of charged Higgs bosons in the NMSSM is the same as in the MSSM. Hence, there is no change in the chargino sector. But due to the addition of the singlino \tilde{S} , there are now five instead of only four neutralinos. The Higgs sector, as well as the neutralino and chargino sector, will be considered in more detail later in this chapter.

3.2 The NMSSM Lagrangian

The Lagrangian of the NMSSM is given by

$$\mathcal{L}_{\text{NMSSM}} = \mathcal{L}_{\text{susy}} + \mathcal{L}_{\text{soft}} + \mathcal{L}_{\text{fix}} + \mathcal{L}_{\text{ghost}} \quad (3.1)$$

$\mathcal{L}_{\text{susy}}$ contains all kinetic terms and interactions of the theory with exact unbroken supersymmetry. Once the particle content, the gauge structure and the superpotential are given, it can

be constructed according to the general rules summarized in Appendix A. The gauge structure of the NMSSM is of course the same as in the SM, namely $SU(3)_C \otimes SU(2)_L \otimes U(1)_Y$. The particle content is given in Table 3.1 and the NMSSM superpotential W is given by

$$W = \hat{u}Y_u(\hat{Q}^T \epsilon \hat{H}_u) - \hat{d}Y_d(\hat{Q}^T \epsilon \hat{H}_d) - \hat{e}Y_e(\hat{L}^T \epsilon \hat{H}_d) + \lambda \hat{S}(\hat{H}_u^T \epsilon \hat{H}_d) + \frac{1}{3}\kappa \hat{S}^3. \quad (3.2)$$

Here the couplings Y_u , Y_d , Y_e , λ and κ are dimensionless and

$$\epsilon = \begin{pmatrix} 0 & 1 \\ -1 & 0 \end{pmatrix}. \quad (3.3)$$

In this notation the generation indices were suppressed – written with all indices $\hat{u}Y_u(\hat{Q}^T \epsilon \hat{H}_u)$ reads $\hat{u}^i Y_u^{ij}(\hat{Q}^{j,a} \epsilon_{ab} \hat{H}_u^b)$ with $a, b \in \{1, 2\}$ and $i, j \in \{1, 2, 3\}$. Furthermore, the Yukawa couplings Y_u , Y_d and Y_e are taken to be diagonal 3×3 matrices. Hence, the model considered here does not allow for generation mixing.

$\mathcal{L}_{\text{soft}}$ contains all soft supersymmetry breaking terms. It is chosen in such a way that all terms, which lead to a mass splitting between the masses of the SM particles and their superpartners, and at the same time do not spoil the cancellation of the quadratic divergences in the loop corrections to the Higgs boson masses, are included [18],

$$\begin{aligned} \mathcal{L}_{\text{soft}} = & -m_{\tilde{Q}_L}^2 \tilde{Q}^\dagger \tilde{Q} - m_{\tilde{u}_R}^2 |\tilde{u}_R|^2 - m_{\tilde{d}_R}^2 |\tilde{d}_R|^2 - \left(T_{Y_u} \tilde{u}_R^* (\tilde{Q}^T \epsilon H_u) - T_{Y_d} \tilde{d}_R^* (\tilde{Q}^T \epsilon H_d) + c.c. \right) + \\ & -m_{\tilde{L}_L}^2 \tilde{L}^\dagger \tilde{L} - m_{\tilde{e}_R}^2 |\tilde{e}_R|^2 + \left(T_{Y_e} \tilde{e}_R^* (\tilde{L}^T \epsilon H_d) + c.c. \right) + \\ & -m_{H_u}^2 H_u^\dagger H_u - m_{H_d}^2 H_d^\dagger H_d - m_S |S|^2 - \left(T_\lambda (H_u^T \epsilon H_d) S + \frac{1}{3} T_\kappa S^3 + c.c. \right) + \\ & -\frac{1}{2} \left(M_1 \tilde{B}^0 \tilde{B}^0 + M_2 \tilde{W}^i \tilde{W}^i + M_3 \tilde{g} \tilde{g} + c.c. \right). \end{aligned} \quad (3.4)$$

In order to parametrize the unknown supersymmetry breaking mechanism, soft supersymmetry breaking mass parameters and trilinear couplings are introduced. The SUSY breaking mass parameters are introduced solely for the scalar superpartners in the chiral supermultiplets, but not for their fermionic superpartners, as well as for the gauginos. The trilinear breaking parameters reflect the structure appearing in the superpotential and are denoted by T_i , with $i = \{\lambda, \kappa, Y_u, Y_d, Y_e\}$, depending on which coupling in the superpotential they correspond to. Note that this notation differs from the often used notation where the trilinear couplings T_i are replaced by $i \cdot A_i$.

The part of the Lagrangian which contains the gauge fixing terms is given by

$$\begin{aligned} \mathcal{L}_{\text{fix}} = & -\frac{1}{2\xi_G} (\partial_\mu G^{a\mu})^2 - \frac{1}{2\xi_A} (\partial_\mu A^\mu)^2 - \frac{1}{2\xi_Z} (\partial_\mu Z^\mu + M_Z \xi_Z G^0)^2 + \\ & -\frac{1}{2\xi_W} |\partial_\mu W^{+\mu} + iM_W \xi_W G^\pm|^2. \end{aligned} \quad (3.5)$$

Here $G^{a\mu}$ stands for the gluon fields, A^μ for the photon field, W^μ for the W -boson, Z^μ for the Z -boson and G^0 and G^\pm for the neutral and charged Goldstone boson, which will be introduced in Section 3.4.3. Throughout this thesis the 't Hooft-Feynman gauge will be used, i.e. $\xi_G = \xi_A = \xi_Z = \xi_W = 1$. This results in the propagators of the vector bosons being proportional to the Minkowski metric $g_{\mu\nu}$. Furthermore this choice of gauge sets the Goldstone boson masses to be $m_{G^0} = M_Z$ and $m_{G^\pm} = M_W$. Fixing the gauge leads to

unphysical polarizations for the vector bosons. In order to eliminate those the Fadeev Popov ghosts [19] are introduced in $\mathcal{L}_{\text{ghost}}$. Since this part is not of any importance for this thesis it will not be considered here any further.

For a detailed discussion of the NMSSM Lagrangian and a derivation of all NMSSM Feynman rules see [16] and [20].

3.3 Motivation for the NMSSM

After having introduced the main features of the NMSSM, it is inevitable to answer the question of why one should go to this more complicated supersymmetric model and why we chose the model set up as we did. As it is always done in physics one starts with the simplest possible model. In supersymmetry this is the MSSM. But the MSSM has some shortcomings. The main issue is the so-called “ μ -problem” [21]. In order to understand this μ -problem it is helpful to have a closer look at the MSSM superpotential

$$W_{\text{MSSM}} = \hat{u}Y_u(\hat{Q}^T\epsilon\hat{H}_u) - \hat{d}Y_d(\hat{Q}^T\epsilon\hat{H}_d) - \hat{e}Y_e(\hat{L}^T\epsilon\hat{H}_d) + \mu(\hat{H}_u^T\epsilon\hat{H}_d). \quad (3.6)$$

Just as in the NMSSM there are the three terms, necessary to generate masses for the quarks and charged leptons, which couple the quarks and leptons to the Higgs doublets. However, the mixing of the Higgs doublets \hat{H}_u and \hat{H}_d is generated by the term $\mu(\hat{H}_u^T\epsilon\hat{H}_d)$. The parameter μ , which has the dimension mass, is already present in the theory before electroweak symmetry breaking (EWSB) takes place. But before electroweak symmetry breaking there are only two natural scales: either $\mu = 0$ or $\mu \approx M_{Pl}$. If, however, μ is set to zero the two Higgs doublets do not mix at all, which causes the minimum of the Higgs potential to occur at $\langle H_d \rangle = 0$, which in turn leads to massless down-type fermions and is therefore not desirable. The other choice is to take μ to be of the order of the Planck scale. Unfortunately, this reintroduces the hierarchy problem all over again because the masses of the scalar Higgs boson acquire corrections proportional to μ^2 . So, the only option we are left with is to adjust μ by hand to be of the order of the electroweak scale. In the NMSSM this adjustment by hand is avoided by generating the μ term dynamically via the new singlet field S . The NMSSM scalar superpotential contains the term $\lambda S(H_u^T\epsilon H_d)$. If S acquires a vacuum expectation value $\langle S \rangle$, this term is comparable to the μ term of the MSSM.

$$\lambda S(H_u^T\epsilon H_d) \xrightarrow{\text{EWSB}} \lambda \langle S \rangle (H_u^T\epsilon H_d) \longleftrightarrow \mu = \lambda \langle S \rangle \quad (3.7)$$

This explains the second to last term in the NMSSM superpotential given in Eq. (3.2) and leaves us to wonder why the last term cubic in \hat{S} was introduced. Without this cubic term the model would possess an additional $U(1)$ symmetry, a Peccei-Quinn (PQ) symmetry [22]. In the MSSM this symmetry is explicitly broken by the μ term. In a NMSSM model without the cubic term, however, the PQ symmetry would be spontaneously broken when S acquires a VEV. This would lead to the appearance of a massless scalar in the Higgs sector, the PQ-axion [23]. Since such an axion has not been observed, this would impose tremendous constraints on the parameter space. Hence, the term cubic in \hat{S} is added to the superpotential to break the PQ symmetry explicitly and to avoid the PQ-axion.

Aside from solving the μ problem the NMSSM provides an extended Higgs sector. This is advantageous since the Higgs sector of the MSSM is highly restricted. In the MSSM the lightest CP-even Higgs boson is at tree-level predicted to be lighter than the Z -boson. Only

large quantum corrections raise the mass above the LEP bounds. In the NMSSM, scenarios with the mass of the lightest CP-even Higgs boson above the mass of the Z -boson already at tree-level are possible. Furthermore, the Higgs sector is less restricted allowing for example for scenarios with a CP-odd Higgs boson so light that the lightest CP-even Higgs boson can decay into two CP-odd ones and thereby escape detection.

Finally, the MSSM Higgs sector is CP-conserving at tree-level and CP-violation is only induced by higher order corrections, whereas in the NMSSM a CP-violating Higgs sector at tree-level is possible.

3.4 The Higgs Sector at Tree-Level

In this section, the Higgs sector of the complex NMSSM will be discussed at tree-level; i.e all parameters are taken to be complex. As the Higgs is the only SM particle not yet discovered, although it plays a crucial role, since it generates the masses of the other particles via the Higgs mechanism, investigating the Higgs sectors of alternative theories is of special interest, since these theories should also be considered in the experimental searches for the Higgs boson.

3.4.1 The Higgs Potential

The Higgs potential¹ of the NMSSM consists of the F-terms, D-terms and the soft SUSY breaking terms

$$V = V_F + V_D + V_{\text{soft}}. \quad (3.8)$$

The F-terms are called F-terms, since they emerge when the auxiliary field F is eliminated from the chiral Lagrangian (see Appendix A). The auxiliary field F has no kinetic term and therefore does not propagate. Such an auxiliary field is needed in a chiral supermultiplet to ensure that the bosonic and fermionic degrees of freedom are equal even off-shell. When going on-shell, the Lagrangian equations of motion for the F field can be used to eliminate it in favor of the other fields. The F-terms of the Higgs potential can be calculated from the scalar superpotential² W and are given by

$$V_F = \sum_i \left| \frac{\delta W}{\delta \phi_i} \right|^2 \quad \text{with} \quad \phi = (H_u, H_d, S) \quad (3.9)$$

$$\Rightarrow V_F = |\lambda|^2 |S|^2 \left(H_u^\dagger H_u + H_d^\dagger H_d \right) + |\lambda (H_u^\dagger \epsilon H_d) + \kappa S^2|^2. \quad (3.10)$$

The D-terms result from the elimination of the auxiliary field \mathcal{D} , required to close the supersymmetry of gauge supermultiplets off-shell. They can be calculated by

$$V_D = \frac{1}{2} \sum_{i,j} g_a^2 (\phi_i^\dagger \mathbf{T}^a \phi_i) (\phi_j^\dagger \mathbf{T}^a \phi_j) \quad \text{with} \quad \phi = (H_u, H_d). \quad (3.11)$$

Here \mathbf{T}^a are the generators of the gauge groups and g_a are the corresponding gauge couplings. For $U(1)_Y$ there is one generator, the hypercharge operator \mathbf{Y} and the gauge coupling is g_1 .

¹The Higgs potential is the part of the potential bilinear in the Higgs fields

²The scalar superpotential is obtained from the superpotential in terms of the superfields by replacing the superfields by their scalar component fields.

The generators for the $SU(2)_L$ are $I_W^a = \sigma^a/2$ (with $a = 1, 2, 3$ and σ^a the Pauli matrices) and the gauge coupling is g_2 . With $\sigma_{ij}^a \sigma_{kl}^a = 2\delta_{il}\delta_{jk} - \delta_{ij}\delta_{kl}$, this leads to the D-terms

$$V_D = \frac{1}{2}g_2^2 |H_u^\dagger H_d|^2 + \frac{1}{8}(g_1^2 + g_2^2) (H_u^\dagger H_u - H_d^\dagger H_d)^2. \quad (3.12)$$

The soft SUSY breaking terms can be read from $\mathcal{L}_{\text{soft}}$ (see Eq. (3.4))

$$V_{\text{soft}} = m_{H_u}^2 H_u^\dagger H_u + m_{H_d}^2 H_d^\dagger H_d + m_S |S|^2 + \left(T_\lambda (H_u^T \epsilon H_d) S + \frac{1}{3} T_\kappa S^3 + c.c. \right). \quad (3.13)$$

The doublets H_u and H_d each consist of one charged and one neutral component. The complex neutral fields can be expanded around the vacuum expectation values $v_{\{u/d\}}/\sqrt{2}$ and written in terms of two real fields $h_{\{u/d\}}$ and $a_{\{u/d\}}$, i.e.

$$H_d = \begin{pmatrix} \frac{1}{\sqrt{2}}(v_d + h_d + ia_d) \\ H_d^- \end{pmatrix} \quad \text{and} \quad H_u = e^{i\phi_u} \begin{pmatrix} H_u^+ \\ \frac{1}{\sqrt{2}}(v_u + h_u + ia_u) \end{pmatrix}. \quad (3.14)$$

The same can be done for the neutral Higgs singlet field

$$S = \frac{1}{\sqrt{2}} e^{i\phi_s} (v_s + h_s + ia_s). \quad (3.15)$$

Due to the phases ϕ_u and ϕ_s , which were introduced in the parametrization for H_u and S , the values for v_d , v_u and v_s can always be chosen to be real and non-negative³. The fields h_u , h_d , h_s , a_u , a_d and a_s are real fields whereas H_u^+ and H_d^- are complex fields, but neither of them are mass eigenstates and are thus usually referred to as interaction eigenstates. In the special case of the real NMSSM (i.e. if all parameters are taken to be real) the h - and the a -fields do not mix, because the h fields are CP-even, while the a -fields are CP-odd and CP-conservation holds for the real NMSSM.

3.4.2 The Tadpole Conditions

The vacuum expectation values of the Higgs fields are given by

$$\langle H_d \rangle = \begin{pmatrix} \frac{v_d}{\sqrt{2}} \\ 0 \end{pmatrix}, \quad \langle H_u \rangle = e^{i\phi_u} \begin{pmatrix} 0 \\ \frac{v_u}{\sqrt{2}} \end{pmatrix} \quad \text{and} \quad \langle S \rangle = e^{i\phi_s} \frac{v_s}{\sqrt{2}}. \quad (3.16)$$

They are called vacuum expectation values (VEVs) since the Higgs potential V has a global nontrivial minimum when the fields assume their VEVs. Therefore, the first derivatives of the Higgs potential V with respect to the Higgs fields obviously have to vanish at the minimum. This fact immediately yields the so-called tadpole conditions:

$$\begin{aligned} t_{h_d} &:= \left\langle \frac{\partial V}{\partial h_d} \right\rangle = \frac{|\lambda|^2}{2} v_d (v_s^2 + v_u^2) + \frac{(g_1^2 + g_2^2)}{8} v_d (v_d^2 - v_u^2) - R_\lambda v_s v_u - \frac{R}{2} v_s^2 v_u + v_d m_{H_d}^2 \stackrel{!}{=} 0, \\ t_{h_u} &:= \left\langle \frac{\partial V}{\partial h_u} \right\rangle = \frac{|\lambda|^2}{2} v_u (v_s^2 + v_d^2) + \frac{(g_1^2 + g_2^2)}{8} v_u (v_u^2 - v_d^2) - R_\lambda v_s v_d - \frac{R}{2} v_s^2 v_d + v_u m_{H_u}^2 \stackrel{!}{=} 0, \\ t_{h_s} &:= \left\langle \frac{\partial V}{\partial h_s} \right\rangle = \frac{|\lambda|^2}{2} v_s (v_d^2 + v_u^2) + |\kappa|^2 v_s^3 - R v_d v_s v_u - R_\lambda v_d v_u + R_\kappa v_s^2 + m_s^2 v_s \stackrel{!}{=} 0, \end{aligned}$$

³Any phase of H_d could be rotated away by gauge transformation. Hence, ϕ_d is taken to be zero.

$$\begin{aligned}
 t_{a_d} &:= \left\langle \frac{\partial V}{\partial a_d} \right\rangle = I_\lambda v_s v_u + \frac{I}{2} v_s^2 v_u \stackrel{!}{=} 0, \\
 t_{a_u} &:= \left\langle \frac{\partial V}{\partial a_u} \right\rangle = I_\lambda v_s v_d + \frac{I}{2} v_s^2 v_d \stackrel{!}{=} 0, \\
 t_{a_s} &:= \left\langle \frac{\partial V}{\partial a_s} \right\rangle = -I v_d v_s v_u + I_\lambda v_d v_u - I_\kappa v_s^2 \stackrel{!}{=} 0,
 \end{aligned} \tag{3.17}$$

where $\langle \dots \rangle$ denotes the vacuum. For simplicity the abbreviations

$$\begin{aligned}
 R &= |\lambda| |\kappa| \cos(\phi_u - 2\phi_s + \phi_\lambda - \phi_\kappa), & I &= |\lambda| |\kappa| \sin(\phi_u - 2\phi_s + \phi_\lambda - \phi_\kappa), \\
 R_\lambda &= \frac{|T_\lambda|}{\sqrt{2}} \cos(\phi_u + \phi_s + \phi_{T_\lambda}), & I_\lambda &= \frac{|T_\lambda|}{\sqrt{2}} \sin(\phi_u + \phi_s + \phi_{T_\lambda}), \\
 R_\kappa &= \frac{|T_\kappa|}{\sqrt{2}} \cos(3\phi_s + \phi_{T_\kappa}) \quad \text{and} & I_\kappa &= \frac{|T_\kappa|}{\sqrt{2}} \sin(3\phi_s + \phi_{T_\kappa})
 \end{aligned} \tag{3.18}$$

were used. In these relations the complex parameters λ , κ , T_λ and T_κ were written as

$$\lambda = |\lambda| \cdot e^{i\phi_\lambda}, \quad \kappa = |\kappa| \cdot e^{i\phi_\kappa}, \quad T_\lambda = |T_\lambda| \cdot e^{i\phi_{T_\lambda}} \quad \text{and} \quad T_\kappa = |T_\kappa| \cdot e^{i\phi_{T_\kappa}}. \tag{3.19}$$

At tree-level the tadpole parameters t_i ($i = h_d, h_u, h_s, a_d, a_u, a_s$) in Eq. (3.17) have to vanish. As mentioned earlier, this is just the minimum condition for the Higgs potential and ensures that no terms linear in the Higgs fields appear in the Lagrangian. The tadpole parameters are only kept for bookkeeping reasons to keep track of where the tadpole relations were used. This is necessary if one considers higher order corrections, since then the tadpole relations have to be modified. The first three tadpole equations can be used to eliminate the soft SUSY breaking mass parameters $m_{H_d}^2$, $m_{H_u}^2$ and m_s^2 in favor of the tadpole parameters t_{h_d} , t_{h_u} and t_{h_s} . In the case of the real NMSSM (i.e. all phases set to zero) the last three tadpole conditions originating from the derivatives with respect to the CP-odd a -fields are not of any interest because they are automatically satisfied (since $I = I_\kappa = I_\lambda = 0$ for real parameters). In the complex case they allow us to eliminate I_κ and I_λ in favor of t_{a_d} and t_{a_s} . Note that the equations for t_{a_d} and t_{a_u} are linearly dependent, hence considering only one is sufficient.

3.4.3 The Mass Matrices for the Neutral Higgs States

Using the tadpole conditions and the fact that the tadpole parameters vanish at Born level, the part of the Lagrangian bilinear in the Higgs fields can be rewritten in the basis

$$\begin{aligned}
 (\phi_a^T, \phi_h^T) &= (a_d, a_u, a_s, h_d, h_u, h_s) \quad \text{as} \\
 \mathcal{L} \Big|_{\text{bil, Higgs}} &= -\frac{1}{2} (\phi_a^T, \phi_h^T) \mathcal{M}_{\text{Higgs}} \begin{pmatrix} \phi_a \\ \phi_h \end{pmatrix} = -\frac{1}{2} (\phi_a^T, \phi_h^T) \begin{pmatrix} \mathcal{M}_{\mathbf{a}} & \mathcal{M}_{\mathbf{ah}} \\ \mathcal{M}_{\mathbf{ha}} & \mathcal{M}_{\mathbf{h}} \end{pmatrix} \begin{pmatrix} \phi_a \\ \phi_h \end{pmatrix}.
 \end{aligned} \tag{3.20}$$

The mass matrix can be split into three submatrices: one for the CP-odd Higgs states $\mathcal{M}_{\mathbf{a}}$, which reads

$$\mathcal{M}_{\mathbf{a}} = \begin{pmatrix} (2R_\lambda + Rv_s) \frac{v_s v_u}{2v_d} & (2R_\lambda + Rv_s) \frac{v_s}{2} & (R_\lambda - Rv_s) v_u \\ (2R_\lambda + Rv_s) \frac{v_s}{2} & (2R_\lambda + Rv_s) \frac{v_d v_s}{2v_u} & (R_\lambda - Rv_s) v_d \\ (R_\lambda - Rv_s) v_u & (R_\lambda - Rv_s) v_d & (R_\lambda + 2Rv_s) \frac{v_d v_u}{v_s} - 3R_\kappa v_s \end{pmatrix}, \tag{3.21}$$

one for the CP-even Higgs states $\mathcal{M}_{\mathbf{h}}$ given by

$$\begin{aligned} \mathcal{M}_{\mathbf{h}} &= \begin{pmatrix} m_{\mathbf{h}}^{(11)} & m_{\mathbf{h}}^{(12)} & m_{\mathbf{h}}^{(13)} \\ m_{\mathbf{h}}^{(12)} & m_{\mathbf{h}}^{(22)} & m_{\mathbf{h}}^{(23)} \\ m_{\mathbf{h}}^{(13)} & m_{\mathbf{h}}^{(23)} & m_{\mathbf{h}}^{(33)} \end{pmatrix}, \\ m_{\mathbf{h}}^{(11)} &= \frac{(g_1^2 + g_2^2)}{4} v_d^2 + (Rv_s + 2R_\lambda) \frac{v_s v_u}{2v_d}, \\ m_{\mathbf{h}}^{(12)} &= \frac{(4|\lambda|^2 - g_1^2 - g_2^2)}{4} v_d v_u - R_\lambda v_s - R \frac{v_s^2}{2}, \\ m_{\mathbf{h}}^{(13)} &= |\lambda|^2 v_d v_s - v_u (Rv_s + R_\lambda), \\ m_{\mathbf{h}}^{(22)} &= (2R_\lambda + Rv_s) \frac{v_d v_s}{2v_u} + \frac{(g_1^2 + g_2^2)}{4} v_u^2, \\ m_{\mathbf{h}}^{(23)} &= |\lambda|^2 v_s v_u - (Rv_s + R_\lambda) v_d, \\ m_{\mathbf{h}}^{(33)} &= 2|\kappa|^2 v_s^2 + R_\lambda \frac{v_d v_u}{v_s} + R_\kappa v_s, \end{aligned} \quad (3.22)$$

and one which indicates the mixing of the CP-even and CP-odd states

$$\mathcal{M}_{\mathbf{ah}} = \mathcal{M}_{\mathbf{ha}}^T = \frac{I}{2} \cdot \begin{pmatrix} 0 & 0 & v_s v_u \\ 0 & 0 & v_d v_s \\ -3v_s v_u & -3v_d v_s & 4v_d v_u \end{pmatrix}. \quad (3.23)$$

It can easily be seen that in general the CP-even and the CP-odd Higgs bosons mix. Only for the case $I = 0$, there is no mixing and CP is conserved. $I = 0$ holds for example for real parameters, but some special phase combinations (e.g. $\phi_u = 2\phi_s = \phi_\lambda = \phi_\kappa$) conserve CP as well, at least at tree-level.

In order to simplify the Higgs mass matrix further, the vacuum expectation values v_u and v_d are usually replaced by the two parameters $\tan\beta$ and v . $\tan\beta$ is the ratio of v_u and v_d and v^2 is the sum of the squares

$$\tan\beta = \frac{v_u}{v_d}, \quad v^2 = v_d^2 + v_u^2, \quad \iff \quad v_d = v \cdot \cos\beta, \quad v_u = v \cdot \sin\beta. \quad (3.24)$$

The Goldstone Boson

Applying a basis change of the form

$$\begin{pmatrix} a_d \\ a_u \end{pmatrix} = \begin{pmatrix} -\cos\beta_n & \sin\beta_n \\ \sin\beta_n & \cos\beta_n \end{pmatrix} \begin{pmatrix} G \\ a \end{pmatrix}, \quad (3.25)$$

will enable us to decouple the massless Goldstone boson G from the Higgs sector. The mass matrix can be written in this new basis $\phi'_a = (G, a, a_s)$

$$\mathcal{L}|_{\text{bil,higgs}} = -\frac{1}{2} (\phi'^T_a, \phi'^T_h) \mathcal{M}'_{\text{Higgs}} \begin{pmatrix} \phi'_a \\ \phi'_h \end{pmatrix} = -\frac{1}{2} (\phi'^T_a, \phi'^T_h) \begin{pmatrix} \mathcal{M}'_{\mathbf{a}} & \mathcal{M}'_{\mathbf{ah}} \\ \mathcal{M}'_{\mathbf{ha}} & \mathcal{M}'_{\mathbf{h}} \end{pmatrix} \begin{pmatrix} \phi'_a \\ \phi'_h \end{pmatrix}. \quad (3.26)$$

At Born level the rotation angle β_n is equal to the angle β from the relation $\tan\beta = v_u/v_d$. The distinction, however, is necessary if one wants to perform the renormalization procedure (see Chapter 4), since β is renormalized whereas β_n is not. But for $\beta = \beta_n$ this rotation

allows us to separate the massless Goldstone boson G . The resulting mass matrices are given by

$$\mathcal{M}'_{\mathbf{a}} = \begin{pmatrix} 0 & 0 & 0 \\ 0 & (2R_\lambda + Rv_s)v_s/\sin(2\beta) & (R_\lambda - Rv_s)v \\ 0 & (R_\lambda - Rv_s)v & \cos\beta \sin\beta (R_\lambda + 2Rv_s)\frac{v^2}{v_s} - 3R_\kappa v_s \end{pmatrix} \quad (3.27a)$$

$$\text{and } \mathcal{M}'_{\mathbf{ah}} = (\mathcal{M}'_{\mathbf{ha}})^T = \frac{Iv}{2} \cdot \begin{pmatrix} 0 & 0 & 0 \\ 0 & 0 & v_s \\ -3v_s \sin\beta & -3v_s \cos\beta & 2v \sin(2\beta) \end{pmatrix}. \quad (3.27b)$$

Since the Goldstone boson decouples completely, it is sufficient to consider a 5×5 mass matrix in the basis $(a, a_s, h_d, h_u, h_s)^T$, instead of the 6×6 matrix which includes the Goldstone boson. In the following the prime will be omitted and the 5×5 matrix will be denoted by $\mathcal{M}_{\text{Higgs}}$. It can once again be split into the submatrices $\mathcal{M}_{\mathbf{a}}$ (2×2), $\mathcal{M}_{\mathbf{h}}$ (3×3) and $\mathcal{M}_{\mathbf{ah}}$ (2×3).

Diagonalizing the Mass Matrices

Let \mathcal{R} be the matrix that diagonalizes $\mathcal{M}_{\text{Higgs}}$. Even in the case of the complex NMSSM the mass matrix $\mathcal{M}_{\text{Higgs}}$ is always real and symmetric. Hence, the rotation matrix \mathcal{R} can always be chosen to be a real orthogonal matrix (i.e. $\mathcal{R}^{-1} = \mathcal{R}^T$).

$$\begin{aligned} \mathcal{R} \mathcal{M}_{\text{Higgs}} \mathcal{R}^T &= \text{diag}(m_{h_1}^2, m_{h_2}^2, m_{h_3}^2, m_{h_4}^2, m_{h_5}^2) & \Rightarrow & h_i = \mathcal{R}_{ij} \phi_j & (3.28) \\ \text{with } m_{h_1}^2 \leq m_{h_2}^2 \leq m_{h_3}^2 \leq m_{h_4}^2 \leq m_{h_5}^2 & & \text{and } \phi &= (a, a_s, h_d, h_u, h_s)^T \end{aligned}$$

The mass eigenstates are denoted as h_i , with $i = 1 \dots 5$. The eigenvalues of the mass matrix, which are of course the squares of the tree-level Higgs masses, are ordered by ascending mass. Hence, h_1 is the lightest neutral Higgs boson.

In the case of the real NMSSM, it is convenient to consider only $\mathcal{M}_{\mathbf{a}}$ and $\mathcal{M}_{\mathbf{h}}$ separately. The rotation matrices diagonalizing these will be denoted as \mathcal{Z}_A and \mathcal{Z}_H .

$$\mathcal{Z}_A \mathcal{M}_{\mathbf{a}} (\mathcal{Z}_A)^T = \text{diag}(m_{a_1}^2, m_{a_2}^2) \quad \Rightarrow \quad a_i = (\mathcal{Z}_A)_{ij} (\phi_a)_j \quad \text{with } \phi_a = (a, a_s)^T \quad (3.29a)$$

$$\mathcal{Z}_H \mathcal{M}_{\mathbf{h}} (\mathcal{Z}_H)^T = \text{diag}(m_{h_1}^2, m_{h_2}^2, m_{h_3}^2) \quad \Rightarrow \quad h_i = (\mathcal{Z}_H)_{ij} (\phi_h)_j \quad \text{with } \phi_h = (h_d, h_u, h_s)^T \quad (3.29b)$$

An analytic expression for the eigenvalues of the Higgs mass matrix, as well as for the elements of the mixing matrix, is only available for special parameter regions which allow simplifying assumptions (see [24]). Hence, we resort to calculating the eigenvalues and mixing matrix elements numerically in our analysis.

3.4.4 The Charged Higgs Boson

So far only the neutral Higgs bosons were taken into consideration. The mass matrix for the charged Higgs boson can also be read from the Higgs potential. In the basis $((H_d^-)^*, H_u^+)$ \mathcal{M}_{H^\pm} is given by

$$\mathcal{M}_{H^\pm} = \left[(2R_\lambda + Rv_s)\frac{v_s}{2} + \sin(2\beta) (g_2^2 - 2|\lambda|^2)\frac{v^2}{8} \right] \cdot \begin{pmatrix} \tan\beta & 1 \\ 1 & \cot\beta \end{pmatrix}. \quad (3.30)$$

Here the tadpole relations and the abbreviations defined in Eq. (3.18) were already applied. \mathcal{M}_{H^\pm} can be diagonalized using the real orthogonal rotation matrix

$$\mathcal{Z}_T = \begin{pmatrix} -\cos\beta_n & \sin\beta_n \\ \sin\beta_n & \cos\beta_n \end{pmatrix} \quad \text{with} \quad \begin{pmatrix} (H_d^-)^* \\ H_u^+ \end{pmatrix} = \mathcal{Z}_T \begin{pmatrix} G^+ \\ H^+ \end{pmatrix}. \quad (3.31)$$

As before, the rotation angle β_n equals β at Born level. This leads to a complete decoupling of the charged Goldstone boson G^+ . The mass squared of the charged Higgs boson is

$$M_{H^\pm}^2 = (2R_\lambda + Rv_s)v_s/\sin(2\beta) + (g_2^2 - 2|\lambda|^2)\frac{v^2}{4}. \quad (3.32)$$

3.4.5 Parameters of the Higgs Sector

Since it will be essential to have a good overview of all the parameters appearing in the Higgs sector when calculating higher order corrections the parameter dependencies discussed above will be summarized briefly here. In the special case of the real NMSSM we start out with the following 12 parameters:

$$g_1, g_2, v_u, v_d, v_s, |\kappa|, |\lambda|, |T_\kappa|, |T_\lambda|, m_{H_d}^2, m_{H_u}^2 \quad \text{and} \quad m_s^2. \quad (3.33)$$

There are of course the gauge couplings g_1 and g_2 , then the vacuum expectation values v_u , v_d and v_s and the couplings $|\kappa|$ and $|\lambda|$ defined in the superpotential. And finally, there are the soft SUSY breaking parameters. If the complex NMSSM is considered, there are six additional phases at first sight:

$$\phi_u, \phi_s, \phi_\kappa, \phi_\lambda, \phi_{T_\kappa} \quad \text{and} \quad \phi_{T_\lambda}. \quad (3.34)$$

But not all of these phases appear independently. A closer look at the Higgs mass matrix reveals that only three phase combinations appear in the Higgs sector, namely those in I , I_λ and I_κ , which are

$$\begin{aligned} \phi_I &= \phi_u - 2\phi_s + \phi_\lambda - \phi_\kappa, \\ \phi_{I_\lambda} &= \phi_u + \phi_s + \phi_{T_\lambda} \quad \text{and} \\ \phi_{I_\kappa} &= 3\phi_s + \phi_{T_\kappa}. \end{aligned} \quad (3.35)$$

The tadpole conditions for t_{a_u} and t_{a_s} , however, relate I_λ and I_κ to I . These relations are

$$I_\lambda = -\frac{I}{2}v_s \quad \text{and} \quad I_\kappa = -\frac{3I}{2} \cdot \frac{v_d v_u}{v_s}. \quad (3.36)$$

Hence, the phases are not independent. If ϕ_I is given, ϕ_{I_λ} and ϕ_{I_κ} can be calculated via

$$\begin{aligned} \phi_{I_\lambda} &= -\arcsin\left(v_s \frac{|\lambda||\kappa|}{\sqrt{2}|T_\lambda|} \cdot \sin(\phi_I)\right) \quad \text{and} \\ \phi_{I_\kappa} &= -\arcsin\left(\frac{3}{\sqrt{2}} \cdot \frac{v_d v_u}{v_s} \cdot \frac{|\lambda||\kappa|}{|T_\kappa|} \cdot \sin(\phi_I)\right). \end{aligned} \quad (3.37)$$

Of course, this gives two possible solutions for each of the two phases. Depending on which solution one picks the sign of R_κ and R_λ changes. Consequently, at tree-level it is sufficient to select one physical phase and the signs of R_κ and R_λ as input values. The relevance of the different phases at higher orders will be discussed in Section 4.9.1.

When calculating the higher order corrections later on, we will use a slightly different parameter set than that given in Eq. (3.33). First of all, the soft SUSY breaking masses ($m_{H_u}^2$, $m_{H_d}^2$ and m_s^2) and $|T_\lambda|$ will be replaced by the tadpole parameters (t_{h_d} , t_{h_u} and t_{h_s}) and the mass of the charged Higgs M_{H^\pm} . The substitution rules for this are

$$|T_\lambda| = \left(2v^3 |\lambda|^2 s_{2\beta} c_{\beta-\beta_n}^2 - 4v |\kappa| |\lambda| v_s^2 c_{\beta-\beta_n}^2 c_{\phi_I} - g_2^2 v^3 s_{2\beta} c_{\beta-\beta_n}^2 - 8c_\beta c_{\beta_n}^2 t_{h_u} + 8s_\beta s_{\beta_n}^2 t_{h_d} + 4v M_{H^\pm}^2 s_{2\beta} \right) / \left(4\sqrt{2} v v_s c_{\beta-\beta_n}^2 c_{\phi_{I\lambda}} \right), \quad (3.38a)$$

$$m_{H_d}^2 = \left(-4v |\lambda|^2 v_s^2 c_{\beta-\beta_n}^2 + t_{h_d} (16c_{\beta_n} s_\beta s_{\beta_n} + 8c_\beta c_{\beta_n}^2) - 8c_{\beta_n}^2 s_\beta t_{h_u} + 8v M_{H^\pm}^2 s_\beta^2 + g_1^2 v^3 c_{2\beta} c_{\beta-\beta_n}^2 - g_2^2 v^3 c_{\beta-\beta_n}^2 \right) / \left(8v c_{\beta-\beta_n}^2 \right), \quad (3.38b)$$

$$m_{H_u}^2 = \left(-4v |\lambda|^2 v_s^2 c_{\beta-\beta_n}^2 - 8c_\beta s_{\beta_n}^2 t_{h_d} + t_{h_u} (16c_\beta c_{\beta_n} s_{\beta_n} + 8s_\beta s_{\beta_n}^2) + 8v c_\beta^2 M_{H^\pm}^2 + g_1^2 v^3 c_{2\beta} c_{\beta-\beta_n}^2 - g_2^2 v^3 c_{\beta-\beta_n}^2 \right) / \left(8v c_{\beta-\beta_n}^2 \right), \quad (3.38c)$$

$$m_s^2 = \left(4v^2 |\kappa| |\lambda| v_s^2 s_{2\beta} c_{\beta-\beta_n}^2 c_{\phi_I} + v^2 |\lambda|^2 (-8v_s^2 c_{\beta-\beta_n}^2 + v^2 c_{\beta-\beta_n}^2 - v^2 c_{4\beta} c_{\beta-\beta_n}^2) + 16|\kappa|^2 v_s^4 c_{\beta-\beta_n}^2 - 8\sqrt{2} |T_\kappa| v_s^3 c_{\beta-\beta_n}^2 c_{\phi_{I\kappa}} - g_2^2 v^4 s_{2\beta}^2 c_{\beta-\beta_n}^2 - 16v c_\beta^2 c_{\beta_n}^2 s_\beta t_{h_u} + 16v_s c_{\beta-\beta_n}^2 t_{h_s} - 8v s_\beta s_{2\beta} s_{\beta_n}^2 t_{h_d} + 4v^2 M_{H^\pm}^2 s_{2\beta}^2 \right) / \left(16v_s^2 c_{\beta-\beta_n}^2 \right). \quad (3.38d)$$

For brevity we used $s_x = \sin x$ and $c_x = \cos x$. Also, the distinction between β originating from the ratio of the VEVs and β_n originating from the mixing matrices was kept. Although $\beta_n = \beta$ at tree-level, we will later on introduce counterterms only for β but not for β_n .

Furthermore, the gauge couplings and v can be replaced by the electric charge e and the vector boson masses M_W and M_Z via the following relations:

$$v = \frac{2M_W}{e} \sqrt{1 - \frac{M_W^2}{M_Z^2}}, \quad g_1 = \frac{eM_Z}{M_W} \quad \text{and} \quad g_2 = e / \sqrt{1 - \frac{M_W^2}{M_Z^2}}. \quad (3.39)$$

After these substitutions the Higgs mass matrix remains a function of the following parameters:

$$M_W, M_Z, e, \tan\beta, v_s, |\kappa|, |\lambda|, |T_\kappa|, M_{H^\pm}^2, t_{h_d}, t_{h_u}, t_{h_s} \quad \text{and all phases.} \quad (3.40)$$

3.5 The Neutralino and Chargino Sectors at Tree-Level

After electroweak symmetry breaking all particles with the same electric charge, the same color charge and the same spin mix. This leads to the neutral Higgsinos (\tilde{H}_u^0 , \tilde{H}_d^0 and \tilde{S}) and neutral gauginos (\tilde{W}^0 and \tilde{B}^0) mixing to yield five neutralinos. The mass eigenstates of the neutralinos will be denoted by χ_i^0 ($i = 1 \dots 5$). The neutralino mass part of the Lagrangian is given by

$$\mathcal{L}_{\chi^0 \text{ mass}} = -\frac{1}{2} (\psi^0)^\text{T} \mathcal{M}_{\chi^0} \psi^0 + c.c. \quad \text{with} \quad \psi^0 = \left(\tilde{B}^0, \tilde{W}^0, \tilde{H}_d^0, \tilde{H}_u^0, \tilde{S} \right)^\text{T} \quad (3.41)$$

$$\text{and} \quad \mathcal{M}_{\chi^0} = \begin{pmatrix} M_1 & 0 & -\frac{g_1 v_d}{2} & \frac{g_1 v_u}{2} e^{-i\phi_u} & 0 \\ 0 & M_2 & \frac{g_2 v_d}{2} & -\frac{g_2 v_u}{2} e^{-i\phi_u} & 0 \\ -\frac{g_1 v_d}{2} & \frac{g_2 v_d}{2} & 0 & -\frac{\lambda v_s}{\sqrt{2}} e^{i\phi_s} & -\frac{\lambda v_u}{\sqrt{2}} e^{i\phi_u} \\ \frac{g_1 v_u}{2} e^{-i\phi_u} & -\frac{g_2 v_u}{2} e^{-i\phi_u} & -\frac{\lambda v_s}{\sqrt{2}} e^{i\phi_s} & 0 & -\frac{\lambda v_d}{\sqrt{2}} \\ 0 & 0 & -\frac{\lambda v_u}{\sqrt{2}} e^{i\phi_u} & -\frac{\lambda v_d}{\sqrt{2}} & \sqrt{2} \kappa v_s e^{i\phi_s} \end{pmatrix}. \quad (3.42)$$

M_1 and M_2 are the gaugino soft SUSY breaking mass parameters which were introduced in Eq. (3.4). Note that generally the parameters M_1 , M_2 , as well as λ and κ can be complex. With the relations given in Eq. (3.39) the neutralino mass matrix can be written in terms of the following parameters: M_1 , M_2 , M_Z , M_W , e , $\tan\beta$, λ , κ , v_s , ϕ_u and ϕ_s . Using the basis transformation

$$\psi_i^0 = N_{ji} \chi_j^0 \quad \Rightarrow \quad N^* \mathcal{M}_{\chi^0} N^\dagger = \text{diag} \left(m_{\chi_1^0}, m_{\chi_2^0}, m_{\chi_3^0}, m_{\chi_4^0}, m_{\chi_5^0} \right) \quad (3.43)$$

\mathcal{M}_{χ^0} can be diagonalized. Here N is a unitary matrix. Once again the convention $m_{\chi_i^0} \leq m_{\chi_{i+1}^0}$ is adopted. Since \mathcal{M}_{χ^0} is a fermionic mass matrix⁴, the eigenvalues of the mass matrix correspond to the masses. In general the eigenvalues can of course be negative. This is not really a problem though, since fermions are allowed to have negative masses. If, however, one wants to avoid negative masses, it is possible to do so by redefining the rotational matrix

$$N'_{ij} = \begin{cases} N_{ij} & \text{if } m_{\chi_i^0} \cdot m_{\chi_j^0} > 0 \\ iN_{ij} & \text{if } m_{\chi_i^0} \cdot m_{\chi_j^0} < 0. \end{cases} \quad (3.44)$$

It might be argued that allowing negative masses is advantageous, since in this case the matrix N is real.

Likewise, the charged Higgsinos and charged gauginos mix to form the two charginos. The mass eigenstates of the charginos will be denoted by χ_i^\pm ($i = 1, 2$). The chargino mass part of the Lagrangian is given by

$$\mathcal{L}_{\chi^\pm \text{mass}} = -\frac{1}{2} (\psi^\pm)^\dagger \begin{pmatrix} 0 & \mathcal{M}_{\chi^\pm}^\dagger \\ \mathcal{M}_{\chi^\pm} & 0 \end{pmatrix} \psi^\pm \quad \text{with} \quad \psi^\pm = \left(\tilde{W}^+, \tilde{H}_u^+, \tilde{W}^-, \tilde{H}_d^- \right)^\dagger \quad (3.45)$$

$$\text{and} \quad \mathcal{M}_{\chi^\pm} = \begin{pmatrix} M_2 & \frac{g_2 v_u}{\sqrt{2}} e^{-i\phi_u} \\ \frac{g_2 v_d}{\sqrt{2}} & \frac{\lambda v_s}{\sqrt{2}} e^{i\phi_s} \end{pmatrix}. \quad (3.46)$$

Of course \mathcal{M}_{χ^\pm} can be written as $\mathcal{M}_{\chi^\pm}(M_2, M_W, \tan\beta, \lambda, v_s, \phi_u, \phi_s)$ and it can be diagonalized using two unitary matrices, denoted by U and V

$$U^* \mathcal{M}_{\chi^\pm} V^\dagger = \text{diag} \left(m_{\chi_1^\pm}, m_{\chi_2^\pm} \right) \\ \text{with} \quad \begin{pmatrix} \chi_1^\pm \\ \chi_2^\pm \end{pmatrix} = U \begin{pmatrix} \tilde{W}^\pm \\ \tilde{H}_d^\pm \end{pmatrix} \quad \text{and} \quad \begin{pmatrix} \chi_1^\pm \\ \chi_2^\pm \end{pmatrix} = V \begin{pmatrix} \tilde{W}^\pm \\ \tilde{H}_u^\pm \end{pmatrix}. \quad (3.47)$$

⁴In fact, the neutralinos are Majorana fermions, which is why one rotation matrix is sufficient to diagonalize the neutralino mass matrix.

Renormalization and Calculation of the One-Loop Higgs Boson Masses

In this chapter the renormalization procedure, which has to be performed when calculating the one-loop corrected masses of the neutral Higgs bosons, is explained. First of all, there are some general remarks on renormalization. Then the counterterm formalism and general renormalization conditions are introduced. After presenting a list of all the counterterms necessary for the renormalization of the NMSSM Higgs sector, the methods used to calculate the one-loop masses and the one-loop mixing matrix in terms of the self-energies of the Higgs sector and the counterterms are described in detail. Finally, a renormalization scheme, which fixes the counterterms, is chosen. The one-loop masses and the choice of renormalization scheme are discussed separately for the real and the complex NMSSM.

4.1 General Remarks on Renormalization

When going beyond Born level and considering higher order corrections usually UV-divergent integrals¹ are encountered. However, it turns out that these UV-divergences always cancel each other when relations of observable parameters (i.e. parameters with physical meaning) are considered. The free² parameters in the original Lagrangian, usually referred to as “bare parameters” are at tree-level directly related to measurable quantities, i.e. physical masses and coupling constants. By going to higher orders this direct relation is destroyed due to the divergent loop integrals. To deal with these divergences, one regularizes the divergent integrals by introducing one or several regularization parameters. There are several possible regularization methods:

Pauli-Villar regularization: This is the simplest method. In the Pauli-Villar regularization [25] one argues that the theory is only valid up to a certain scale and therefore introduces a cutoff parameter. So, if the original upper integration limit was infinity, this infinity is simply replaced by a cutoff parameter, which is taken to be fairly large but finite.

¹For a short summary on loop integrals see Appendix B

²In this context “free” means that they are undetermined by the theory.

Although this method is straightforward, it has a considerable flaw: it breaks gauge invariance.

Dimensional Regularization: This is the method usually used in SM calculations, since it preserves Lorentz and gauge invariance. In dimensional regularization [26] the four dimensions of spacetime are extended to $D = 4 - \epsilon$ dimensions and the divergences are expressed as powers of $1/\epsilon$. For supersymmetric calculations, however, this method is not appropriate. By extending the spacetime to D dimensions, additional bosonic degrees of freedom are introduced and supersymmetry is broken thereby.

Dimensional Reduction: This method is a modification of dimensional regularization. The general idea, however, is the same. But instead of considering both the fields and the momenta in D dimensions, only the momenta are treated in D dimensions, while the fields are kept four dimensional. This way dimensional reduction [27] conserves supersymmetry, and is therefore the method of choice for supersymmetric calculations.

The regularization parameters have of course no physical meaning. So, if one wants to predict a physical parameter in terms of other physical parameters, one needs a renormalization procedure which systematically removes parameters with no physical meaning. One possible approach is to first calculate physical quantities in terms of the bare parameters. These equations can be solved for the bare parameters. The expressions for the bare parameters in terms of the physical quantities can be reinserted into the original relations between the physical quantities and the bare parameters. If there are more physical observables than bare parameters this results in relations between the physical quantities or rather a prediction for a physical observable in terms of other observables. If the theory is renormalizable these relations do not depend on the regularization method anymore, i.e. the divergences cancel. Although this approach to renormalization always works it can get really complicated. Therefore a different method which is more formalized is used: the so-called counterterm formalism.

4.1.1 Counterterm Formalism

In the counterterm formalism each bare parameter (e.g. p^{bare}) of the original Lagrangian is split into the so-called “renormalized parameter” p^{ren} , which is finite and a counterterm $\delta^i p$ which contains the divergent part corresponding to the corrections of i^{th} order

$$p^{\text{bare}} = p^{\text{ren}} + \delta^1 p + \delta^2 p + \dots \quad (4.1)$$

Since we only deal with one-loop corrections here, the superscript will be omitted from now on and δp will denote the first order counterterm. Now, one has to choose renormalization conditions which link the renormalized parameters to physical observables by fixing the counterterms. There are different kinds of renormalization conditions. The two types of renormalization conditions that are relevant for this thesis are:

On-Shell Renormalization: Applying on-shell renormalization conditions fixes the counterterms, so that the renormalized parameters are equal to the physical observables to all orders of perturbation theory. So, for example if one of the parameters is a mass, the counterterm δm is chosen so that m^{ren} is equal to the physical mass³. Then δm consists

³Physical mass in this context means that the square of the mass is given by the real part of the momentum squared at which the propagator has its pole.

of a finite and a divergent part. If on-shell renormalization is used for all parameters the result does not depend on the renormalization scale⁴ Q .

$\overline{\text{DR}}$ Renormalization: Only the part of the bare parameter proportional to Δ is absorbed by the counterterm. Δ consists of the divergent part of the bare parameter and the constants γ_E and $\ln 4\pi$:

$$\Delta = \frac{2}{\epsilon} - \gamma_E + \ln 4\pi. \quad (4.2)$$

Here γ_E is the Euler-Mascheroni constant, $\gamma_E \approx 0.5772$. If $\overline{\text{DR}}$ renormalization is used the result still depends on the renormalization scale Q . $\overline{\text{DR}}$ conditions are nevertheless useful when the parameters cannot easily be connected to physical observables or if the observables cannot be measured with good accuracy. The $\overline{\text{DR}}$ renormalization is in principle the same as the $\overline{\text{MS}}$ renormalization, which is usually used in the SM. The only difference is that $\overline{\text{DR}}$ renormalization uses dimensional reduction, whereas $\overline{\text{MS}}$ renormalization uses dimensional regularization.

The choice of the set of independent parameters and renormalization conditions for these parameters is called a renormalization scheme. If the calculations were performed up to all orders, all renormalization schemes would yield the same results. Of course, this is not possible. Therefore the difference between several renormalization schemes is a measure for the theoretical uncertainty due to missing higher order corrections.

Defining the counterterms for all the independent parameters in the Lagrangian is sufficient to obtain finite S-matrix elements. If one, however, also desires finite Green functions the fields have to be renormalized as well. In order to do that, the bare field (e.g. ϕ^{bare}) is replaced by the renormalized field ϕ^{ren} multiplied with the square root of a so-called field renormalization constant Z_ϕ

$$\begin{aligned} \phi^{\text{bare}} &= \sqrt{Z_\phi} \phi^{\text{ren}} = \sqrt{1 + \delta^1 Z_\phi + \delta^2 Z_\phi + \dots} \phi^{\text{ren}} \\ \Rightarrow \phi^{\text{bare}} &= \left(1 + \frac{1}{2} \delta^1 Z_\phi + \frac{1}{8} (\delta^1 Z_\phi)^2 + \frac{1}{2} \delta^2 Z_\phi + \dots \right) \phi^{\text{ren}}. \end{aligned} \quad (4.3)$$

Combining the parameter and field renormalization the bare Lagrangian \mathcal{L}_0 can be split into the renormalized Lagrangian \mathcal{L} and the counterterm Lagrangian $\delta\mathcal{L}$

$$\mathcal{L}_0 = \mathcal{L} + \delta\mathcal{L}. \quad (4.4)$$

The bare Lagrangian and the renormalized Lagrangian are generally of the same form. The only difference is that the former depends on bare parameters, whereas the latter depends on renormalized parameters. Thus, the renormalized Lagrangian is finite and all the divergences of the bare Lagrangian are absorbed into the counterterm Lagrangian.

4.1.2 Renormalization Conditions

As already mentioned above we need renormalization conditions which tell us what parts of the bare parameters are to be absorbed into the counterterms, i.e. these renormalization conditions fix the counterterms. This is usually done by using one-particle irreducible two-point functions. The two-point function is basically equivalent to the inverse propagator. Hence, the statement that the real part of the pole of the propagator is at $p^2 = m^2$, is

⁴Appendix B explains why this scale is introduced.

equivalent to the statement that the real part of the two-point vertex function vanishes if the external momentum p^2 is equal to the mass m^2 . The renormalized⁵ two-point function $\hat{\Gamma}_S$ for a scalar with the physical mass m_S is given by

$$\hat{\Gamma}_S = S \text{---} \text{---} \text{---} \text{---} \text{---} \text{---} \text{---} \text{---} \text{---} S = i(p^2 - m_S^2) + i\hat{\Sigma}_S(p^2). \quad (4.5)$$

Here $\hat{\Sigma}_S(p^2)$ is the renormalized self-energy, which consists of the self-energy $\Sigma_S(p^2)$ creating the UV-divergent loop corrections to the mass m_S and the counterterm part, which includes the counterterm δm_S^2 and the field renormalization constant δZ_S

$$\hat{\Sigma}_S(p^2) = \Sigma_S(p^2) + (p^2 - m_S^2) \delta Z_S - \delta m_S^2. \quad (4.6)$$

The form of $\hat{\Sigma}_S(p^2)$ can be understood, when considering the bare Lagrangian

$$\mathcal{L} = \frac{1}{2}(p^2 - m_S^2)S^2 + \dots, \quad (4.7)$$

and making the replacements

$$m_S^2 \rightarrow m_S^2 + \delta m_S^2 \quad \text{and} \quad S \rightarrow (1 + \frac{1}{2}\delta Z_S)S. \quad (4.8)$$

The counterterms δm_S^2 and δZ_S have to be chosen in such a manner that they cancel the divergences of the loop integrals in the unrenormalized self-energy $\Sigma_S(p^2)$, so that the renormalized self-energy $\hat{\Sigma}(p^2)$ is finite. If m_S^2 is to be renormalized on-shell the renormalization condition reads

$$\text{Re } \hat{\Gamma}_S(m_S^2) \stackrel{!}{=} 0 \quad \Rightarrow \quad \text{Re } \hat{\Sigma}_S(m_S^2) = 0 \quad \Rightarrow \quad \delta m_S^2 = \text{Re } \Sigma_S(m_S^2). \quad (4.9)$$

So, if an on-shell renormalization condition is applied the mass counterterm for a scalar is determined by the real part of the self-energy evaluated at m_S^2 .

Similar relations can be derived for vector bosons and fermions. The two-point function $\hat{\Gamma}_{\mu\nu}^V$ for vector bosons with the mass M_V displays an additional Lorentz structure. In the 't Hooft-Feynman gauge the two-point function reads

$$\hat{\Gamma}_{\mu\nu}^V(p^2) = V_\mu \text{---} \text{---} \text{---} \text{---} \text{---} \text{---} \text{---} V_\nu = -ig_{\mu\nu}(p^2 - M_V^2) - i\hat{\Sigma}_{\mu\nu}^V(p^2). \quad (4.10)$$

The on-shell renormalization condition for vector bosons is given by

$$\text{Re } \hat{\Gamma}_{\mu\nu}^V(p^2)\epsilon^\nu(p^2) \Big|_{p^2=M_V^2} \stackrel{!}{=} 0. \quad (4.11)$$

Here ϵ_ν is the polarization vector. The renormalized self-energy for the vector bosons $\hat{\Sigma}_{\mu\nu}^V(p^2)$ can be split into a transverse and a longitudinal part

$$\hat{\Sigma}_{\mu\nu}^V(p^2) = \left(g_{\mu\nu} - \frac{p_\mu p_\nu}{p^2}\right) \hat{\Sigma}_V^T(p^2) + \frac{p_\mu p_\nu}{p^2} \hat{\Sigma}_V^L(p^2). \quad (4.12)$$

⁵Renormalized parameters are always denoted by a hat.

$\hat{\Sigma}_V^T(p^2)$ and $\hat{\Sigma}_V^L(p^2)$ have the same form as the scalar renormalized self-energy. Thus condition (4.11) together with $p_\nu \epsilon^\nu = 0$ leads to the mass counterterm for the vector bosons

$$\delta M_V^2 = \text{Re} \Sigma_V^T(M_V^2). \quad (4.13)$$

Finally, the two-point function for fermions is given by

$$\hat{\Gamma}_F(p) = F \xrightarrow{p^2} \text{---} \text{---} \text{---} \text{---} \text{---} \text{---} \text{---} \text{---} \text{---} \text{---} \text{---} \xrightarrow{p^2} F = i(\not{p} - m_F) + i\hat{\Sigma}(p). \quad (4.14)$$

The on-shell renormalization condition for fermions with the mass m_F is

$$\text{Re} \hat{\Gamma}_F(p)u(p) \Big|_{p^2=m_F^2} \stackrel{!}{=} 0. \quad (4.15)$$

Here $u(p)$ denotes the spinor. The fermionic self-energy can be written in the following form

$$\hat{\Sigma}(p) = \not{p}\omega_L \hat{\Sigma}_{VL}(p) + \not{p}\omega_R \hat{\Sigma}_{VR}(p) + \omega_L \hat{\Sigma}_{SL}(p) + \omega_R \hat{\Sigma}_{SR}(p), \quad (4.16)$$

where $\omega_L = \frac{1-\gamma_5}{2}$ and $\omega_R = \frac{1+\gamma_5}{2}$ are the left- and right-handed projection operators. $\hat{\Sigma}_{VL}$ and $\hat{\Sigma}_{VR}$ are called the left- and right-handed vectorial self-energies, while $\hat{\Sigma}_{SL}$ and $\hat{\Sigma}_{SR}$ are called the left- and right-handed scalar self-energies⁶. This decomposition can be performed both for the renormalized and the unrenormalized self-energy. The components of the renormalized self-energy can be expressed in terms of the unrenormalized self-energy components, the mass counterterm δm_F and the field renormalization constants⁷ δZ_R and δZ_L

$$\begin{aligned} \hat{\Sigma}_{VL}(p) &= \Sigma_{VL}(p) + \frac{1}{2}(\delta Z_L^* + \delta Z_L), \\ \hat{\Sigma}_{VR}(p) &= \Sigma_{VR}(p) + \frac{1}{2}(\delta Z_R^* + \delta Z_R), \\ \hat{\Sigma}_{SL}(p) &= \Sigma_{SL}(p) - \frac{1}{2}m_F(\delta Z_R + \delta Z_L) - \delta m_F, \\ \hat{\Sigma}_{SR}(p) &= \Sigma_{SR}(p) - \frac{1}{2}m_F(\delta Z_R^* + \delta Z_L^*) - \delta m_F. \end{aligned} \quad (4.18)$$

Using the relations

$$\not{p}\omega_L = \omega_R \not{p}, \quad \not{p}\omega_R = \omega_L \not{p} \quad \text{and} \quad \not{p}u(p) \xrightarrow{p^2 \rightarrow m_F^2} m_F u(m_F^2) \quad (4.19)$$

it can be derived that the mass counterterm has to be fixed to

$$\delta m_F = \frac{1}{2} \left(m_F \text{Re} \Sigma_{VL}(m_F) + m_F \text{Re} \Sigma_{VR}(m_F) + \text{Re} \Sigma_{SL}(m_F) + \text{Re} \Sigma_{SR}(m_F) \right) \quad (4.20)$$

in order to renormalize the fermion mass on-shell.

Note that during this whole discussing of general renormalization conditions, all parameters were taken to be real. The subtleties that arise when working with complex parameters will be considered later on when needed. A nice overview of these general renormalization conditions is given in [28].

⁶“vectorial” and “scalar” might be misleading here. Of course the “vectorial” self-energy is still a scalar.

⁷It is necessary to introduce two field renormalization constants, one for the left-handed field and one for the right-handed field.

4.2 Counterterms in the NMSSM Higgs Sector

When calculating the one-loop Higgs masses the renormalization procedure for the Higgs sector has to be performed. So, all bare parameters appearing in the Higgs mass matrix are split into a renormalized parameter and a counterterm as described in Section 4.1.1. The parameters of the Higgs sector are listed in Eq. (3.40). For real parameters (e.g. the vector boson masses) it is straightforward to introduce one counterterm which is automatically real. For complex parameters (e.g. λ or κ), however, it is possible to introduce either one complex counterterm or two real counterterms. Here we take the latter choice. All complex parameters are split into their absolute value and their phase. Then one real counterterm for the absolute value and one real counterterm for the phase is introduced. All necessary counterterms are listed in Table 4.1. As mentioned earlier only three different phase combinations (ϕ_I, ϕ_{I_λ}

real parameters and absolute values	phases
$e \rightarrow e(1 + \delta Z_e)$	
$M_W^2 \rightarrow M_W^2 + \delta M_W^2$	$\phi_\lambda \rightarrow \phi_\lambda + \delta\phi_\lambda$
$M_Z^2 \rightarrow M_Z^2 + \delta M_Z^2$	$\phi_\kappa \rightarrow \phi_\kappa + \delta\phi_\kappa$
$M_{H^\pm}^2 \rightarrow M_{H^\pm}^2 + \delta M_{H^\pm}^2$	$\phi_{T_\kappa} \rightarrow \phi_{T_\kappa} + \delta\phi_{T_\kappa}$
$t_{h_d} \rightarrow t_{h_d} + \delta t_{h_d}$	$\phi_{T_\lambda} \rightarrow \phi_{T_\lambda} + \delta\phi_{T_\lambda}$
$t_{h_u} \rightarrow t_{h_u} + \delta t_{h_u}$	$\phi_u \rightarrow \phi_u + \delta\phi_u$
$t_{h_s} \rightarrow t_{h_s} + \delta t_{h_s}$	$\phi_s \rightarrow \phi_s + \delta\phi_s$
$ \lambda \rightarrow \lambda + \delta\lambda$	or
$ \kappa \rightarrow \kappa + \delta\kappa$	$\phi_I \rightarrow \phi_I + \delta\phi_I$
$ v_s \rightarrow v_s + \delta v_s$	$t_{a_d} \rightarrow t_{a_d} + \delta t_{a_d}$
$ T_\kappa \rightarrow T_\kappa + \delta T_\kappa$	$t_{a_s} \rightarrow t_{a_s} + \delta t_{a_s}$
$\tan\beta \rightarrow \tan\beta + \delta\tan\beta$	

Table 4.1: Counterterms of the Higgs sector.

and ϕ_{I_κ}) appear in the Higgs sector. Hence, it is sufficient to introduce counterterms for these three phase combinations. Using the tadpole equations for t_{a_d} and t_{a_s} Eq. (3.17) the counterterms $\delta\phi_{I_\lambda}$ and $\delta\phi_{I_\kappa}$ can be replaced by δt_{a_d} and δt_{a_s} . Obviously, $\delta\phi_I, \delta t_{a_d}$ and δt_{a_s} are just functions of the counterterms of the initial six phases.

In order to obtain the counterterm mass matrix $\delta\mathcal{M}_{\text{Higgs}}$ one has to:

1. Express the Higgs mass matrix in terms of the parameters

$$M_W, M_Z, e, \tan\beta, v_s, |\kappa|, |\lambda|, |T_\kappa|, M_{H^\pm}^2, t_{h_d}, t_{h_u}, t_{h_s}, \phi_I, \phi_{I_\lambda} \quad \text{and} \quad \phi_{I_\kappa}. \quad (4.21)$$

The necessary substitution rules for this are given in Eq. (3.38a-3.38d) and Eq. (3.39). Note that it is important to distinguish between β_n coming from the rotation matrices and β coming from the ratio of the VEVs, since in contrast to $\tan\beta_n$, $\tan\beta$ receives a counterterm.

2. Carry out the replacements listed in Table 4.1.

3. Expand around the counterterms and keep only the terms linear in the counterterms. All terms of higher order in the counterterms are only needed for higher order calculations. Thus, we obtain

$$\mathcal{M}_{\text{Higgs}} \rightarrow \mathcal{M}_{\text{Higgs}} + \delta\mathcal{M}_{\text{Higgs}} \quad (4.22)$$

and can read off the counterterm mass matrix $\delta\mathcal{M}_{\text{Higgs}}$.

4. Insert the tree-level relations

$$t_{h_u} = t_{h_d} = t_{h_s} = 0 \quad \text{and} \quad \beta_n = \beta. \quad (4.23)$$

The resulting counterterm mass matrix $\delta\mathcal{M}_{\text{Higgs}}$ is given in Appendix D.

We already mentioned several times that the angle β originating from the ratio of the VEVs is renormalized, whereas the angle β_n appearing in the rotation matrices to separate the charged and neutral Goldstone bosons is not. The reason for this distinction is that the whole renormalization procedure could also be performed for the interaction eigenstates, i.e. before the separation of the Goldstone bosons. But the angle β_n has not even entered the calculation before the separation of the Goldstone bosons, therefore it does not need to be renormalized.

Note, that in the special case of the real NMSSM the counterterm mass matrices $\delta\mathcal{M}_{\mathbf{h}}$ and $\delta\mathcal{M}_{\mathbf{a}}$ are given by

$$\delta\mathcal{M}_{\mathbf{a}} = \begin{pmatrix} \delta\mathcal{M}_{\text{Higgs}} \Big|_{11} & \delta\mathcal{M}_{\text{Higgs}} \Big|_{12} \\ \delta\mathcal{M}_{\text{Higgs}} \Big|_{21} & \delta\mathcal{M}_{\text{Higgs}} \Big|_{22} \end{pmatrix}_{\delta\phi_I = \delta t_{a_d} = \delta t_{a_s} = 0} \quad (4.24a)$$

$$\text{and} \quad \delta\mathcal{M}_{\mathbf{h}} = \begin{pmatrix} \delta\mathcal{M}_{\text{Higgs}} \Big|_{33} & \delta\mathcal{M}_{\text{Higgs}} \Big|_{34} & \delta\mathcal{M}_{\text{Higgs}} \Big|_{35} \\ \delta\mathcal{M}_{\text{Higgs}} \Big|_{43} & \delta\mathcal{M}_{\text{Higgs}} \Big|_{44} & \delta\mathcal{M}_{\text{Higgs}} \Big|_{45} \\ \delta\mathcal{M}_{\text{Higgs}} \Big|_{53} & \delta\mathcal{M}_{\text{Higgs}} \Big|_{54} & \delta\mathcal{M}_{\text{Higgs}} \Big|_{55} \end{pmatrix}_{\delta\phi_I = \delta t_{a_d} = \delta t_{a_s} = 0} \quad (4.24b)$$

The other matrix elements of $\delta\mathcal{M}_{\text{Higgs}}$ vanish in the real case and naturally the counterterms for the phases are not needed.

In addition to the counterterms for the parameters, it is necessary to introduce field renormalization constants. Here we will introduce one single field renormalization constant for each Higgs doublet and one for the singlet field

$$H_d \rightarrow \sqrt{Z_{H_d}} H_d, \quad H_u \rightarrow \sqrt{Z_{H_u}} H_u \quad \text{and} \quad S \rightarrow \sqrt{Z_S} S. \quad (4.25)$$

4.3 One-Loop Higgs Masses in the Real NMSSM

For now we restrict ourselves to the special case of the real NMSSM. Hence, there is no mixing between the CP-even and CP-odd eigenstates and they can be considered separately. In contrast to the simple examples given in Section 4.1.2 the renormalized two-point functions in the Higgs sector are matrices instead of scalars. The renormalized two-point functions for the CP-even and CP-odd Higgs mass eigenstates are

$$\hat{\Gamma}_{\mathbf{h}} = i \begin{pmatrix} p^2 - m_{h_1}^2 + \hat{\Sigma}_{h_1 h_1}(p^2) & \hat{\Sigma}_{h_1 h_2}(p^2) & \hat{\Sigma}_{h_1 h_3}(p^2) \\ \hat{\Sigma}_{h_2 h_1}(p^2) & p^2 - m_{h_2}^2 + \hat{\Sigma}_{h_2 h_2}(p^2) & \hat{\Sigma}_{h_2 h_3}(p^2) \\ \hat{\Sigma}_{h_3 h_1}(p^2) & \hat{\Sigma}_{h_3 h_2}(p^2) & p^2 - m_{h_3}^2 + \hat{\Sigma}_{h_3 h_3}(p^2) \end{pmatrix} \quad (4.26)$$

and

$$\hat{\Gamma}_{\mathbf{a}} = i \begin{pmatrix} p^2 - m_{a_1}^2 + \hat{\Sigma}_{a_1 a_1}(p^2) & \hat{\Sigma}_{a_1 a_2}(p^2) \\ \hat{\Sigma}_{a_2 a_1}(p^2) & p^2 - m_{a_2}^2 + \hat{\Sigma}_{a_2 a_2}(p^2) \end{pmatrix}. \quad (4.27)$$

Here p^2 is the external momentum, m_{h_i} and m_{a_i} are the tree-level masses and $\hat{\Sigma}_{h_i h_j}$ and $\hat{\Sigma}_{a_i a_j}$ are the renormalized self-energies. The matrix valued renormalized self-energy for the CP-even mass eigenstates is given by

$$\hat{\Sigma}_{\mathbf{h}}^{(1)}(p^2) = \Sigma_{\mathbf{h}}^{(1)}(p^2) + \frac{1}{2} p^2 (\delta \tilde{Z}_{\mathbf{h}}^\dagger + \delta \tilde{Z}_{\mathbf{h}}) - \frac{1}{2} (\delta \tilde{Z}_{\mathbf{h}}^\dagger \mathcal{M}_{\mathbf{h}}^{\text{dia}} + \mathcal{M}_{\mathbf{h}}^{\text{dia}} \delta \tilde{Z}_{\mathbf{h}}) - \mathcal{Z}_H \delta \mathcal{M}_{\mathbf{h}} \mathcal{Z}_H^T$$

(4.28)

with $\delta \tilde{Z}_{\mathbf{h}} = \mathcal{Z}_H \begin{pmatrix} \delta Z_{H_d} & 0 & 0 \\ 0 & \delta Z_{H_u} & 0 \\ 0 & 0 & \delta Z_S \end{pmatrix} \mathcal{Z}_H^T$.

Since the field renormalization constants were introduced for the interaction eigenstates, it is necessary to apply the rotation matrix \mathcal{Z}_H , which diagonalizes $\mathcal{M}_{\mathbf{h}}$, to obtain the field renormalization constants $\delta \tilde{Z}_{\mathbf{h}}$ for the mass eigenstates. The unrenormalized self-energy $\Sigma_{h_i h_j}(p^2) = \Sigma_{\mathbf{h}}(p^2)|_{ij}$ can be obtained by calculating all contributing one-loop diagrams with external particles h_i and h_j . The generic diagrams are given in Fig. 4.1. If one inserts the

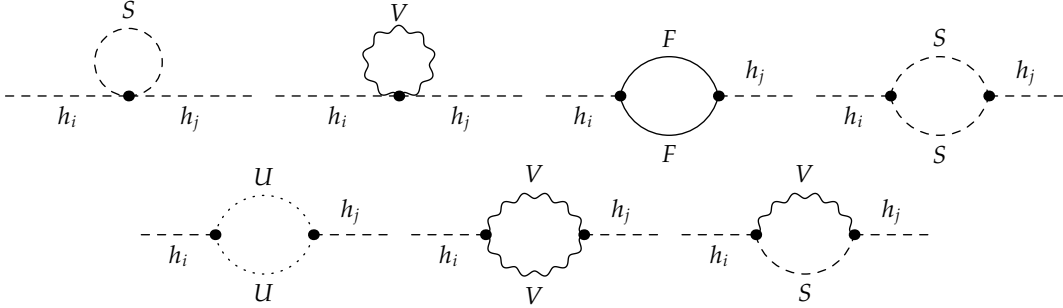


Figure 4.1: Generic diagrams contributing to $\Sigma_{h_i h_j}(p^2)$. There are scalars (S), vector bosons (V), fermions (F) or ghosts (U) in the loop.

particles, this results in a total of 126 diagrams at particle level, which have to be calculated to obtain one component of the self-energy matrix. The one-loop self-energies are calculated analytically in terms of the loop functions A_0 and B_0 (for more details see Appendix B). The particles to be inserted are:

- **scalars (S):** Higgs particles (h_i , a_i and H^\pm), Goldstone bosons (G and G^\pm), sleptons (\tilde{e} and $\tilde{\nu}$) and squarks (\tilde{u} and \tilde{d})
- **vector bosons (V):** Z- and W-bosons (Z and W^\pm)
- **fermions (F):** charged leptons (e), quarks (u and d), neutralinos (χ^0) and charginos (χ^\pm)
- **ghosts (U):** ghost corresponding to the Z- and W-bosons (η_Z and η_\pm)

For the CP-odd Higgs fields the renormalized self-energy is given by

$$\hat{\Sigma}_{\mathbf{a}}^{(1)}(p^2) = \Sigma_{\mathbf{a}}^{(1)}(p^2) + \frac{1}{2} p^2 (\delta \tilde{Z}_{\mathbf{a}}^\dagger + \delta \tilde{Z}_{\mathbf{a}}) - \frac{1}{2} (\delta \tilde{Z}_{\mathbf{a}}^\dagger \mathcal{M}_{\mathbf{a}}^{\text{dia}} + \mathcal{M}_{\mathbf{a}}^{\text{dia}} \delta \tilde{Z}_{\mathbf{a}}) - \mathcal{Z}_A \delta \mathcal{M}_{\mathbf{a}} \mathcal{Z}_A^T$$

(4.29)

with $\delta \tilde{Z}_{\mathbf{a}} = \mathcal{Z}_A \begin{pmatrix} \cos^2 \beta \delta Z_{H_u} + \sin^2 \beta \delta Z_{H_d} & 0 \\ 0 & \delta Z_S \end{pmatrix} \mathcal{Z}_A^T$.

The generic diagrams for $\Sigma_{a_i a_j}$ are the same as for $\Sigma_{h_i h_j}$.

Now that we understand the structure of the two-point functions, it remains to explain how the one-loop masses can be derived from it. Since the two-point function has a matrix structure the physical masses are given by the real part of the roots of the determinant of $\hat{\Gamma}(p^2)$. Since the momentum p^2 appears not only in the diagonal elements, but also as an argument of the self-energies, it is impossible to solve the resulting equations analytically. There are different approximations which can be applied to obtain numerical results.

$p^2 = 0$ Approximation: In this approximation the momentum appearing in the self-energies is set to zero. So, the two-point function for the CP-even fields becomes

$$\hat{\Gamma}_{\mathbf{h}} = i \begin{pmatrix} p^2 - m_{h_1}^2 + \hat{\Sigma}_{h_1 h_1}(0) & \hat{\Sigma}_{h_1 h_2}(0) & \hat{\Sigma}_{h_1 h_3}(0) \\ \hat{\Sigma}_{h_2 h_1}(0) & p^2 - m_{h_2}^2 + \hat{\Sigma}_{h_2 h_2}(0) & \hat{\Sigma}_{h_2 h_3}(0) \\ \hat{\Sigma}_{h_3 h_1}(0) & \hat{\Sigma}_{h_3 h_2}(0) & p^2 - m_{h_3}^2 + \hat{\Sigma}_{h_3 h_3}(0) \end{pmatrix}. \quad (4.30)$$

The condition $\det(\hat{\Gamma}_{\mathbf{h}}(p^2)) = 0$ results in a polynomial cubic in p^2 . The three possible solutions for p^2 are the one-loop masses for the CP-even Higgs fields we have been looking for. This approximation is only suitable if one is interested in the masses of the light Higgs bosons.

On-Shell Approximation: In the on-shell approximation the momentum dependence in the self-energy $\hat{\Sigma}_{h_i h_j}$ is replaced by $\frac{1}{2}(m_{h_i}^2 + m_{h_j}^2)$. This has the convenient effect that the dependence on the field renormalization constants in the renormalized self-energies drops out completely. To avoid complex contributions the real part of $\Sigma_{\mathbf{h}}$ is taken. The condition $\det(\hat{\Gamma}_{\mathbf{h}}(p^2)) = 0$ once again results in a cubic equation for p^2 . In fact solving this equation is the same as determining the eigenvalues of the following matrix

$$\mathcal{M}_{\mathbf{h}}^{\text{dia}} + \mathcal{Z}_H \delta \mathcal{M}_{\mathbf{h}} \mathcal{Z}_H^T - \text{Re} \Sigma_{\mathbf{h}}(p^2) \Big|_{p^2 \rightarrow \frac{1}{2}(m_{h_i}^2 + m_{h_j}^2)}. \quad (4.31)$$

Iterative Approximation: Since this is the most exact approximation of those listed here, this is the one used throughout this thesis. As the name already suggest, an iterative procedure is applied to determine the one-loop masses. Let's say we are interested in the one-loop mass of the k -th Higgs boson. First of all, the p^2 appearing in the self-energies has to be set to a starting value. One possible choice is to set p^2 equal to the tree-level mass ($p^2 = m_{h_k}^2$). Then the k -th eigenvalue $M_{h_k}^2$ of the matrix

$$\mathcal{M}_{\mathbf{h}}^{\text{1loop}} = \mathcal{M}_{\mathbf{h}}^{\text{dia}} - \hat{\Sigma}_{\mathbf{h}}(p^2) \Big|_{p^2 \rightarrow m_{h_k}^2} \quad (4.32)$$

yields the first approximation for the one-loop mass of the k -th Higgs boson. The idea now is to take this first approximation, set p^2 to $M_{h_k}^2$ and once again calculate the k -th eigenvalue of $\mathcal{M}_{\mathbf{h}}^{\text{1loop}}$. However, there is a slight complication because the eigenvalue $M_{H_k}^2$ can be complex. The physical mass is of course given by the square root of the real part of the eigenvalue. But for the iterative procedure we actually keep using the complex value $M_{H_k}^2$. Since `LoopTools` [29], the program used to evaluate the loop functions, is not able to deal with complex arguments in the loop functions, we use the following expansion

$$\mathcal{M}_{\mathbf{h}}^{\text{1loop}} \approx \mathcal{M}_{\mathbf{h}}^{\text{dia}} - \hat{\Sigma}_{\mathbf{h}}\left(\text{Re}(M_{H_k}^2)\right) - i \text{Im}(M_{H_k}^2) \frac{\partial \hat{\Sigma}_{\mathbf{h}}(p^2)}{\partial p^2} \Big|_{p^2 \rightarrow \text{Re}(M_{H_k}^2)} \quad (4.33)$$

Now, the k -th eigenvalue gives a new approximation, which we can reenter into Eq. (4.33). This procedure is repeated until the physical mass remains the same to a certain precision which we chose to be 10^{-9} in our analysis.

Note that all of the above approximations are not strict one-loop calculations. In fact all of them include terms quadratic in the self-energies, which are formally of higher order. All of the above approximations were explained using the example of the CP-even Higgs sector. Of course the procedures for the CP-odd Higgs sector are analogous. Explanations of the different approximations can also be found e.g. in [30] and [31].

4.4 Mixing Matrix Elements at One-Loop in the Real Higgs Sector

The fact that $\hat{\Gamma}_{\mathbf{h}}$ and $\hat{\Gamma}_{\mathbf{a}}$ as given in Eq. (4.26) and Eq. (4.27) are non-diagonal matrices reveals that the tree-level mass eigenstates h_i and a_i mix to the one-loop mass eigenstates H_i and A_j . Since we already know how the interaction eigenstates mix to the tree-level mass eigenstates, the mixing of the interaction eigenstates to the one-loop mass eigenstates can easily be inferred. This mixing shall be described by the mixing matrices $\mathcal{Z}_H^{1\text{-loop}}$ and $\mathcal{Z}_A^{1\text{-loop}}$,

$$\begin{pmatrix} H_1 \\ H_2 \\ H_3 \end{pmatrix} = \mathcal{Z}_H^{1\text{-loop}} \begin{pmatrix} h_d \\ h_u \\ h_s \end{pmatrix} \quad \text{and} \quad \begin{pmatrix} A_1 \\ A_2 \end{pmatrix} = \mathcal{Z}_A^{1\text{-loop}} \begin{pmatrix} a \\ a_s \end{pmatrix}. \quad (4.34)$$

Knowing these mixing matrices is essential, when discussing Higgs phenomenology, as the elements of the mixing matrices are a strong indicator of how a particular Higgs boson couples to the other particles of the model. By construction the Higgs singlet, which is of course an interaction eigenstate, does not couple at all to the gauge bosons or to the quarks and leptons. A Higgs state which is mostly singlet-like can therefore escape detection even if it is light. $(\mathcal{Z}_H^{1\text{-loop}})_{i3}^2$ is a measure for the strength of the singlet component in the i -th CP-even Higgs boson just like $(\mathcal{Z}_A^{1\text{-loop}})_{i2}^2$ is a measure for the strength of the singlet component in the i -th CP-odd Higgs boson.

$p^2 = 0$ Approximation

One way to calculate the mixing matrix is to use the $p^2 = 0$ approximation. Here the one-loop mixing matrices are defined as the matrices that diagonalize the one-loop corrected mass matrices with the external momentum in the one-loop corrections set to zero:

$$\mathcal{Z}_H^{1\text{-loop}} \left(\mathcal{M}_{\mathbf{h}} - (\mathcal{Z}_H)^T \hat{\Sigma}_{\mathbf{h}}(0) \mathcal{Z}_H \right) (\mathcal{Z}_H^{1\text{-loop}})^T = \text{diag}(M_{H_1}^2, M_{H_2}^2, M_{H_3}^2), \quad (4.35a)$$

$$\mathcal{Z}_A^{1\text{-loop}} \left(\mathcal{M}_{\mathbf{a}} - (\mathcal{Z}_A)^T \hat{\Sigma}_{\mathbf{a}}(0) \mathcal{Z}_A \right) (\mathcal{Z}_A^{1\text{-loop}})^T = \text{diag}(M_{A_1}^2, M_{A_2}^2). \quad (4.35b)$$

Setting the external momentum to zero guarantees that the one-loop corrections are real, which in turn leads to an orthogonal mixing matrix. It is obvious that the relation

$$\sum_{i=1}^3 (\mathcal{Z}_H^{1\text{-loop}})_{i3}^2 = 1 \quad (4.36)$$

holds for an orthogonal matrix. This relation is equivalent to the statement that all singlet components of the one-loop mass eigenstates add up to one. The mixing elements obtained in the $p^2 = 0$ approximation are equivalent to those obtained in an effective field approach.

External On-Shell Higgs Bosons

The $p^2 = 0$ approximation does, however, not take care of correctly normalizing the S-matrix. But if one is working with external Higgs bosons this is crucial. The correct normalization can be achieved by finite wave function normalization constants. Having to introduce these here, could be avoided by applying an on-shell scheme to the field renormalization constants instead of the $\overline{\text{DR}}$ renormalization we will use. The formulas to determine the mixing matrices which account for the correct external on-shell properties were taken from [30], where the mixing matrices for the case of two and three mixing particles are derived.

CP-odd Higgs Bosons: As there are two CP-odd Higgs Bosons, we need to consider two particle mixing. Let

$$\hat{\Gamma}_{ij} = i\delta_{ij}(p^2 - m_{a_i}^2) + i\hat{\Sigma}_{ij} \quad \text{with } i, j = a_1, a_2 \quad (4.37)$$

be the renormalized two-point function for the tree-level mass eigenstates a_i going to a_j . To abbreviate the notation the index \mathbf{a} on $\hat{\Sigma}$ and $\hat{\Gamma}$ and their p^2 dependence will be omitted in the following. After inverting the matrix valued two-point function the so-called effective self-energy can be read off the diagonal elements by presuming that the diagonal elements should read

$$(\hat{\Gamma}^{-1})_{ii} = \frac{-i}{p^2 - m_{a_i}^2 + \hat{\Sigma}_{\text{eff},ii}}. \quad (4.38)$$

The effective self-energy is then given by

$$\hat{\Sigma}_{\text{eff},ii} = \hat{\Sigma}_{ii} + i \frac{\hat{\Gamma}_{ij}^2}{\hat{\Gamma}_{jj}}. \quad (4.39)$$

There is no summation over j here. Instead j is given by $j \neq i$ (i.e. if $i = 1$ then $j = 2$ and vice versa). The mixing matrix is given by

$$\left(\mathcal{Z}_A^{1\text{-loop}}\right)_{il} = \sum_{j=1}^2 \sqrt{\hat{Z}_i} \hat{Z}_{ij} (\mathcal{Z}_A)_{jl}. \quad (4.40)$$

With the wave function normalization constants

$$\hat{Z}_i = \left(\frac{1}{1 + \text{Re} \hat{\Sigma}'_{\text{eff},ii}(p^2)} \right) \Big|_{p^2=M_{A_i}^2}, \quad (4.41)$$

$$\hat{Z}_{ij} \stackrel{i \neq j}{=} \left(\frac{-\hat{\Sigma}_{ij}(p^2)}{M_{A_i}^2 - m_{a_j}^2 + \hat{\Sigma}_{jj}(p^2)} \right) \Big|_{p^2=M_{A_i}^2} \quad \text{and} \quad \hat{Z}_{ii} = 1. \quad (4.42)$$

Here $\hat{\Sigma}'_{\text{eff},ii}$ denotes the derivative of the effective self-energy with respect to the external momentum squared which is set to the one-loop mass $M_{A_i}^2$.

CP-even Higgs Bosons: For the CP-even Higgs bosons we have to consider the mixing of three particles. The renormalized two-point function for h_i going to h_j is denoted by

$$\hat{\Gamma}_{ij} = i\delta_{ij}(p^2 - m_{h_i}^2) + i\hat{\Sigma}_{ij} \quad \text{with } i, j = h_1, h_2, h_3. \quad (4.43)$$

In the case of three particle mixing the effective self-energy is slightly more complicated and reads

$$\hat{\Sigma}_{\text{eff},ii} = \hat{\Sigma}_{ii} - i \frac{\hat{\Gamma}_{ij}^2 \hat{\Gamma}_{kk} + \hat{\Gamma}_{ik}^2 \hat{\Gamma}_{jj} - 2\hat{\Gamma}_{ij} \hat{\Gamma}_{ik} \hat{\Gamma}_{jk}}{\hat{\Gamma}_{jk}^2 - \hat{\Gamma}_{jj} \hat{\Gamma}_{kk}}. \quad (4.44)$$

Again there is no summation over any of the indices here. The index i is given and j and k are determined by the demand that all indices need to differ (e.g. $i = 1$ leads to $j = 2$ and $k = 3$ or $j = 3$ and $k = 2$, which one does not matter due to symmetry). The mixing matrix is then given by

$$\left(\mathcal{Z}_H^{1\text{-loop}}\right)_{il} = \sum_{j=1}^3 \sqrt{\hat{Z}_i} \hat{Z}_{ij} (\mathcal{Z}_H)_{jl}. \quad (4.45)$$

With the wave function normalization constants

$$\hat{Z}_i = \left(\frac{1}{1 + \text{Re} \hat{\Sigma}'_{\text{eff},ii}} \right) \Big|_{p^2=M_{H_i}^2}, \quad (4.46)$$

$$\hat{Z}_{ij} \stackrel{i \neq j}{=} \left(\frac{\hat{\Sigma}_{ij}(M_{H_i}^2 - m_{h_k}^2 + \hat{\Sigma}_{kk}) - \hat{\Sigma}_{jk} \hat{\Sigma}_{ki}}{\hat{\Sigma}_{jk}^2 - (M_{H_i}^2 - m_{h_j}^2 + \hat{\Sigma}_{jj})(M_{H_i}^2 - m_{h_k}^2 + \hat{\Sigma}_{kk})} \right) \Big|_{p^2=M_{H_i}^2} \quad \text{and} \quad \hat{Z}_{ii} = 1. \quad (4.47)$$

Note that the mixing matrices determined this way cannot be regarded as rotation matrices, since they are not unitary let alone orthogonal. But still the matrix elements $(\mathcal{Z}_H^{1\text{-loop}})_{i3}^2$ and $(\mathcal{Z}_A^{1\text{-loop}})_{i2}^2$ can be used to determine the singlet component of the one-loop mass eigenstates. However, the relation given in Eq. (4.36) is only fulfilled approximately

$$\sum_{i=1}^3 \left(\mathcal{Z}_H^{1\text{-loop}}\right)_{i3}^2 \approx 1. \quad (4.48)$$

But since the imaginary parts of the mixing matrix determined by the approximation for external on-shell Higgs bosons are relatively small compared to the real part the deviation from the exact relation is small.

4.5 Mixing with the Goldstone Boson at One-Loop

In the two previous sections we always neglected the mixing with the Goldstone boson which takes place at one-loop level when calculating the one-loop masses and mixing matrix elements. To be more precise we neglected the mixing of the CP-odd Higgs bosons with the Goldstone boson. Since CP is conserved in the real NMSSM, the CP-even Higgs bosons do

not mix with the Goldstone boson. But for the CP-odd Higgs bosons we should really have considered the 3×3 two-point function

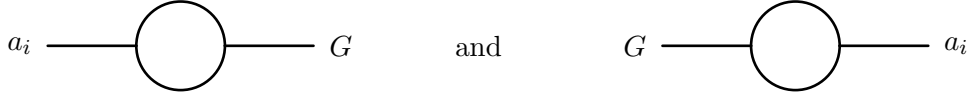
$$\hat{\Gamma}_{G,\mathbf{a}} = i \begin{pmatrix} p^2 + \hat{\Sigma}_{GG} & \hat{\Sigma}_{Ga_1} & \hat{\Sigma}_{Ga_2} \\ \hat{\Sigma}_{a_1G} & p^2 - m_{a_1}^2 + \hat{\Sigma}_{a_1a_1}(p^2) & \hat{\Sigma}_{a_1a_2}(p^2) \\ \hat{\Sigma}_{a_2G} & \hat{\Sigma}_{a_2a_1}(p^2) & p^2 - m_{a_2}^2 + \hat{\Sigma}_{a_2a_2}(p^2) \end{pmatrix}, \quad (4.49)$$

in the basis (G, a_1, a_2) . The additional subscript G indicates that the respective 3×3 matrix is considered. The renormalized self-energy in this case is given by

$$\hat{\Sigma}_{G,\mathbf{a}}^{(1)}(p^2) = \Sigma_{G,\mathbf{a}}^{(1)}(p^2) + \frac{1}{2}p^2 \left(\delta\tilde{Z}_{G,\mathbf{a}}^\dagger + \delta\tilde{Z}_{G,\mathbf{a}} \right) - \frac{1}{2} \left(\delta\tilde{Z}_{G,\mathbf{a}}^\dagger \mathcal{M}_{G,\mathbf{a}}^{\text{dia}} + \mathcal{M}_{G,\mathbf{a}}^{\text{dia}} \delta\tilde{Z}_{G,\mathbf{a}} \right) - \mathcal{Z}_A \delta\mathcal{M}_{G,\mathbf{a}} \mathcal{Z}_A^T$$

with $\delta\tilde{Z}_{G,\mathbf{a}} = \mathcal{Z}_A \begin{pmatrix} c_\beta^2 \delta Z_{H_d} + s_\beta^2 \delta Z_{H_u} & s_\beta c_\beta (\delta Z_{H_u} - \delta Z_{H_d}) & 0 \\ s_\beta c_\beta (\delta Z_{H_u} - \delta Z_{H_d}) & s_\beta^2 \delta Z_{H_d} + c_\beta^2 \delta Z_{H_u} & 0 \\ 0 & 0 & \delta Z_S \end{pmatrix} \mathcal{Z}_A^T. \quad (4.50)$

So, on the one hand the mixing occurs due to contributions of one-loop diagrams such as



with any particles in the loop. On the other hand we argued that the Goldstone boson decouples since the first row and the first column of $\mathcal{M}_{\mathbf{a}}$ (see Eq.(3.27a)) vanish after applying the rotation with the angle β_n . However, this is only the case if the tree-level relations $\beta_n = \beta$, $t_{h_d} = t_{h_u} = t_{h_s} = 0$ are inserted. Before these relations are inserted the element of the mass matrix that describes the mixing of the Goldstone boson G and the interaction eigenstate a reads

$$\mathcal{M}_{G,\mathbf{a}} \Big|_{12} = \frac{M_W^2 s_{2\Delta\beta}}{2} \left(1 - \frac{s_{\theta_W}^2 \lambda^2}{e^2} \right) - M_{H^\pm}^2 t_{\Delta\beta} + \frac{e}{2M_W s_{\theta_W} c_{\Delta\beta}} \left(t_{h_u} c_{\beta_n} - t_{h_d} s_{\beta_n} \right), \quad (4.51)$$

where we used the abbreviations $\sin x = s_x$, $\cos x = c_x$, $\tan x = t_x$ and $\Delta\beta = \beta - \beta_n$. The Weinberg angle θ_W is given by $\cos \theta_W = M_Z/M_W$. It can easily be seen that the above expression vanishes at tree-level. If we now perform the expansion around the counterterms and then plug in the simplifying tree-level relations, we obtain

$$\delta\mathcal{M}_{G,\mathbf{a}} \Big|_{12} = \delta \tan \beta c_\beta^2 \left[M_W^2 \left(1 - \frac{2s_{\theta_W}^2 \lambda^2}{e^2} \right) - M_{H^\pm}^2 \right] + \frac{e}{2M_W s_{\theta_W}} \left(\delta t_{h_u} c_\beta - \delta t_{h_d} s_\beta \right). \quad (4.52)$$

The other elements of $\delta\mathcal{M}_{G,\mathbf{a}}$ can be derived accordingly.

These mixing terms were not presented in Section 4.3, since including them only led to minor changes in the one-loop masses. Actually, the effect was less than 10^{-4} . Therefore, although implemented, these terms were neglected in the standard calculation. The fact that they are so small is not really a surprise as this is already known for the MSSM.

4.6 Renormalization Schemes for the Real Higgs Sector

Before we can actually calculate the one-loop masses and mixing matrix elements, it is necessary to fix the counterterms. In other words: we need to adopt a renormalization scheme, which defines renormalization conditions for the twelve counterterms of the real Higgs sector. The main renormalization scheme we use is a scheme that mixes on-shell and $\overline{\text{DR}}$ renormalization conditions, therefore it is referred to as “mixed scheme”. To get a grasp on the theoretical uncertainties a pure on-shell scheme and a pure $\overline{\text{DR}}$ scheme were implemented as well for comparison. The different schemes will be described in more detail in the following. The renormalization procedures presented here are inspired by the procedures used for the renormalization of the Higgs sector, as well as of the neutralino and chargino sectors as performed for the MSSM in [32] and [33].

4.6.1 Mixed Renormalization Scheme

In the mixed scheme the parameters with a clear physical meaning are renormalized on-shell, whereas the parameters which cannot be linked to a physical observable straightaway are renormalized using $\overline{\text{DR}}$ conditions.

$$\underbrace{e, M_W, M_Z, M_{H^\pm}, t_{h_d}, t_{h_u}, t_{h_s}}_{\text{on-shell}}, \underbrace{\lambda, \kappa, v_s, T_\kappa, \tan\beta}_{\overline{\text{DR}}} \quad (4.53)$$

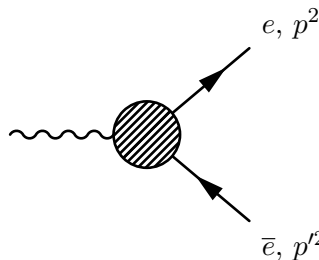
From the twelve parameters which need to be renormalized in the real Higgs sector seven can be linked to physical observables and are therefore renormalized on-shell. These parameters are: the electric charge, the vector boson masses M_Z and M_W , the mass of the charged Higgs boson and the tadpole parameters t_{h_d} , t_{h_u} and t_{h_s} . Hence, we are left with five parameters to be $\overline{\text{DR}}$ renormalized, see Eq. (4.53). To fix these five $\overline{\text{DR}}$ counterterms it would be sufficient to employ renormalization conditions solely from the Higgs sector. But in order to have a nontrivial crosscheck we will use renormalization conditions from the Higgs, the neutralino and the chargino sector. For convenience the parameters which are renormalized on-shell are taken to be on-shell input parameters, whereas the parameters which are $\overline{\text{DR}}$ renormalized are taken to be $\overline{\text{DR}}$ input parameters.

Charge Renormalization

The charge counterterm is chosen so that the corrections to the electron-electron-photon vertex vanish for on-shell external particles, i.e. vanishing photon momentum. This is the so-called Thomson limit. The renormalization condition

$$\bar{u}(p)\hat{\Gamma}_\mu^{Ae\bar{e}}(p,p')u(p')\Big|_{p^2=p'^2=m_e^2} = e\bar{u}(p)\gamma_\mu u(p')\Big|_{p^2=p'^2=m_e^2}, \quad (4.54)$$

with

$$\hat{\Gamma}_\mu^{Ae\bar{e}}(p,p') = A_\mu \text{ (diagram)} \quad (4.55)$$


do not need to be considered in the Higgs self-energies. Note that the one-loop corrections are given in terms of the mass eigenstates, whereas the tadpole parameters are given in terms of the interaction eigenstates. Hence, the rotation matrix appears in the renormalization conditions

$$\begin{pmatrix} \delta t_{h_d} \\ \delta t_{h_u} \\ \delta t_{h_s} \end{pmatrix} = (\mathcal{Z}_H)^T \begin{pmatrix} T_{h_1} \\ T_{h_2} \\ T_{h_3} \end{pmatrix}. \quad (4.64)$$

Field Renormalization Constants

The field renormalization constants are renormalized in the $\overline{\text{DR}}$ scheme to circumvent unphysically large corrections, since in the MSSM this has proven to be numerically stable even close to thresholds [30, 32, 34]. They are chosen so that the residua of the poles of the propagators of the CP-even Higgs fields are set to one. This is equivalent to the demand that the derivative of the renormalized self-energy with respect to the momentum squared vanishes on-shell (i.e. $p^2 = m_{h_i}^2$). Since we renormalize the field renormalization constants in the $\overline{\text{DR}}$ scheme we only take the divergent part

$$\text{Re} \left(\frac{\partial \hat{\Sigma}_{h_i h_i}(p^2)}{\partial p^2} \right) \Big|_{p^2=m_{h_i}^2}^{\text{div}} = 0. \quad (4.65)$$

With the renormalized self-energies as given in Eq. (4.28) this yields the following three equations

$$\text{Re} \left(\frac{\partial \Sigma_{h_i h_i}(p^2)}{\partial p^2} \right) \Big|_{p^2=m_{h_i}^2}^{\text{div}} + |(\mathcal{Z}_H)_{i1}|^2 \delta Z_{H_d} + |(\mathcal{Z}_H)_{i2}|^2 \delta Z_{H_u} + |(\mathcal{Z}_H)_{i3}|^2 \delta Z_S = 0 \quad (4.66)$$

with $i = 1, 2, 3$. The field renormalization constants can be obtained by solving these equations for δZ_{H_u} , δZ_{H_d} and δZ_S and then taking the divergent part only.

The Counterterm $\delta \tan \beta$

The counterterm $\delta \tan \beta$ is fixed using the $\overline{\text{DR}}$ -scheme. Since $\tan \beta$ was introduced as the ratio of the VEVs v_u and v_d , it is apparent that

$$\delta \tan \beta = \tan \beta \left(\frac{1}{2} (\delta Z_{H_u} - \delta Z_{H_d}) + \frac{\delta v_u}{v_u} - \frac{\delta v_d}{v_d} \right) \Big|_{\text{div}}. \quad (4.67)$$

The divergent parts $\frac{\delta v_u}{v_u} \Big|_{\text{div}}$ and $\frac{\delta v_d}{v_d} \Big|_{\text{div}}$ are equal as shown for the MSSM in [35, 36]. Hence these two terms cancel and we are left with

$$\delta \tan \beta = \frac{1}{2} \tan \beta (\delta Z_{H_u} - \delta Z_{H_d}) \Big|_{\text{div}}. \quad (4.68)$$

So, $\delta \tan \beta$ is determined by the field renormalization constants which in turn are given by the solution to Eq. (4.66).

The Counterterm $\delta\lambda$

To fix $\delta\lambda$ we search for an entry in the Higgs mass matrices $\mathcal{M}_{\mathbf{h}}$ and $\mathcal{M}_{\mathbf{a}}$ in which λ appears as isolated as possible. The (1,1) entry of $\mathcal{M}_{\mathbf{a}}$ fulfills this requirement

$$\mathcal{M}_{\mathbf{a}}\Big|_{11} \equiv M_{a,a}^2 = M_{H^\pm}^2 - M_W^2 + \frac{2\lambda^2 M_W^2}{e^2} \left(1 - \frac{M_W^2}{M_Z^2}\right). \quad (4.69)$$

Although this is an interaction eigenstate, one can still apply the renormalization condition for scalars given in Eq. (4.9)

$$\delta M_{a,a}^2 = \text{Re} \Sigma_{a,a}(M_{a,a}^2). \quad (4.70)$$

Here $\Sigma_{a,a}$ is the self-energy in the interaction eigenstates. The Feynman rules being given in mass eigenstates implies that we usually obtain the self-energies in the basis of the mass eigenstates (denoted as $\Sigma_{\mathbf{a}}$ for the CP-odd Higgs fields). But these two are related by

$$\Sigma_{a,a} = \left((\mathcal{Z}_A)^T \Sigma_{\mathbf{a}} \mathcal{Z}_A \right)\Big|_{11}. \quad (4.71)$$

The counterterm $\delta M_{a,a}$ can be expressed in terms of the counterterms δM_{H^\pm} , δZ_e , δM_W^2 and δM_Z^2 (see Eq. (D.3)), all of which were already determined in the renormalization conditions above. Eventually this provides an expression for $\delta\lambda$ in terms of the already known counterterms and the self-energies of the CP-odd Higgs sector:

$$\delta\lambda = \frac{1}{4\lambda M_W^2 \sin^2\theta_W} \left[e^2 \left((\mathcal{Z}_A)^T \text{Re} \Sigma_{\mathbf{a}}(M_{a,a}^2) \mathcal{Z}_A \right)\Big|_{11} - e^2 \delta M_{H^\pm}^2 + 4\lambda^2 M_W^2 \sin^2\theta_W \delta Z_e + \left. \left(e^2 - 2\lambda^2(1 - 2\cos^2\theta_W) \right) \delta M_W^2 - 2\lambda^2 \cos^4\theta_W \delta M_Z^2 \right]_{\text{div}} \quad (4.72)$$

Since λ is to be $\overline{\text{DR}}$ renormalized, we only take the divergent part as indicated by the subscript div .

The Counterterm δv_s

Applying the renormalization condition for fermions given in Eq. (4.20) to the counterterm of the (2,2) element of the chargino mass matrix (see Eq. (3.46)) fixes δv_s . The counterterm of the (2,2) entry of the chargino mass matrix is given by

$$\delta \mathcal{M}_{\chi^\pm}\Big|_{22} \equiv \delta m_{\chi_{22}^\pm} = \delta \left(\frac{\lambda v_s}{\sqrt{2}} \right). \quad (4.73)$$

Solving for δv_s and taking only the divergent part results in

$$\delta v_s = \left(\frac{\sqrt{2}}{\lambda} \delta m_{\chi_{22}^\pm} - \frac{v_s}{\lambda} \delta\lambda \right)\Big|_{\text{div}}, \quad (4.74)$$

where $\delta m_{\chi_{22}^\pm}$ is given by

$$\delta m_{\chi_{22}^\pm} = \frac{1}{2} \left(m_{\chi_{22}^\pm} \text{Re} \Sigma_{\chi_{22}^\pm}^{\text{VL}}(m_{\chi_{22}^\pm}) + m_{\chi_{22}^\pm} \text{Re} \Sigma_{\chi_{22}^\pm}^{\text{VR}}(m_{\chi_{22}^\pm}) + \text{Re} \Sigma_{\chi_{22}^\pm}^{\text{SL}}(m_{\chi_{22}^\pm}) + \text{Re} \Sigma_{\chi_{22}^\pm}^{\text{SR}}(m_{\chi_{22}^\pm}) \right). \quad (4.75)$$

The self-energies $\Sigma_{\chi_{22}^{\pm}}^{\text{VL}}$, $\Sigma_{\chi_{22}^{\pm}}^{\text{VR}}$, $\Sigma_{\chi_{22}^{\pm}}^{\text{SL}}$ and $\Sigma_{\chi_{22}^{\pm}}^{\text{SR}}$ are once again in the basis of the interaction eigenstates. The following relations link them to the self-energies of the mass eigenstates:

$$\Sigma_{\chi_{22}^{\pm}}^{\text{VL}} = \Sigma_{\chi^{\pm},\text{int}}^{\text{VL}} \Big|_{22} = \left(V^{\dagger} \Sigma_{\chi^{\pm},\text{mass}}^{\text{VL}} V \right) \Big|_{22}, \quad (4.76a)$$

$$\Sigma_{\chi_{22}^{\pm}}^{\text{VR}} = \Sigma_{\chi^{\pm},\text{int}}^{\text{VR}} \Big|_{22} = \left(U^{\text{T}} \Sigma_{\chi^{\pm},\text{mass}}^{\text{VR}} U^* \right) \Big|_{22}, \quad (4.76b)$$

$$\Sigma_{\chi_{22}^{\pm}}^{\text{SL}} = \Sigma_{\chi^{\pm},\text{int}}^{\text{SL}} \Big|_{22} = \left(U^{\text{T}} \Sigma_{\chi^{\pm},\text{mass}}^{\text{SL}} V \right) \Big|_{22}, \quad (4.76c)$$

$$\Sigma_{\chi_{22}^{\pm}}^{\text{SR}} = \Sigma_{\chi^{\pm},\text{int}}^{\text{SR}} \Big|_{22} = \left(V^{\dagger} \Sigma_{\chi^{\pm},\text{mass}}^{\text{SR}} U^* \right) \Big|_{22}. \quad (4.76d)$$

Here the matrices U and V are the unitary matrices introduced in Section 3.5 to diagonalize the chargino mass matrix. $\Sigma_{\chi^{\pm},\text{int}}$ is the 2×2 chargino self-energy matrix the basis of the interaction eigenstates, whereas $\Sigma_{\chi^{\pm},\text{mass}}$ is the 2×2 chargino self-energy matrix in the basis of the mass eigenstates.

Thus, if the four self-energies of the chargino sector are known, the counterterm δv_s is known, as $\delta\lambda$ has already been determined.

The Counterterm $\delta\kappa$

The neutralino sector offers a nice solution to fix $\delta\kappa$. The (5,5) entry of the neutralino mass matrix depends only on κ and v_s

$$\mathcal{M}_{\chi^0} \Big|_{55} \equiv m_{\chi_{55}^0} = \sqrt{2}\kappa v_s. \quad (4.77)$$

We choose to fix $\delta m_{\chi_{55}^0}$ by the renormalization condition for fermions

$$\delta m_{\chi_{55}^0} = \frac{1}{2} \left(m_{\chi_{55}^0} \text{Re} \Sigma_{\chi_{55}^0}^{\text{VL}}(m_{\chi_{55}^0}) + m_{\chi_{55}^0} \text{Re} \Sigma_{\chi_{55}^0}^{\text{VR}}(m_{\chi_{55}^0}) + \text{Re} \Sigma_{\chi_{55}^0}^{\text{SL}}(m_{\chi_{55}^0}) + \text{Re} \Sigma_{\chi_{55}^0}^{\text{SR}}(m_{\chi_{55}^0}) \right) \quad (4.78)$$

where

$$\begin{aligned} \Sigma_{\chi_{55}^0}^J &= \Sigma_{\chi^0,\text{int}}^J \Big|_{55} = \left(N^{\dagger} \Sigma_{\chi^0,\text{mass}}^J N \right) \Big|_{55} & \text{for } J = \text{VL, SR} \\ \Sigma_{\chi_{55}^0}^J &= \Sigma_{\chi^0,\text{int}}^J \Big|_{55} = \left(N^{\text{T}} \Sigma_{\chi^0,\text{mass}}^J N^* \right) \Big|_{55} & \text{for } J = \text{VR, SL}. \end{aligned} \quad (4.79)$$

Here N is the unitary matrix introduced in Section 3.5 to diagonalize the neutralino mass matrix. Since there are 5 neutralinos in the NMSSM the self-energy is a 5×5 matrix. The counterterm $\delta\kappa$ is given in terms of the already known counterterms δv_s and $\delta m_{\chi_{55}^0}$, with the latter depending on the 25 self-energies of the neutralino sector:

$$\delta\kappa = \left(\frac{1}{\sqrt{2}v_s} \delta m_{\chi_{55}^0} - \frac{\kappa}{v_s} \delta v_s \right) \Big|_{\text{div}} \quad (4.80)$$

The Counterterm δT_{κ}

Finally, the only counterterm left to fix is δT_{κ} . T_{κ} was introduced as the trilinear SUSY breaking parameter in Eq. (3.4). It appears only in combination with the Higgs singlet field. Hence, we are left with two options: either fix $\delta\mathcal{M}_{\mathbf{a}} \Big|_{22}$ or $\delta\mathcal{M}_{\mathbf{h}} \Big|_{33}$, i.e. the singlet components

of the CP-odd or CP-even fields. They are given in Eq. (D.8) and Eq. (D.17), respectively. Unfortunately both expressions are very lengthy. Here we choose to fix $\delta\mathcal{M}_{\mathbf{a}}|_{22}$ by

$$\delta\mathcal{M}_{\mathbf{a}}|_{22} \equiv \delta M_{a_s, a_s}^2 = \left((\mathcal{Z}_A)^T \Sigma_{\mathbf{a}}(M_{a_s, a_s}^2) \mathcal{Z}_A \right) \Big|_{22}. \quad (4.81)$$

Solving this equation for δT_κ and taking only the divergent part yields the last missing counterterm

$$\delta T_\kappa = \left\{ -\frac{\sqrt{2}}{3v_s} \left[\left((\mathcal{Z}_A)^T \Sigma_{\mathbf{a}}(M_{a_s, a_s}^2) \mathcal{Z}_A \right) \Big|_{22} - \delta f \right] - T_\kappa \frac{\delta v_s}{v_s} \right\} \Big|_{\text{div}}, \quad (4.82)$$

with

$$\begin{aligned} f = & \frac{t_{h_s}}{v_s} - \frac{2M_W s_{\theta_W} s_\beta c_\beta^2 c_{\beta_n}^2}{e v_s^2 c_{\Delta\beta}^2} [t_{h_u} + t_{h_d} t_\beta t_{\beta_n}^2] + \frac{M_W^2 s_{\theta_W}^2 s_{2\beta}^2}{e^2 v_s^2 c_{\Delta\beta}^2} [M_{H^\pm}^2 - M_W^2 c_{\Delta\beta}^2] \\ & + \frac{\lambda M_W^2 s_{\theta_W}^2 s_{2\beta}}{e^4 v_s^2} [2\lambda M_W^2 s_{\theta_W}^2 s_{2\beta} + 3\kappa e^2 v_s^2], \end{aligned} \quad (4.83)$$

where $\Delta\beta = \beta - \beta_n$.

4.6.2 $\overline{\text{DR}}$ Renormalization Scheme

The $\overline{\text{DR}}$ renormalization scheme uses the same renormalization conditions as the mixed scheme with the only difference that the finite parts of all counterterms are discarded. Now, if one takes the experimentally determined values for the electric charge and the vector boson masses as input values, these are in fact on-shell values. But since we now use $\overline{\text{DR}}$ conditions for these parameters we need to convert the on-shell input values to $\overline{\text{DR}}$ input values. The same applies to the tadpole parameters and the mass of the charged Higgs boson. They also need to be converted, if we want to compare the mixed renormalization scheme, where they were taken to be on-shell input values, to the $\overline{\text{DR}}$ scheme. The bare parameter p can either be split into an on-shell parameter p^{OS} and an on-shell counterterm δp^{OS} or into a $\overline{\text{DR}}$ parameter $p^{\overline{\text{DR}}}$ and a $\overline{\text{DR}}$ counterterm $\delta p^{\overline{\text{DR}}}$. The on-shell counterterm δp^{OS} also includes a finite part, whereas the $\overline{\text{DR}}$ counterterm $\delta p^{\overline{\text{DR}}}$ consists only of a divergent part

$$p = p^{\text{OS}} + \delta p^{\text{OS}} = p^{\overline{\text{DR}}} + \delta p^{\overline{\text{DR}}}. \quad (4.84)$$

Since the divergent parts of the on-shell and $\overline{\text{DR}}$ counterterms are equal ($\delta p^{\text{OS}}|_{\text{div}} = \delta p^{\overline{\text{DR}}}|_{\text{div}}$), this leads to the following relation to convert an on-shell input to a $\overline{\text{DR}}$ input

$$p^{\overline{\text{DR}}} = p^{\text{OS}} + \delta p^{\text{OS}}|_{\text{fin}} \quad (4.85)$$

The input conversion enters the calculation of the one-loop Higgs masses in the Higgs mass matrix. As described in Section 4.3 the one-loop masses are calculated starting from

$$\mathcal{M}_{\mathbf{h}}^{\text{1loop}} = \mathcal{Z}_H \mathcal{M}_{\mathbf{h}} (\mathcal{Z}_H)^T - \hat{\Sigma}_{\mathbf{h}}(p^2). \quad (4.86)$$

The mass matrix $\mathcal{M}_{\mathbf{h}}$ depends on the twelve parameters of the Higgs sector. Since all of these parameters are renormalized in the $\overline{\text{DR}}$ scheme the $\overline{\text{DR}}$ values need to be entered to obtain the numerical mass matrix

$$\mathcal{M}_{\mathbf{h}}(e^{\overline{\text{DR}}}, M_W^{\overline{\text{DR}}}, M_Z^{\overline{\text{DR}}}, M_{H^\pm}^{\overline{\text{DR}}}, t_{h_d}^{\overline{\text{DR}}}, t_{h_u}^{\overline{\text{DR}}}, t_{h_s}^{\overline{\text{DR}}}, \lambda^{\overline{\text{DR}}}, \kappa^{\overline{\text{DR}}}, v_s^{\overline{\text{DR}}}, T_\kappa^{\overline{\text{DR}}}, \tan\beta^{\overline{\text{DR}}}). \quad (4.87)$$

As mentioned above the on-shell values for e , M_W , M_Z , M_{H^\pm} , t_{h_d} , t_{h_u} and t_{h_s} have to be converted to $\overline{\text{DR}}$ input values.

4.6.3 On-Shell Renormalization Scheme

In the on-shell scheme all parameters except $\tan\beta$ are renormalized on-shell. For $\tan\beta$ the same $\overline{\text{DR}}$ renormalization condition as in the mixed scheme is used

$$\delta\tan\beta = \frac{1}{2}\tan\beta\left(\delta Z_{H_u} - \delta Z_{H_d}\right)\Big|_{\text{div}} \quad (4.88)$$

to avoid unphysically large corrections close to threshold. The field renormalization constant are also $\overline{\text{DR}}$ renormalized as in Eq. (4.66). Furthermore, we can reuse the following on-shell renormalization conditions from the mixed scheme:

$$\begin{aligned} \delta M_W^2 &= \text{Re } \Sigma_W^{\text{T}}(M_W^2), & \delta M_Z^2 &= \text{Re } \Sigma_Z^{\text{T}}(M_Z^2), & \delta M_{H^\pm}^2 &= \text{Re } \Sigma_{H^\pm}(M_{H^\pm}^2), \\ \delta Z_e &= \frac{1}{2} \frac{\partial \Sigma_{AA}^{\text{T}}(p^2)}{\partial p^2} \Big|_{p^2=0} + \frac{\sin\theta_W}{\cos\theta_W} \frac{\Sigma_{AZ}^{\text{T}}(0)}{M_Z^2} & \text{and} & & \begin{pmatrix} \delta t_{h_d} \\ \delta t_{h_u} \\ \delta t_{h_s} \end{pmatrix} &= (\mathcal{Z}_H)^{\text{T}} \begin{pmatrix} T_{h_1} \\ T_{h_2} \\ T_{h_3} \end{pmatrix}. \end{aligned} \quad (4.89)$$

Now, we have to find on-shell renormalization conditions for the five parameters which were $\overline{\text{DR}}$ renormalized in the mixed scheme. On-shell renormalization conditions are applied to mass eigenstates, in contrast to the interaction eigenstates we used for the $\overline{\text{DR}}$ renormalization. If we once again include conditions originating from the chargino and neutralino sectors, the counterterms for the soft SUSY breaking gaugino masses M_1 and M_2 will enter the equations as well. So, we need to find a set of equations to solve for the six counterterms: $\delta\lambda$, $\delta\kappa$, δT_κ , δv_s , δM_1 and δM_2 . We choose to renormalize the two CP-odd Higgs bosons, both charginos and the two lightest neutralinos on-shell. The renormalization conditions then read:

$$\begin{aligned} \left(\mathcal{Z}_A \delta\mathcal{M}_{\mathbf{a}} (\mathcal{Z}_A)^{\text{T}}\right)\Big|_{11} &= \text{Re } \Sigma_{a_1 a_1}(m_{a_1}^2), & \left(\mathcal{Z}_A \delta\mathcal{M}_{\mathbf{a}} (\mathcal{Z}_A)^{\text{T}}\right)\Big|_{22} &= \text{Re } \Sigma_{a_2 a_2}(m_{a_2}^2), \\ \left(U^* \delta\mathcal{M}_{\chi^\pm} V^\dagger\right)\Big|_{11} &= \frac{1}{2} \left[m_{\chi_1^\pm} \left(\text{Re } \Sigma_{\chi_1^\pm \chi_1^\pm}^{\text{VL}}(m_{\chi_1^\pm}) + \text{Re } \Sigma_{\chi_1^\pm \chi_1^\pm}^{\text{VR}}(m_{\chi_1^\pm}) \right) + \right. \\ & \quad \left. + \text{Re } \Sigma_{\chi_1^\pm \chi_1^\pm}^{\text{SL}}(m_{\chi_1^\pm}) + \text{Re } \Sigma_{\chi_1^\pm \chi_1^\pm}^{\text{SR}}(m_{\chi_1^\pm}) \right], \\ \left(U^* \delta\mathcal{M}_{\chi^\pm} V^\dagger\right)\Big|_{22} &= \frac{1}{2} \left[m_{\chi_2^\pm} \left(\text{Re } \Sigma_{\chi_2^\pm \chi_2^\pm}^{\text{VL}}(m_{\chi_2^\pm}) + \text{Re } \Sigma_{\chi_2^\pm \chi_2^\pm}^{\text{VR}}(m_{\chi_2^\pm}) \right) + \right. \\ & \quad \left. + \text{Re } \Sigma_{\chi_2^\pm \chi_2^\pm}^{\text{SL}}(m_{\chi_2^\pm}) + \text{Re } \Sigma_{\chi_2^\pm \chi_2^\pm}^{\text{SR}}(m_{\chi_2^\pm}) \right], \\ \left(N^* \delta\mathcal{M}_{\chi^0} N^\dagger\right)\Big|_{11} &= \frac{1}{2} \left[m_{\chi_1^0} \left(\text{Re } \Sigma_{\chi_1^0 \chi_1^0}^{\text{VL}}(m_{\chi_1^0}) + \text{Re } \Sigma_{\chi_1^0 \chi_1^0}^{\text{VR}}(m_{\chi_1^0}) \right) + \right. \\ & \quad \left. + \text{Re } \Sigma_{\chi_1^0 \chi_1^0}^{\text{SL}}(m_{\chi_1^0}) + \text{Re } \Sigma_{\chi_1^0 \chi_1^0}^{\text{SR}}(m_{\chi_1^0}) \right], \\ \left(N^* \delta\mathcal{M}_{\chi^0} N^\dagger\right)\Big|_{22} &= \frac{1}{2} \left[m_{\chi_2^0} \left(\text{Re } \Sigma_{\chi_2^0 \chi_2^0}^{\text{VL}}(m_{\chi_2^0}) + \text{Re } \Sigma_{\chi_2^0 \chi_2^0}^{\text{VR}}(m_{\chi_2^0}) \right) + \right. \\ & \quad \left. + \text{Re } \Sigma_{\chi_2^0 \chi_2^0}^{\text{SL}}(m_{\chi_2^0}) + \text{Re } \Sigma_{\chi_2^0 \chi_2^0}^{\text{SR}}(m_{\chi_2^0}) \right]. \end{aligned} \quad (4.90)$$

Here $\delta\mathcal{M}_{\chi^\pm}$ and $\delta\mathcal{M}_{\chi^0}$ are the counterterm matrices to the chargino and neutralino mass matrices. They are given explicitly in Appendix E. The self-energies are in the basis of the mass eigenstates and for the fermionic self-energies we once again assumed the decomposition

$$\Sigma(p) = \not{p}\omega_L \Sigma_{\text{VL}}(p) + \not{p}\omega_R \Sigma_{\text{VR}}(p) + \omega_L \Sigma_{\text{SL}}(p) + \omega_R \Sigma_{\text{SR}}(p). \quad (4.91)$$

This system of equations can be solved for $\delta\lambda$, $\delta\kappa$, δT_κ , δv_s , δM_1 and δM_2 . When comparing the on-shell scheme to the mixed scheme all input values given as $\overline{\text{DR}}$ values need to be converted to on-shell input values:

$$\begin{aligned}\lambda^{\text{OS}} &= \lambda^{\overline{\text{DR}}} - \delta\lambda^{\text{OS}}|_{\text{fin}}, & \kappa^{\text{OS}} &= \kappa^{\overline{\text{DR}}} - \delta\kappa^{\text{OS}}|_{\text{fin}} \\ T_\kappa^{\text{OS}} &= T_\kappa^{\overline{\text{DR}}} - \delta T_\kappa^{\text{OS}}|_{\text{fin}}, & v_s^{\text{OS}} &= v_s^{\overline{\text{DR}}} - \delta v_s^{\text{OS}}|_{\text{fin}}.\end{aligned}\quad (4.92)$$

These on-shell values are the ones to be inserted into the Higgs mass matrix

$$\mathcal{M}_h(e^{\text{OS}}, M_W^{\text{OS}}, M_Z^{\text{OS}}, M_{H^\pm}^{\text{OS}}, t_{h_d}^{\text{OS}}, t_{h_u}^{\text{OS}}, t_{h_s}^{\text{OS}}, \lambda^{\text{OS}}, \kappa^{\text{OS}}, v_s^{\text{OS}}, T_\kappa^{\text{OS}}, \tan\beta^{\text{OS}}) \quad (4.93)$$

when calculating the one-loop masses.

4.7 One-Loop Higgs Masses in the Complex NMSSM

In the case of the complex NMSSM CP-violation occurs and the mixing of all five Higgs bosons needs to be taken into account. The elements of the 5×5 two-point function are given by

$$\left(\hat{\Gamma}_{\text{Higgs}}(p^2)\right)_{ij} = i\delta_{ij}(p^2 - m_{h_i}^2) + i\hat{\Sigma}_{h_i h_j}(p^2) \quad \text{with } i = 1\dots 5; j = 1\dots 5. \quad (4.94)$$

With the renormalized self-energy

$$\begin{aligned}\hat{\Sigma}_{h_i h_j}(p^2) &= \Sigma_{h_i h_j}(p^2) + \frac{1}{2}p^2 \left(\delta\tilde{Z}^\dagger + \delta\tilde{Z}\right)|_{ij} + \\ &\quad - \frac{1}{2} \left(\delta\tilde{Z}^\dagger \mathcal{M}_{\text{Higgs}}^{\text{dia}} + \mathcal{M}_{\text{Higgs}}^{\text{dia}} \delta\tilde{Z}\right)|_{ij} - \left(\mathcal{R} \delta\mathcal{M}_{\text{Higgs}} \mathcal{R}^T\right)|_{ij}.\end{aligned}\quad (4.95)$$

Here $\mathcal{M}_{\text{Higgs}}^{\text{dia}}$ is the diagonal matrix with the square of the tree-level Higgs masses $m_{h_i}^2$ on the diagonal and $\delta\mathcal{M}_{\text{Higgs}}$ is the counterterm mass matrix as given in Appendix D. The field renormalization constants for the mass eigenstates read

$$\delta\tilde{Z} = \mathcal{R} \text{diag}(\cos^2 \beta \delta Z_{H_u} + \sin^2 \beta \delta Z_{H_d}, \delta Z_S, \delta Z_{H_d}, \delta Z_{H_u}, \delta Z_S) \mathcal{R}^T, \quad (4.96)$$

where \mathcal{R} is the orthogonal matrix that diagonalizes the Higgs mass matrix as defined in Eq. (3.28). The squared one-loop masses of the neutral Higgs bosons, which will be denoted by $M_{H_i}^2$ in the following and ordered by ascending mass (i.e. $M_{H_i}^2 < M_{H_j}^2$ if $i < j$), are given by the roots of the determinant of the renormalized two-point function $\hat{\Gamma}_{\text{Higgs}}$. Of course, the same approximations as described in Section 4.3 can be used. The only difference being that we need to work with a 5×5 matrix instead of a 2×2 (real case, CP-odd Higgs bosons) or a 3×3 matrix (real case, CP-even Higgs bosons). In the numerical analysis in Chapter 5 we will always apply the iterative procedure if not noted otherwise. Once again, the mixing with the Goldstone boson is negligible as we explicitly verified and is therefore not taken into account in the actual calculation.

4.8 Mixing Matrix Elements at One-Loop in the Complex Higgs Sector

For the complex NMSSM we will generally use the $p^2 = 0$ approximation to determine the one-loop Higgs mixing matrix $\mathcal{R}^{1\text{-loop}}$. In this approximation $\mathcal{R}^{1\text{-loop}}$ is defined as the unitary matrix that diagonalizes

$$\left(\mathcal{M}_{\text{Higgs}} - \mathcal{R}^T \hat{\Sigma}_{\text{Higgs}}(0) \mathcal{R} \right) \quad (4.97)$$

with $\mathcal{M}_{\text{Higgs}}$ being the 5×5 mass matrix in the basis of the interaction eigenstates and $\hat{\Sigma}_{\text{Higgs}}(0)$ the renormalized self-energy at vanishing external momentum.

The formalism for external Higgs bosons as described for the real NMSSM gets quite complicated for the mixing of five particles. Therefore the explicit formulas are not given here, although they were derived and implemented. The results, however, hardly differed from the $p^2 = 0$ approximation. Since the latter runs a lot faster than the former, this is the one we applied in the actual calculations.

4.9 Renormalization of the Complex Higgs Sector

As listed in Table 4.1 fifteen counterterms are required to renormalize the Higgs sector of the complex NMSSM. Now, we have to define a renormalization scheme to fix these fifteen counterterms. We once again choose a scheme which mixes on-shell and $\overline{\text{DR}}$ renormalization. The parameters with a clear physical meaning are renormalized on-shell and all other parameters are $\overline{\text{DR}}$ renormalized:

$$\underbrace{e, M_W, M_Z, M_{H^\pm}, t_{h_d}, t_{h_u}, t_{h_s}, t_{a_d}, t_{a_s}}_{\text{on-shell}}, \underbrace{\lambda, \kappa, v_s, T_\kappa, \tan\beta, \phi_I}_{\overline{\text{DR}}} \quad (4.98)$$

On-Shell Conditions

The renormalization conditions for the on-shell parameters only need to be slightly modified in comparison to the real NMSSM. What basically needs to be done, is to replace all “Re” appearing in the renormalization conditions by “ $\widetilde{\text{Re}}$ ”. $\widetilde{\text{Re}}$ is defined to act only on the loop functions. So, if it acts on the product of any complex number with a loop function, $\widetilde{\text{Re}}$ ensures that the imaginary part of the loop function is discarded while the imaginary part of the complex number is kept, e.g.

$$\widetilde{\text{Re}}\left(c \cdot B_0(p^2, m_1^2, m_2^2)\right) = c \cdot \text{Re} B_0(p^2, m_1^2, m_2^2) \quad \text{with } c \in \mathbb{C}. \quad (4.99)$$

Hence, the counterterms for the vector boson masses, the mass of the charged Higgs boson and the electric charge read

$$\begin{aligned} \delta M_W^2 &= \widetilde{\text{Re}} \Sigma_W^T(M_W^2), & \delta M_Z^2 &= \widetilde{\text{Re}} \Sigma_Z^T(M_Z^2), & \delta M_{H^\pm}^2 &= \widetilde{\text{Re}} \Sigma_{H^\pm}(M_{H^\pm}^2), \\ \text{and } \delta Z_e &= \frac{1}{2} \frac{\partial \Sigma_{AA}^T(p^2)}{\partial p^2} \Bigg|_{p^2=0} + \frac{\sin \theta_W}{\cos \theta_W} \frac{\Sigma_{AZ}^T(0)}{M_Z^2}. \end{aligned} \quad (4.100)$$

The counterterms for the tadpole parameters read

$$\begin{aligned} \delta t_{a_d} &= \sin\beta \mathcal{R}_{i1} T_i, & \delta t_{a_s} &= \mathcal{R}_{i2} T_i, & \delta t_{h_d} &= \mathcal{R}_{i3} T_i \\ \delta t_{h_u} &= \mathcal{R}_{i4} T_i & \text{and} & & \delta t_{h_s} &= \mathcal{R}_{i5} T_i. \end{aligned} \quad (4.101)$$

Here T_i is the one-loop tadpole diagram in the basis of the mass eigenstates with the external Higgs boson h_i .

$\overline{\text{DR}}$ Conditions

We once again want to use the neutralino and chargino sectors, as well as the Higgs sector, to determine the remaining counterterms. However, in the chargino and neutralino sector the phases ϕ_u , ϕ_s , ϕ_λ and ϕ_κ appear on their own and not only in the combination

$$\phi_I = \phi_u + \phi_\lambda - 2\phi_s - \phi_\kappa$$

as they do in the Higgs sector. This can easily be seen in the mass matrices given in Eq. (3.42) and Eq. (3.46). Therefore, we will introduce the counterterms $\delta\phi_u$, $\delta\phi_s$, $\delta\phi_\lambda$ and $\delta\phi_\kappa$ explicitly. Furthermore, the additional counterterms δM_1 , $\delta\phi_{M_1}$, δM_2 and $\delta\phi_{M_2}$ are required for the chargino and neutralino sectors. The field renormalization constants and $\tan\beta$ are fixed similarly to the renormalization scheme for the real Higgs sector. So, this leaves the counterterms

$$\delta\lambda, \delta\kappa, \delta v_s, \delta T_\kappa, \delta M_1, \delta M_2, \delta\phi_u, \delta\phi_s, \delta\phi_\lambda, \delta\phi_\kappa, \delta\phi_{M_1} \text{ and } \delta\phi_{M_2} \quad (4.102)$$

to be fixed via renormalization conditions from the Higgs, chargino and neutralino sectors.

Field Renormalization Constants and $\tan\beta$

The field renormalization constants are once again fixed by $\overline{\text{DR}}$ conditions. The residuum of the pole of the propagator is set to one by

$$\widetilde{\text{Re}} \left(\frac{\partial \hat{\Sigma}_{h_i h_i}(p^2)}{\partial p^2} \right) \Big|_{p^2=m_{h_i}^2}^{\text{div}} = 0. \quad (4.103)$$

With $\hat{\Sigma}_{h_i h_i}(p^2)$ as given in Eq. (4.95) this leads to the following five equations

$$\widetilde{\text{Re}} \left(\frac{\partial \Sigma_{h_i h_i}(p^2)}{\partial p^2} \right) \Big|_{p^2=m_{h_i}^2}^{\text{div}} + \delta \tilde{Z} \Big|_{ii} = 0 \quad i = 1 \dots 5, \quad (4.104)$$

$$\text{with} \quad \delta \tilde{Z} = \mathcal{R} \text{diag}(\cos^2\beta \delta Z_{H_u} + \sin^2\beta \delta Z_{H_d}, \delta Z_S, \delta Z_{H_d}, \delta Z_{H_u}, \delta Z_S) \mathcal{R}^T.$$

This is an overdetermined set of equations, which yields a solution for δZ_{H_u} , δZ_{H_d} and δZ_S .

Chargino Sector

The chargino sector provides four renormalization conditions. When Eq. (4.20) is modified for the 2×2 chargino mass matrix including complex parameters, it reads

$$\begin{aligned} \left(U^* \delta \mathcal{M}_{\chi^\pm} V^\dagger \right) \Big|_{ii}^{\text{div}} &= \frac{1}{2} \left(m_{\chi_i^\pm} \left(\widetilde{\text{Re}} \Sigma_{\chi_i^\pm \chi_i^\pm}^{\text{VL}}(m_{\chi_i^\pm}) \right)^* + m_{\chi_i^\pm} \widetilde{\text{Re}} \Sigma_{\chi_i^\pm \chi_i^\pm}^{\text{VR}}(m_{\chi_i^\pm}) + \right. \\ &\quad \left. + \widetilde{\text{Re}} \Sigma_{\chi_i^\pm \chi_i^\pm}^{\text{SL}}(m_{\chi_i^\pm}) + \left(\widetilde{\text{Re}} \Sigma_{\chi_i^\pm \chi_i^\pm}^{\text{SR}}(m_{\chi_i^\pm}) \right)^* \right)^{\text{div}} \end{aligned} \quad (4.105)$$

with $i = 1, 2$. Here $\delta \mathcal{M}_{\chi^\pm}$ is the counterterm mass matrix for the charginos (see Appendix E), which is rotated to mass eigenstates with the matrices U and V . The self-energy of χ_i^\pm going to χ_i^\pm is denoted by $\Sigma_{\chi_i^\pm \chi_i^\pm}$ and $m_{\chi_i^\pm}$ is the tree-level mass of χ_i^\pm . Eq. (4.105) yields four equations, since the real part and the imaginary part of the equations for the two mass eigenstates have to be satisfied individually.

Neutralino Sector

The neutralino sector provides ten renormalization conditions. They are given by the real and imaginary parts of the following five equations

$$\begin{aligned} \left(N^* \delta \mathcal{M}_{\chi^0} N^\dagger \right) \Big|_{ii}^{\text{div}} &= \frac{1}{2} \left(m_{\chi_i^0} \left(\widetilde{\text{Re}} \Sigma_{\chi_i^0 \chi_i^0}^{\text{VL}}(m_{\chi_i^0}) \right)^* + m_{\chi_i^0} \widetilde{\text{Re}} \Sigma_{\chi_i^0 \chi_i^0}^{\text{VR}}(m_{\chi_i^0}) + \right. \\ &\quad \left. + \widetilde{\text{Re}} \Sigma_{\chi_i^0 \chi_i^0}^{\text{SL}}(m_{\chi_i^0}) + \left(\widetilde{\text{Re}} \Sigma_{\chi_i^0 \chi_i^0}^{\text{SR}}(m_{\chi_i^0}) \right)^* \right)^{\text{div}} \end{aligned} \quad (4.106)$$

with $i = 1 \dots 5$. The counterterm mass matrix $\delta \mathcal{M}_{\chi^0}$ is rotated to mass eigenstates with the matrix N . The tree-level mass of χ_i^0 is denoted by $m_{\chi_i^0}$ and $\Sigma_{\chi_i^0 \chi_i^0}$ stands for the self-energy of χ_i^0 going to χ_i^0 .

Higgs Sector

The Higgs Sector provides only five renormalization conditions. Of course there are five mass eigenstates, so we can impose the five conditions

$$\left(\mathcal{R} \delta \mathcal{M}_{\text{Higgs}} \mathcal{R}^T \right) \Big|_{ii}^{\text{div}} = \widetilde{\text{Re}} \Sigma_{h_i h_i}^{\text{div}}(m_{h_i}^2) \quad \text{with} \quad i = 1 \dots 5. \quad (4.107)$$

But in contrast to the chargino and neutralino sector these conditions are always real for the Higgs sector and therefore only yield five equations.

Combining the Chargino, Neutralino and Higgs Sector Conditions

On the one hand we have altogether nineteen renormalization conditions from these sectors, on the other hand we only need twelve to fix the remaining counterterms listed in Eq. (4.102). Hence, we are dealing with an overdetermined system of equations. We solved this by first taking a subset of twelve equations and then later on verifying that the remaining seven equations were satisfied as well. Since the parameter T_κ only appears in the Higgs sector, we need at least one condition from the Higgs sector. Furthermore, we chose all four conditions of the chargino sector and seven of the neutralino conditions.

4.9.1 Remark on the Counterterms of the Phases

After performing the numerical analysis, it turned out that the counterterms for the phases $\delta\phi_u$, $\delta\phi_s$, $\delta\phi_\lambda$, $\delta\phi_\kappa$, $\delta\phi_{M_1}$ and $\delta\phi_{M_2}$ were always zero. In other words: these counterterms are not needed to renormalize the Higgs sector. These phases remain at their tree-level values and can be interpreted as mixing parameters. Just like the rotation matrices introduced to diagonalize the mass matrices these mixing parameters do not have to be renormalized⁹. Hence, when going from the real NMSSM to the complex NMSSM only two more counterterms are needed, namely δt_{a_d} and δt_{a_s} . It remains to be seen whether a conclusive explanation for this observation can be found.

⁹In [37] a similar conclusion for the neutralino and chargino sector of the MSSM is presented.

Finally, everything we need to proceed to the numerical analysis has been presented. In this chapter some example scenarios will be analyzed. We will always fix all input parameters except for one and then investigate the dependence of the tree-level and one-loop masses of the neutral Higgs bosons on this parameter. First, we consider three scenarios for the Higgs sector of the real NMSSM. For the real NMSSM we also apply the exclusion limits set by the experimental data acquired at LEP, Tevatron and LHC. Then, we move on to the Higgs sector of the complex NMSSM. On the one hand, the complex NMSSM allows for CP-violation in the Higgs sector already at tree-level. On the other hand, CP-violation in the Higgs sector can also be induced at one-loop level by setting a phase of a parameter that does not appear in the Higgs sector but enters only in the higher order corrections. Both kinds of scenarios will be discussed later on.

But before diving into the actual analysis, let us shortly summarize how the calculation was performed, i.e. which programs were used, etc. The Feynman rules needed for the calculation of the self-energies were derived using the `Mathematica` package `Sarah` [38]. Provided with the particle content of any supersymmetric theory and the superpotential `Sarah` can derive all mass matrices and all Feynman rules analytically. The Feynman rules can be written to a `Feynarts` [39] model file. The Feynman rules derived this way were cross-checked against those given in [16] and [20]. Using the `Feynarts` and `FormCalc` [40] packages, the analytic self-energies required for the renormalization procedure could be calculated. Since these analytic self-energies are very lengthy, they are not given here. To perform the numerical evaluation a `Mathematica` program was written. Provided with the input values (see Section 5.1) it calculates the whole NMSSM spectrum, i.e. all particle masses and all mixing matrices. Furthermore, the different renormalization schemes as described in Section 4.6 and Section 4.9 and the procedures to determine the one-loop masses and mixing elements (see Section 4.3 and Section 4.4, respectively Section 4.7 and Section 4.8) were implemented. The program `LoopTools` [29] was used to evaluate the loop functions appearing in the self-energies numerically. In the end this resulted in a `Mathematica` program which, starting from some input parameters, calculates the whole tree-level spectrum of the NMSSM, the one-loop Higgs masses and the one-loop Higgs mixing matrices. The output is provided in SUSY Les Houches Accord (SLHA) [41] compliant form.

5.1 Input Parameters

To perform the numerical analysis we need to set all input parameters. First of all, there are the SM input values such as the gauge boson masses, the quark masses, the lepton masses and the electroweak and strong coupling constants. The SM input values were taken from the “Review of Particle Physics” by the “Particle Data Group” [42]. The SM input values are given by:

- **Electroweak Input Values**

If the Fermi coupling constant G_F , the mass of the Z -boson M_Z and the electromagnetic coupling constant α_{em} are given¹, the W -boson mass M_W and the electric charge e can be inferred from those.

$$\begin{aligned} G_F &= 1.16637 \cdot 10^{-5} \text{ GeV}^{-2}, & M_Z &= 91.1876 \text{ GeV}, & \alpha_{\text{em}} &= 1/137. \\ \Rightarrow M_W &= 80.9388 \text{ GeV} & \text{and} & & e &= 0.302822. \end{aligned}$$

- **Strong coupling constant**

The strong coupling α_s at the scale M_Z is given by

$$\alpha_s(M_Z) = 0.1184 \quad \Rightarrow \quad g_s(M_Z) = \sqrt{4\pi\alpha_s} = 1.21978.$$

- **Quark Masses**

The quark masses are given by:

$$\begin{aligned} m_t(\text{pole}) &= 173.3 \text{ GeV}, & m_b^{\overline{\text{MS}}}(m_b) &= 4.19 \text{ GeV}, & m_c(2\text{GeV}) &= 1.27 \text{ GeV}, \\ m_s(2\text{GeV}) &= 101 \text{ MeV}, & m_u(2\text{GeV}) &= 2.5 \text{ MeV}, & m_d(2\text{GeV}) &= 4.95 \text{ MeV}. \end{aligned}$$

For the top quark the pole mass is given. The bottom mass is given as the $\overline{\text{MS}}$ running mass at the scale of the bottom mass. The masses of the light quarks are given at the scale of 2 GeV. If not stated otherwise we use the pole masses for the top quark and the bottom quark² and the masses for the light quarks as given above throughout this thesis. Only when comparing our results to those of [44], we set the masses of the light quarks to zero and calculate the running $\overline{\text{DR}}$ top and bottom masses at the renormalization scale Q (for further details see Appendix C).

- **Lepton Masses**

The masses of the charged leptons are given by:

$$m_e = 511 \text{ keV}, \quad m_\mu = 105.7 \text{ MeV}, \quad m_\tau = 1.777 \text{ GeV}.$$

The neutrinos are taken to be massless. When comparing to [44] the masses of the light generations are set to zero, i.e. $m_e = 0$ and $m_\mu = 0$.

All other input parameters cannot be linked directly to any observables. With the exception of the mass of the charged Higgs boson, we take all other input values to be $\overline{\text{DR}}$ input values at the renormalization scale Q . To simplify matters even further, we assume a restricted scenario, in which all soft breaking parameters can be calculated from the three parameters

¹Here we follow the SLHA convention, which suggests these three parameters as input values from which the other electroweak input values can be derived.

²The conversion of the $\overline{\text{MS}}$ bottom mass to the pole mass was done using SUSY-HIT [43], $m_b(\text{pole}) = 4.88 \text{ GeV}$.

M_{SUSY} , M_0 and A_0 . The parameter M_{SUSY} is a common soft SUSY breaking mass parameter which fixes all soft SUSY breaking mass parameters of the squarks and sleptons

$$m_{\tilde{Q}_L}^2 = m_{\tilde{u}_R}^2 = m_{\tilde{d}_R}^2 = m_{\tilde{L}_L}^2 = m_{\tilde{e}_R}^2 = M_{\text{SUSY}}^2. \quad (5.1)$$

The parameter M_0 determines the absolute value of the gaugino mass parameters

$$M_1 = \frac{1}{3}M_0 \cdot e^{i\phi_{M_1}}, \quad M_2 = \frac{2}{3}M_0 \cdot e^{i\phi_{M_2}}, \quad M_3 = 2M_0 \cdot e^{i\phi_{M_3}}. \quad (5.2)$$

Their phases are denoted by ϕ_{M_1} , ϕ_{M_2} and ϕ_{M_3} . The parameter A_0 fixes the absolute values of the trilinear breaking parameters T_{Y_u} , T_{Y_d} and T_{Y_e}

$$\begin{aligned} T_{Y_u} &= A_0 \cdot Y_u \cdot e^{i\phi_{A_u}} & \text{with} & \quad Y_u = \frac{\sqrt{2}}{v_u} \cdot \text{diag}(m_u, m_c, m_t), \\ T_{Y_d} &= A_0 \cdot Y_d \cdot e^{i\phi_{A_d}} & \text{with} & \quad Y_d = \frac{\sqrt{2}}{v_d} \cdot \text{diag}(m_d, m_s, m_b), \\ T_{Y_e} &= A_0 \cdot Y_e \cdot e^{i\phi_{A_e}} & \text{with} & \quad Y_e = \frac{\sqrt{2}}{v_d} \cdot \text{diag}(m_e, m_\mu, m_\tau). \end{aligned} \quad (5.3)$$

Note that the Yukawa couplings are assumed to be diagonal. Hence, we do not allow for generation mixing. The Yukawa couplings are determined by the squark and slepton masses and the VEVs v_u and v_d . As discussed in Section 3.4.5 the absolute values for six of the Higgs sector parameters have to be provided. We choose to set $\tan\beta$, $|\lambda|$, $|\kappa|$, $|T_\lambda|$, $|T_\kappa|$ and $|\mu|$ as input values with $|\mu|$ given by $|\mu| = |\lambda|v_s/\sqrt{2}$. Furthermore, the four phases ϕ_u , ϕ_s , ϕ_λ and ϕ_κ are assigned values. Setting these phases automatically determines the phases ϕ_{T_κ} and ϕ_{T_λ} up to an ambiguity which can be resolved by defining the sign of R_λ and R_κ (see Eq. (3.37)). Moreover, it is necessary to choose a renormalization scale Q , which enters the one-loop calculation due to the regularization procedure.

Hence, we need to assign numerical values to the following parameters in order to calculate the one-loop masses at a specific parameter point:

the absolute values of the Higgs sector parameters	$\tan\beta, \lambda , \kappa , T_\lambda , T_\kappa , \mu $
the phases of the Higgs sector parameters	$\phi_u, \phi_s, \phi_\lambda, \phi_\kappa, \text{sgn } R_\lambda, \text{sgn } R_\kappa$
the absolute values of the soft breaking parameters	$M_{\text{SUSY}}, M_0, A_0$
the phases of the soft breaking parameters	$\phi_{M_1}, \phi_{M_2}, \phi_{M_3}, \phi_{A_u}, \phi_{A_d}, \phi_{A_e}$
the renormalization scale	Q

In the following the values for the phases will only be stated explicitly if they are nonzero.

5.2 Real Higgs Sector

In this section the results of three different scenarios which exemplify some of the various higher order effects are presented. First, we adopt the scenario presented in [44] and analyze the differences between the different renormalization schemes as well as the influence of the top mass and the renormalization scale on the one-loop masses. Then, we adopt two more

scenarios. In the first we examine the dependence of the one-loop Higgs boson masses on T_κ . In the second we investigate the dependence on the mass of the charged Higgs boson M_{H^\pm} . Finally, we apply LEP, Tevatron and LHC exclusion limits to these scenarios.

For all scenarios the VEV of the singlet v_s is chosen to be of the order of the vacuum expectation value $v \approx 246$ GeV. Furthermore, to avoid violation of unitary bounds the parameters λ and κ are nearly always chosen so that $\sqrt{\lambda^2 + \kappa^2} \lesssim 0.7$.

To cross-check our calculation, the whole procedure to obtain the one-loop Higgs boson masses in the NMSSM was also implemented independently by Thorben Graf [20]. Other scenarios can be found in his diploma thesis. The results presented here for the real NMSSM can also be found in [45].

5.2.1 Variation of λ

In [44] the one-loop masses of the two lightest CP-even Higgs bosons of the real NMSSM were calculated in dependence on λ using a $\overline{\text{DR}}$ renormalization scheme. To verify that we reproduce their results we adopt their parameter settings

$$\begin{aligned} \tan\beta = 2, \quad \kappa = \lambda/5, \quad T_\lambda = (500 \text{ GeV}) \cdot \lambda, \quad T_\kappa = (-10 \text{ GeV}) \cdot \kappa, \quad \mu = 250 \text{ GeV} \\ M_{\text{SUSY}} = 300 \text{ GeV}, \quad M_0 = 300 \text{ GeV}, \quad A_0 = -450 \text{ GeV}, \quad Q = 300 \text{ GeV}. \end{aligned}$$

The parameter λ is varied between 0 and 1. Furthermore, the masses of the light generations of quarks and leptons are set to zero and we use the running $\overline{\text{DR}}$ top and bottom masses (see Appendix C) as input values. Here the $\overline{\text{DR}}$ scheme is considered as the main renormalization scheme. Hence, T_λ is taken to be a $\overline{\text{DR}}$ input value at the renormalization scale Q . Since the mixed and on-shell renormalization schemes require the mass of the charged Higgs boson as an input value instead of T_λ , the input values need to be converted accordingly.

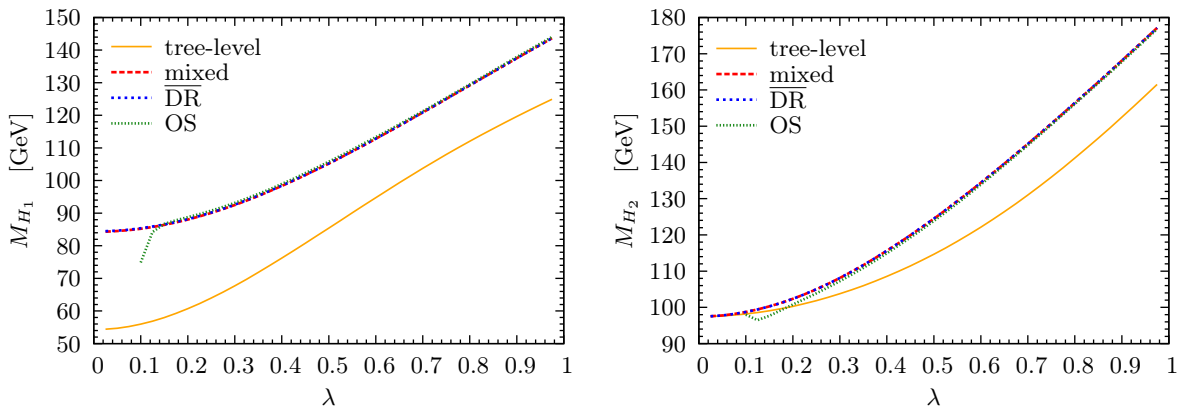


Figure 5.1: The mass M_{H_1} of the lightest (left) and the mass M_{H_2} of the next-to-lightest (right) CP-even Higgs boson in dependence on λ at tree-level (orange/solid) and at one-loop in the $\overline{\text{DR}}$ (blue/dotted), the mixed (red/dashed) and the on-shell (green/small dotted) renormalization scheme.

Fig. 5.1 shows the masses of the lightest and next-to-lightest CP-even Higgs boson at tree-level and at one-loop in the different renormalization schemes. The one-loop masses were obtained using the iterative procedure described in Section 4.3. We find agreement with [44] for the

one-loop masses. Both masses increase with λ at tree-level and at one-loop. The difference in the renormalization schemes is negligible except for small λ . In fact, for small λ the on-shell renormalization scheme becomes unstable and is therefore only plotted for $\lambda \geq 0.1$. This numerical instability is probably due to the finite parts of some of the counterterms going with $1/\lambda$ which blow up for small λ and cause a problem when converting the $\overline{\text{DR}}$ input values to on-shell values for the on-shell scheme. For small values of λ the mass of the lightest CP-even Higgs boson M_{H_1} receives corrections of up to 55% compared to the tree-level mass, i.e.

$$\Delta M_{H_1} = \frac{|M_{H_1}^{\text{1loop}} - M_{H_1}^{\text{tree}}|}{M_{H_1}^{\text{tree}}} \lesssim 55\%. \quad (5.4)$$

For small λ these corrections lift M_{H_1} from ~ 55 GeV at tree-level to ~ 85 GeV at one-loop. For bigger λ , the correction relative to the tree-level mass of H_1 is smaller but still about 15%. For this parameter variation the tree-level mass of the next-to-lightest CP-even Higgs boson M_{H_2} ranges from about 98 GeV to 162 GeV, whereas the one-loop mass ranges from 98 GeV to 176 GeV. For small λ the next-to-lightest Higgs boson mass M_{H_2} is hardly corrected at all, while the correction for larger values of λ is up to 11%.

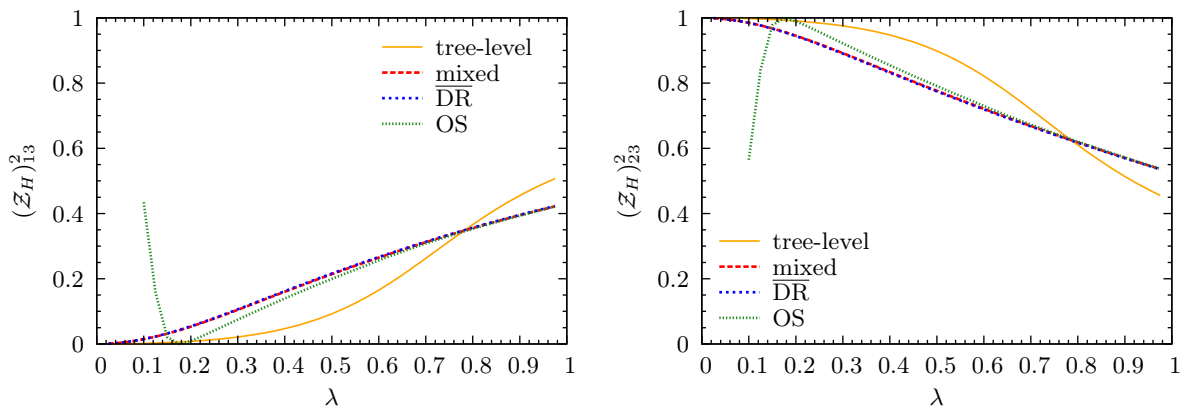


Figure 5.2: The singlet component of the lightest (left) and next-to-lightest (right) CP-even Higgs boson at tree-level (orange/solid) and at one-loop obtained using the $p^2 = 0$ approximation in the $\overline{\text{DR}}$ (blue/dotted), the mixed (red/dashed) and the on-shell (green/small dotted) renormalization scheme.

This behavior can be explained when considering the singlet components of H_1 and H_2 . The singlet component is given by the square of the corresponding element of the mixing matrix, i.e. by $(Z_H)_{13}^2$ and $(Z_H)_{23}^2$, respectively. Here the mixing matrix was calculated using the $p^2 = 0$ approximation to be consistent with the calculation of [44]. The singlet component is of interest because it is an indicator for the strengths with which the Higgs boson couples to the other particles. By construction the singlet does not couple to the SM fermions or gauge bosons at all. The coupling to all the other particles (i.e. sfermions, neutralinos, charginos and Higgs bosons) is proportional to λ . Hence, if a Higgs boson is mostly singlet-like, it can only receive corrections from these other particles and these corrections are roughly proportional to λ^2 . As can be seen in Fig. 5.2, H_2 is mostly singlet like for small values of λ . Therefore, it receives hardly any corrections. But as λ increases the singlet component of H_2 decreases and with this the corrections increase. H_1 on the other hand is dominantly MSSM-like³ for

³By MSSM-like we mean that it mainly consists of h_u and h_d , which originate from the Higgs doublets also present in the MSSM.

small λ and becomes more singlet-like with increasing λ , so that the corrections get smaller.

The corrections to the Higgs boson masses and the strength of the singlet component strongly depend on the top quark mass. To investigate this dependence, we calculated the one-loop masses in the $\overline{\text{DR}}$ scheme, one time using the pole mass and another time using the running mass as an input value. Fig. 5.3 shows the tree-level and one-loop masses for the lightest and next-to-lightest CP-even Higgs boson for the input values $m_t^{\text{pole}} = 173.3$ GeV and $m_t^{\overline{\text{DR}}} = 150.6$ GeV. It is apparent that the corrections are larger for the larger value of the top quark mass. In fact, the strong influence of the top quark mass on the one-loop masses suggests that the main corrections originate from top loops just as in the MSSM.

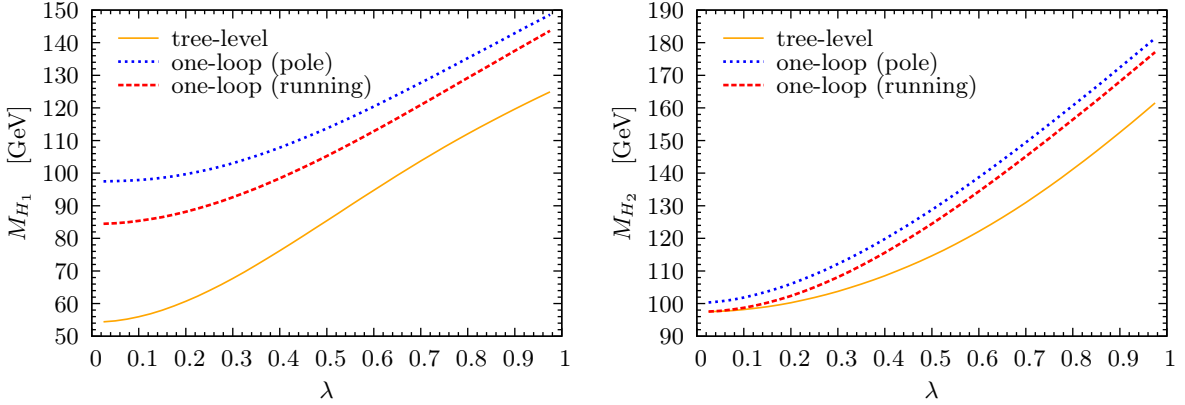


Figure 5.3: The mass M_{H_1} of the lightest (left) and the mass M_{H_2} of the next-to-lightest (right) CP-even Higgs boson in dependence on λ at tree-level (orange/solid) and at one-loop in the $\overline{\text{DR}}$ scheme with the top and bottom pole masses (blue/dotted) and running top and bottom masses (red/dashed) as input.

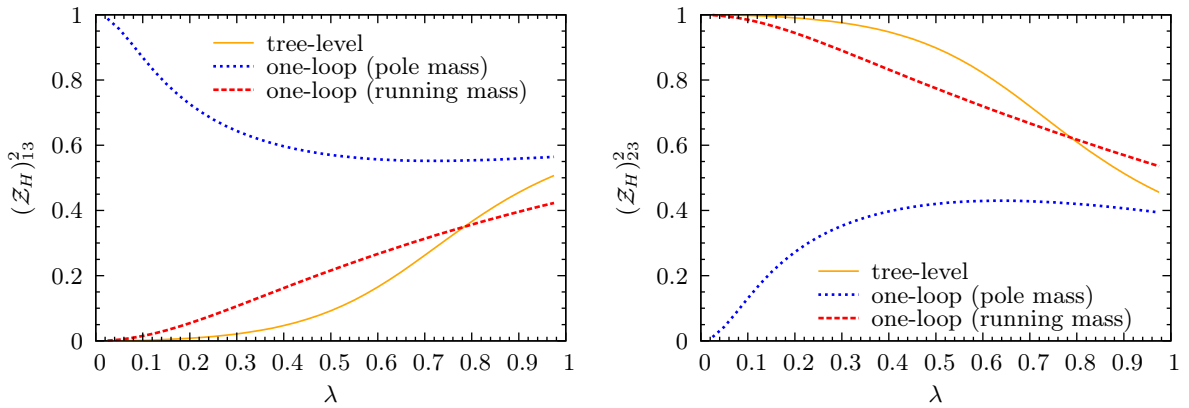


Figure 5.4: The singlet component of the lightest (left) and next-to-lightest (right) CP-even Higgs boson at tree-level (orange/solid) and at one-loop obtained using the $p^2 = 0$ approximation in the $\overline{\text{DR}}$ scheme with the top and bottom pole masses (blue/dotted) and running top and bottom masses (red/dashed) as input.

The strength of the singlet components of H_1 and H_2 for the different top quark masses are plotted in Fig. 5.4. At tree-level H_1 is mostly MSSM-like and H_2 is mostly singlet-like for small λ . For the running top mass this still holds true at one-loop. For the top pole mass, however, this is reversed. In fact, this is simply due to our convention of ordering the one-loop masses by ascending mass. For the top pole mass the one-loop corrections to H_1 are so large that they get shifted above the one-loop corrections to H_2 . So the one-loop corrected mass to the tree-level H_1 is assigned to the one-loop H_2 and vice versa.

The influence of the renormalization scale Q on the results provides an estimate of the missing higher order corrections. Fig. 5.5 shows the masses of the lightest and next-to-lightest CP-even Higgs boson at tree-level and at one-loop for the renormalization scales $Q = 150$ GeV, $Q = 300$ GeV and $Q = 600$ GeV. Taking half or double of the renormalization scale $Q = 300$ GeV changes the mass of the lightest CP-even Higgs boson up to $\sim 7\%$ relative to the one-loop mass at 300 GeV, whereas the mass of the next-to-lightest CP-even Higgs boson is only changed by about 3% at most. The mixing matrix elements (not plotted here) are even more sensitive to the scale variation. But all in all, the residual theoretical uncertainties due to missing higher order corrections are below 10%.

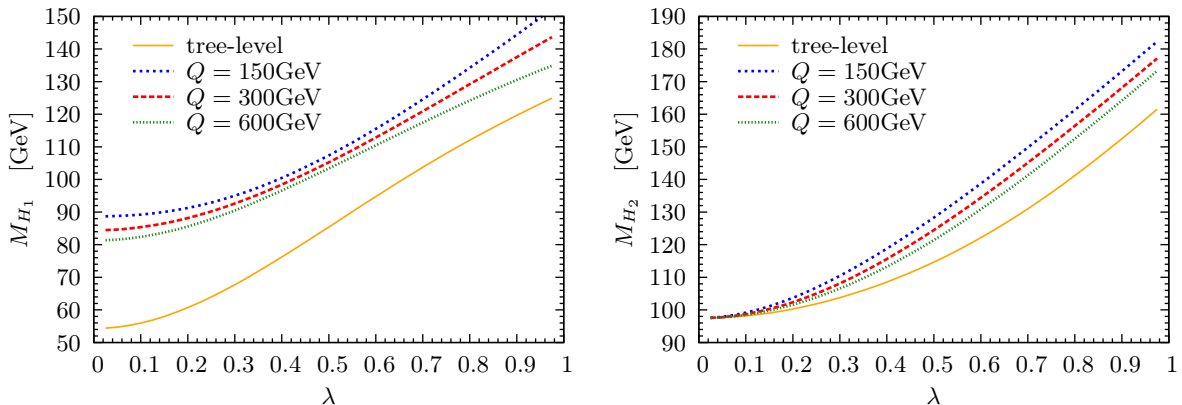


Figure 5.5: The mass M_{H_1} of the lightest (left) and the mass M_{H_2} of the next-to-lightest (right) CP-even Higgs boson in dependence on λ at tree-level (orange/solid) and at one-loop in the $\overline{\text{DR}}$ scheme for the renormalization scales $Q = 150$ GeV (blue/dotted), $Q = 300$ GeV (red/dashed) and $Q = 600$ GeV (green/small dotted).

The masses of the CP-odd Higgs bosons A_1 and A_2 as well as the mass of the heavy CP-even Higgs boson H_3 are not plotted here, since they are hardly affected by the one-loop corrections. The mass of the light CP-odd Higgs boson M_{A_1} increases with λ and ranges from 40 GeV to 140 GeV at tree-level. It receives small negative corrections which amount to 2% of the tree-level value at their maximum. The light CP-odd Higgs boson is nearly completely singlet-like, leaving the heavy CP-odd Higgs boson to be mainly MSSM-like. Both heavy Higgs bosons H_3 and A_2 receive small negative mass corrections of the order of 0.5% and their one-loop masses are between 580 GeV and 600 GeV.

5.2.2 Variation of T_κ

In this section the dependence of the Higgs boson masses and the mixing matrix elements on the parameter T_κ is investigated. We choose the following parameter set:

$$\begin{aligned} \tan\beta = 2, \quad \lambda = 0.6, \quad \kappa = \lambda/3, \quad T_\lambda = 325 \text{ GeV}, \quad \mu = 275 \text{ GeV} \\ M_{\text{SUSY}} = 1.1 \text{ TeV}, \quad M_0 = 600 \text{ GeV}, \quad A_0 = -900 \text{ GeV}, \quad Q = 300 \text{ GeV}. \end{aligned}$$

The soft breaking parameters M_0 and M_{SUSY} were chosen, so that the resulting squark masses of the first two generations and the gluino mass are in agreement with the current exclusion limits set by the LHC [46]. Furthermore we work with the pole masses for the top and the bottom quark mass and the masses for the light quarks as given in Section 5.1. From these input parameters we calculate the mass of the charged Higgs boson, which is then taken to be an on-shell input value.

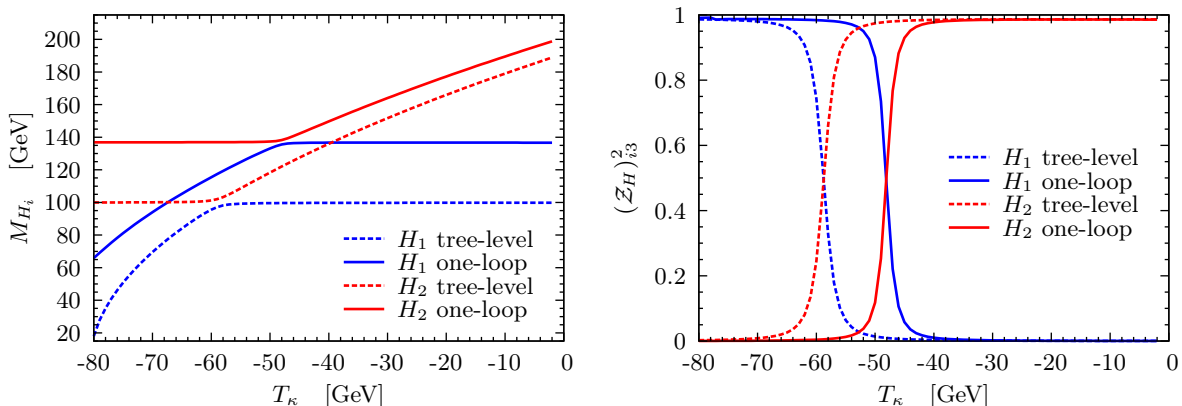


Figure 5.6: The mass (left) and the singlet component (right) of the lightest (blue/dark gray) and next-to-lightest (red/light gray) CP-even Higgs boson at tree-level (dashed) and at one-loop (solid) in dependence on T_κ . The one-loop masses were calculated in the mixed renormalization scheme and the method for external on-shell Higgs bosons was used to calculate the one-loop mixing.

On the left of Fig. 5.6 the masses of the lightest and next-to-lightest CP-even Higgs boson are plotted at tree-level and at one-loop. The one-loop masses were calculated using the mixed renormalization scheme. The singlet components plotted on the right of Fig. 5.6 were obtained using the method for external on-shell Higgs bosons to determine the mixing matrix elements as described in Section 4.4. But we also checked that the difference to the $p^2 = 0$ approximation is negligible here. It is striking that the mass of the lightest CP-even Higgs boson steadily increases with increasing T_κ up to a certain value of T_κ and then remains more or less constant. The opposite happens for the mass of the next-to-lightest CP-even Higgs boson, which starts out as a constant and then starts to increase at the same value of T_κ from where on M_{H_1} is constant. This behavior appears both at tree-level and at one-loop. However, the value of T_κ at which this happens is shifted. Once again, the singlet component is the key to understanding this behavior. T_κ was introduced as the trilinear soft SUSY breaking parameter. It appears in the Lagrangian in the form

$$\mathcal{L}_{\text{soft}} = \dots - \frac{1}{3} T_\kappa S^3. \quad (5.5)$$

Hence, only the masses of Higgs bosons with a sizeable singlet component dependent on T_κ . At tree-level H_1 is mostly singlet like below $T_\kappa \approx -59$ GeV, while H_2 is mostly MSSM-like. At $T_\kappa \approx -59$ GeV there is a cross-over and H_1 becomes MSSM-like whereas H_2 becomes singlet-like. As long as it is mainly singlet-like the mass of the corresponding Higgs boson increases with increasing T_κ and if it is mainly MSSM-like the mass remains constant. At one-loop the cross-over is shifted to $T_\kappa \approx -48$ GeV. The one-loop corrections are quite sizeable especially for M_{H_1} . At the low end of the T_κ range the lightest CP-even Higgs boson is very light (only about 18 GeV) but receives corrections of ~ 48 GeV. The corrections for M_{H_2} are not as large, but they still amount to 37% of the tree-level mass at their maximum.

The lightest CP-odd Higgs boson is mostly singlet-like and therefore its mass (not plotted here) depends strongly on T_κ . Its mass decreases with rising T_κ from around 345 GeV down to 110 GeV. The one-loop corrections to M_{A_1} are around 3–7 GeV and negative. The heavy Higgs bosons H_3 and A_2 are both dominantly MSSM-like. Hence, their masses are nearly constant. Both masses are around 640 GeV in the considered T_κ range. The corrections to the mass of the heavy Higgs bosons are only about 1 GeV.

5.2.3 Variation of M_{H^\pm}

Now, we set all parameters except for T_λ :

$$\begin{aligned} \tan\beta = 2, \quad \lambda = 0.65, \quad \kappa = \lambda/3, \quad T_\kappa = (-10 \text{ GeV}) \cdot \kappa, \quad \mu = 225 \text{ GeV} \\ M_{\text{SUSY}} = 1.1 \text{ TeV}, \quad M_0 = 600 \text{ GeV}, \quad A_0 = -900 \text{ GeV}, \quad Q = 300 \text{ GeV}. \end{aligned}$$

With all other parameters fixed, varying T_λ is equivalent to varying the mass of the charged Higgs boson, since M_{H^\pm} can be written as a function of T_λ :

$$M_{H^\pm}^2(T_\lambda) = M_W^2 \left[1 - \frac{2\lambda^2}{e^2} \left(1 - \frac{M_W^2}{M_Z^2} \right) \right] + \frac{v_s}{\sin(2\beta)} \left(\sqrt{2}T_\lambda + \lambda\kappa v_s \right). \quad (5.6)$$

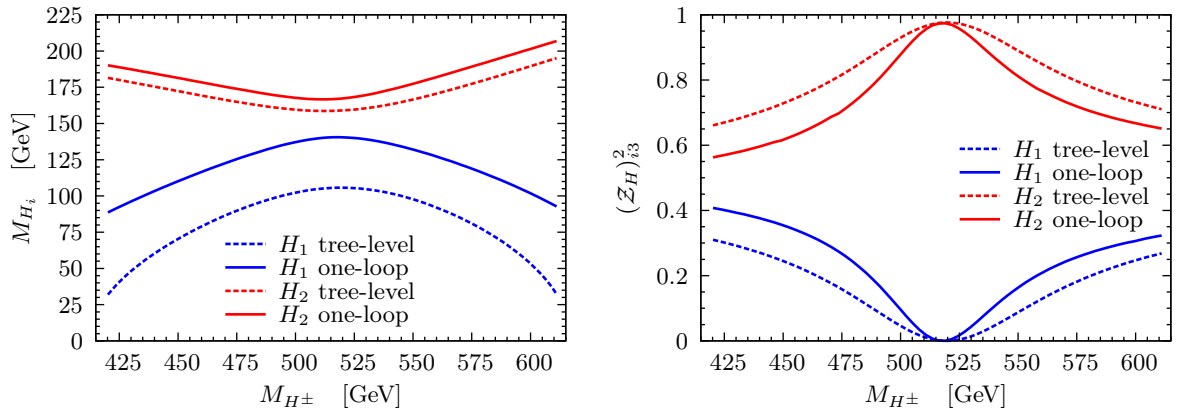


Figure 5.7: The mass (left) and the singlet component (right) of the lightest (blue/dark gray) and next-to-lightest (red/light gray) CP-even Higgs boson at tree-level (dashed) and at one-loop (solid) in dependence on M_{H^\pm} . The one-loop masses were calculated in the mixed renormalization scheme and the method for external on-shell Higgs bosons was used to calculate the one-loop mixing.

The masses of the lightest and next-to-lightest CP-even Higgs boson as well as their singlet components are shown in Fig. 5.7. The one-loop masses were calculated using the mixed renormalization scheme and we applied the method for external Higgs bosons to determine the mixing matrix elements. Both at tree-level and at one-loop the mass of the lightest CP-even Higgs boson first increases with M_{H^\pm} , until it reaches a maximum somewhere between $M_{H^\pm} \approx 515$ GeV and $M_{H^\pm} \approx 520$ GeV and then decreases again. The mass of the next-to-lightest CP-even Higgs boson decreases at first, displays a minimum and increases again. For the entire M_{H^\pm} range H_2 is mostly singlet-like. However, its singlet component becomes maximal when M_{H_2} reaches its minimum and mixing with the non-singlet-components is increased away from this minimum. Furthermore, the maximum in the singlet component of M_{H_2} becomes more pronounced at one-loop. But note that although its singlet component is maximal, H_2 is not completely singlet-like. Since H_1 is more or less completely MSSM-like at this point, the remaining singlet component is taken over by H_3 . Due to the fact that it is mainly MSSM-like the corrections to the mass of H_1 are fairly large. This holds especially for small tree-level masses of H_1 , for which the one-loop corrections nearly triple the mass. For H_2 the one-loop mass corrections are between 5% and 7% of the corresponding tree-level value.

The influence of the different renormalization schemes on the one-loop Higgs boson masses is shown in Fig. 5.8. The mixed and the on-shell renormalization scheme differ only slightly, but M_{H_1} in the $\overline{\text{DR}}$ scheme differs by up to 8 GeV from the other schemes. This difference turned out to originate from the conversion of the input parameters; to be more precise from the conversion of the tadpole parameters. In the $\overline{\text{DR}}$ scheme the tadpole parameters are renormalized using $\overline{\text{DR}}$ conditions, but since they are on-shell input values, they have to be converted. If one defines a renormalization scheme that uses $\overline{\text{DR}}$ conditions for all parameters with the exception of the tadpole parameters, this difference we observed does not occur.

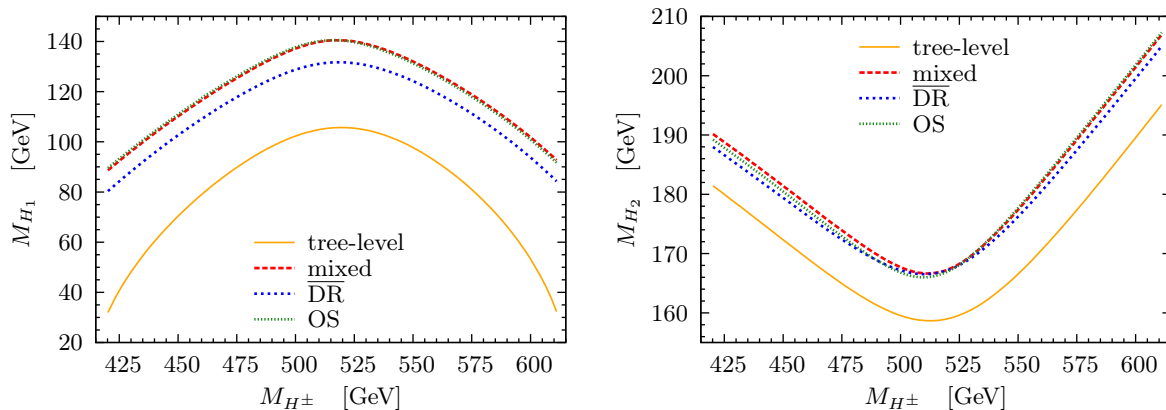


Figure 5.8: The mass M_{H_1} of the lightest (left) and the mass M_{H_2} of the next-to-lightest (right) CP-even Higgs boson in dependence on M_{H^\pm} at tree-level (orange/solid) and at one-loop in the $\overline{\text{DR}}$ (blue/dotted), the mixed (red/dashed) and the on-shell (green/small dotted) renormalization scheme.

In Fig. 5.9 the masses of two CP-odd Higgs bosons at tree-level and at one-loop are displayed. The mass of the light CP-odd Higgs boson M_{A_1} receives negative corrections of up to 6.5 GeV which amount to 5% of the corresponding tree-level value. So the tree-level mass of A_1 which ranges between 118.4 GeV and 125 GeV is corrected to a mass range of 116.5 GeV to

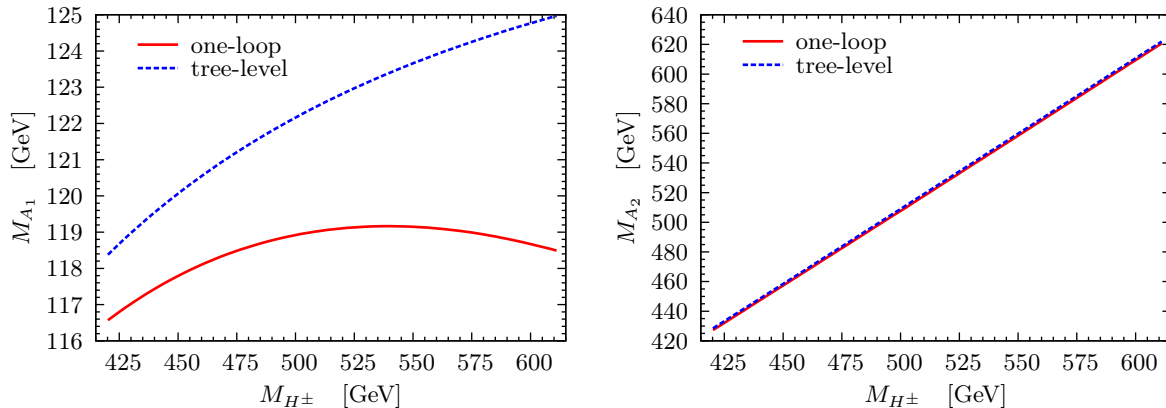


Figure 5.9: The mass of the lightest M_{A_1} (left) and next-to-lightest M_{A_2} (right) CP-odd Higgs boson at tree-level (blue/dashed) and at one-loop (red/solid).

119.2 GeV. The mass of the heavy CP-odd Higgs boson, which is nearly mass degenerate with the heavy CP-even Higgs boson, ranges from 420 GeV to 620 GeV and receives corrections of maximally 1.5 GeV.

5.2.4 Exclusion Limits

After discussing several example scenarios it is inevitable to check the exclusion limits set by the experiments for these scenarios. Note that we do not perform a sophisticated analysis here, but consider only the dominant channels. For LEP these are $e^+e^- \rightarrow ZH \rightarrow b\bar{b}$ and $e^+e^- \rightarrow ZH \rightarrow \gamma\gamma$. For the Tevatron we consider Higgs production via vector boson fusion (VBF) or gluon-gluon fusion with the Higgs decaying into W^-W^+ or $\tau^-\tau^+$ subsequently. For the LHC we use combined exclusion limits, which set a limit on the cross-section relative to the SM, $\sigma/\sigma^{\text{SM}}$.

The NLO SM cross sections and branching ratios required for the calculation were obtained using HIGLU [47] and HDECAY [48]. The NMSSM couplings and branching ratios were taken from NMSSMHDECAY [49], which is a version of HDECAY modified for the NMSSM.

LEP exclusion $ZH \rightarrow b\bar{b}$:

A 95% CL upper limit on the normalized cross-section $e^+e^- \rightarrow ZH$, assuming that the Higgs exclusively decays into $b\bar{b}$ pairs, relative to the corresponding SM value is provided in Table 14 (b) of [50]. Hence,

$$Q_{\text{obs}} = \frac{\sigma(ZH) \text{BR}(b\bar{b})}{\sigma(ZH)^{\text{SM}}} \quad (5.7)$$

is given. Q_{obs} is the observed upper bound on the cross-section $\sigma(ZH)$ times the branching ratio of the Higgs decaying into a $b\bar{b}$ pair (denoted by $\text{BR}(b\bar{b})$) normalized to the SM cross-section⁴ $\sigma(ZH)^{\text{SM}}$. To check if a parameter point is excluded we have to calculate

$$Q_{\text{model}} = \frac{\sigma(ZH)^{\text{NM}} \text{BR}(b\bar{b})^{\text{NM}}}{\sigma(ZH)^{\text{SM}}} = (g_{ZZH_i}^{\text{NM}})^2 \text{BR}(b\bar{b})^{\text{NM}}. \quad (5.8)$$

⁴The SM branching ratio $\text{BR}(b\bar{b})^{\text{SM}}$ does not appear in the denominator since it is assumed to be one.

Here the superscript NM stands for the NMSSM. The ratio of the NMSSM cross-section $\sigma(ZH)^{\text{NM}}$ and the SM cross-section is given by $(g_{ZZH_i}^{\text{NM}})^2$ which denotes the squared coupling of the NMSSM Higgs boson to two Z -bosons normalized to the SM coupling.

If $\frac{Q_{\text{model}}}{Q_{\text{obs}}} > 1$, the respective parameter point is excluded.

LEP exclusion $ZH \rightarrow \gamma\gamma$:

For this channel the 95% CL upper limit on cross-section times branching ratio for a Higgs boson decaying into a photon pair relative to the SM is given in [51]. Hence, [51] provides

$$Q_{\text{obs}} = \frac{\sigma(ZH) \text{BR}(\gamma\gamma)}{\sigma(ZH)^{\text{SM}}}. \quad (5.9)$$

We calculate

$$Q_{\text{model}} = (g_{ZZH_i}^{\text{NM}})^2 \text{BR}(\gamma\gamma)^{\text{NM}}. \quad (5.10)$$

If $\frac{Q_{\text{model}}}{Q_{\text{obs}}} > 1$, the respective parameter point is excluded.

Tevatron exclusion $H \rightarrow WW$

The 95% CL upper limit on cross-section times branching ratio relative to the SM for a Higgs boson produced in vector boson or gluon-gluon-fusion, which subsequently decays into a W -boson pair is given in [52], i.e.

$$Q_{\text{obs}} = \frac{(\sigma(gg) + \sigma(\text{VBF})) \text{BR}(WW)}{(\sigma(gg)^{\text{SM}} + \sigma(\text{VBF})^{\text{SM}}) \text{BR}(WW)^{\text{SM}}}. \quad (5.11)$$

Hence we need to calculate

$$Q_{\text{model}} = \frac{(\sigma(gg)^{\text{NM}} + \sigma(\text{VBF})^{\text{NM}}) \text{BR}(WW)^{\text{NM}}}{(\sigma(gg)^{\text{SM}} + \sigma(\text{VBF})^{\text{SM}}) \text{BR}(WW)^{\text{SM}}} \quad (5.12)$$

with

$$\sigma(gg)^{\text{NM}} = (g_{t\bar{t}H_i}^{\text{NM}})^2 \cdot \sigma(gg)^{\text{SM}} \quad \text{and} \quad \sigma(\text{VBF})^{\text{NM}} = (g_{WWH_i}^{\text{NM}})^2 \cdot \sigma(\text{VBF})^{\text{SM}}. \quad (5.13)$$

Here $g_{t\bar{t}H_i}^{\text{NM}}$ denotes the coupling of the i -th Higgs boson of the NMSSM to the top quark normalized to the SM coupling and $g_{WWH_i}^{\text{NM}}$ denotes the coupling of the i -th Higgs boson of the NMSSM to the W boson normalized to the SM coupling. Note that we only included the dominant contributions for the gluon-gluon-fusion cross-section. Since we always chose small values for $\tan\beta$ the dominant contributions come from the top loops. The respective parameter point is excluded if Q_{model} is bigger than Q_{obs} .

Tevatron exclusion $H \rightarrow \tau\tau$

D0 and CDF [52] provide limits on the cross-section times branching ratio for the $H \rightarrow \tau\tau$ decay channel. So they give Q_{obs} as

$$Q_{\text{obs}} = \sigma \text{BR}(\tau\tau). \quad (5.14)$$

We have to calculate

$$Q_{\text{model}} = \sigma^{\text{NM}} \text{BR}(\tau\tau)^{\text{NM}} \quad (5.15)$$

with the NMSSM cross-section given by

$$\begin{aligned} \sigma^{\text{NM}} = & (g_{WWH_i}^{\text{NM}})^2 \left(\sigma(WH)^{\text{SM}} + \sigma(ZH)^{\text{SM}} + \sigma(\text{VBF})^{\text{SM}} \right) + \\ & + (g_{t\bar{t}H_i}^{\text{NM}})^2 \sigma(gg)^{\text{SM}}, \end{aligned} \quad (5.16)$$

where $g_{t\bar{t}H_i}^{\text{NM}}$ and $g_{WWH_i}^{\text{NM}}$ once again denote the NMSSM coupling of H_i to the top quark and to the W -boson, respectively, normalized to the SM coupling. If Q_{model} is bigger than Q_{obs} the parameter point is excluded.

LHC exclusion

For the LHC exclusion limits we refer to [53], wherein the results from Atlas and CMS are combined to a 95% CL limit on $\sigma/\sigma^{\text{SM}}$. We rescale $\sigma/\sigma^{\text{SM}}$ to $\sigma/\sigma^{\text{NM}}$ by multiplying with $\sigma^{\text{SM}}/\sigma^{\text{NM}}$. If the value obtained in this way is smaller than one the corresponding parameter point is excluded. The total SM and NMSSM cross-sections necessary for the rescaling are given by

$$\begin{aligned} \sigma^{\text{SM}} = & \sigma(WH)^{\text{SM}} + \sigma(ZH)^{\text{SM}} + \sigma(\text{VBF})^{\text{SM}} + \sigma(gg)^{\text{SM}} + \sigma(t\bar{t}H)^{\text{SM}} \\ \sigma^{\text{NM}} = & (g_{WWH_i}^{\text{NM}})^2 \left(\sigma(WH)^{\text{SM}} + \sigma(ZH)^{\text{SM}} + \sigma(\text{VBF})^{\text{SM}} \right) + \\ & + (g_{t\bar{t}H_i}^{\text{NM}})^2 \sigma(t\bar{t}H)^{\text{SM}} + \sigma(gg)^{\text{NM}} \end{aligned} \quad (5.17)$$

with

$$\begin{aligned} \sigma(gg)^{\text{NM}} = & \sigma(gg)_{\text{top}}^{\text{NM}} (g_{t\bar{t}H_i}^{\text{NM}})^2 + \sigma(gg)_{\text{bot}}^{\text{NM}} (g_{b\bar{b}H_i}^{\text{NM}})^2 + \\ & + \left(\sigma(gg)_{\text{total}}^{\text{NM}} - \sigma(gg)_{\text{top}}^{\text{NM}} - \sigma(gg)_{\text{bot}}^{\text{NM}} \right) (g_{t\bar{t}H_i}^{\text{NM}} g_{b\bar{b}H_i}^{\text{NM}}). \end{aligned}$$

In contrast to Eq. (5.16), all contributions to the gluon-gluon-fusion cross-section are considered. On the one hand there are the contributions from top and from bottom loops, but on the other hand there are also interference effect, which are taken into account in the last term of $\sigma(gg)^{\text{NM}}$. The NMSSM couplings normalized to the SM coupling of H_i to the top or bottom quark are denoted by $g_{t\bar{t}H_i}^{\text{NM}}$ and $g_{b\bar{b}H_i}^{\text{NM}}$. Furthermore, $\sigma(gg)_{\text{total}}^{\text{NM}}$ denotes the total cross-section of $gg \rightarrow H$, whereas $\sigma(gg)_{\text{top}}^{\text{NM}}$ and $\sigma(gg)_{\text{bot}}^{\text{NM}}$ denote the top and bottom contributions to this cross-section.

The exclusion limits applied

Now, we can apply the exclusion limits to the one-loop results of our scenarios. It turns out that part of the parameter range of the λ and M_{H^\pm} variation has already been excluded by LEP, more precisely by the channel $ZH \rightarrow b\bar{b}$. The exclusion limits for these scenarios are shown in Fig. 5.10 (compare to Fig. 5.1 and Fig. 5.7).

For the λ variation all parameter points at which the mass of the lightest Higgs boson is smaller than 113 GeV (at one-loop) are excluded. This corresponds to the region $\lambda \leq 0.6$. The SM Higgs is already excluded for $M_H \leq 114.4$ GeV [50]. But the fact that in our case this limit is lowered is not surprising, since the NMSSM Higgs boson has a reduced HZZ -coupling.

For the M_{H^\pm} variation the regions of $M_{H^\pm} \lesssim 452$ GeV (corresponds to $M_{H_1} \lesssim 112.5$ GeV) and $M_{H^\pm} \gtrsim 585$ GeV (corresponds to $M_{H_1} \lesssim 113.5$ GeV) are excluded. Furthermore, the maximal value of M_{H_1} in the M_{H^\pm} variation is approximately 140.5 GeV, which is just below

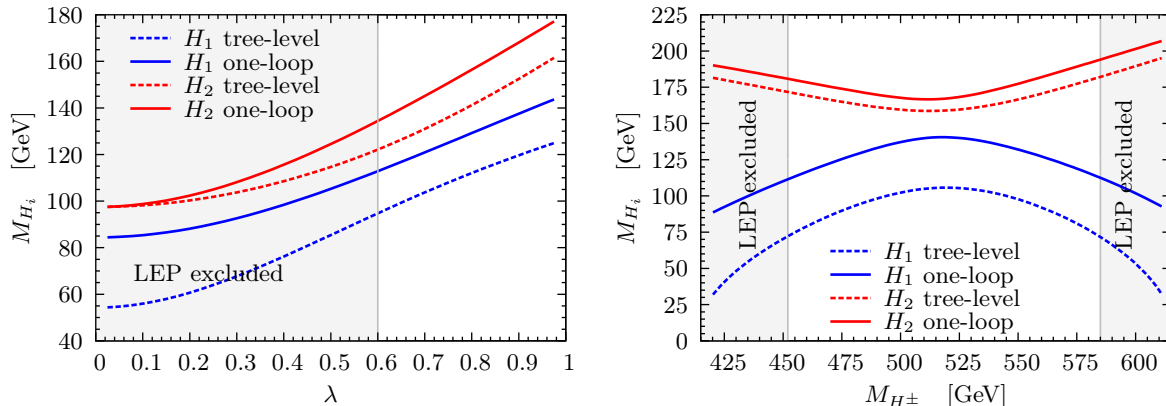


Figure 5.10: Excluded parameter regions for the λ (left) and M_{H^\pm} (right) variation. The exclusion limits were applied to the one-loop masses.

the newest LHC exclusion limits. But taking the uncertainties of the one-loop calculation and the fact that our exclusion limits are only a rough estimate into account, part of the M_{H^\pm} region around $M_{H^\pm} \approx 515$ GeV might actually be excluded.

For all three scenarios the Tevatron results do not exclude any parameter points. In fact, for the scenario of the T_κ variation the complete parameter range is not excluded yet by any of the channels investigated here.

Moreover, we checked our exclusion limits against those obtained with `HiggsBounds` [54] and found complete agreement.

5.3 Complex Higgs Sector

When introducing complex parameters, CP-violation is introduced simultaneously. As discussed earlier, we can set any of the phases $\phi_u, \phi_s, \phi_\lambda, \phi_\kappa, \phi_{A_e}, \phi_{A_d}, \phi_{A_u}, \phi_{M_1}, \phi_{M_2}$ and ϕ_{M_3} to a nonzero value. Depending on which of these phases we choose, different effects can be observed in the tree-level and one-loop Higgs boson masses. For example setting the phase ϕ_{M_3} , so that the soft SUSY breaking gluino mass parameter becomes complex has no effect at all, neither on the tree-level Higgs boson masses nor on the one-loop Higgs boson masses.

That ϕ_{M_3} cannot have any effect on the tree-level masses is obvious, since it does not appear in the tree-level mass matrices of the Higgs sector. That it does not affect the one-loop masses can also be understood easily, since the one-loop corrections to the Higgs boson masses do not include gluinos in the loop. Hence, choosing a complex M_3 can only have an effect for two-loop or even higher order Higgs masses. Following the same arguments it can be concluded that choosing the other soft SUSY breaking gaugino mass parameters or the trilinear soft SUSY sfermion breaking parameters complex by setting an appropriate phase ϕ_{M_i} ($i = 1, 2$) or ϕ_{A_j} ($j = e, d, u$), does not influence the tree-level Higgs boson masses but induces CP-violation at one-loop order, since the neutralinos, charginos and sfermions contribute to the one-loop corrections of the Higgs boson masses. This leaves the phases which appear in the tree-level Higgs mass matrix $\phi_u, \phi_s, \phi_\lambda$ and ϕ_κ . Any of these can create CP-violation already at tree-level.

In the following we will first discuss two scenarios within which CP-violation occurs already at tree-level. The dependence of the tree-level and one-loop Higgs boson masses on the values of the phases is investigated as well as the extent of the CP-violation. Then we have a closer look at a scenario where CP-violation is induced at one-loop level.

5.3.1 CP-Violation at Tree-Level

In contrast to the MSSM, the NMSSM presents the possibility of CP-violation at tree-level. In the MSSM the only phase in the Higgs sector is the relative phase of the Higgs doublets. Due to the tadpole conditions this phase is forced to be a multiple of π . Since the matrix elements of the Higgs mass matrix which are responsible for the mixing of the CP-even and CP-odd states are proportional to the sine of this phase, no mixing between the CP-even and CP-odd states can occur at tree-level in the MSSM. A closer look at \mathcal{M}_{ah} as given in Eq. (3.27b) reveals that the matrix elements responsible for the mixing of the CP-even and CP-odd states at tree-level in the NMSSM are all proportional to $I \propto \sin(\phi_I)$ which was defined in Eq. (3.18). So at tree-level not the explicit individual values of the phases ϕ_u , ϕ_s , ϕ_λ and ϕ_κ matter but only the phase combination

$$\phi_I = \phi_u - 2\phi_s + \phi_\lambda - \phi_\kappa. \quad (5.18)$$

However, at one-loop the explicit values for the individual phases should make a difference, since these phases appear separately in the chargino and neutralino mass matrices, see Eq. (3.46) and Eq. (3.42). So for example changing ϕ_u and ϕ_λ while keeping ϕ_I constant has no effect on the tree-level masses of the Higgs bosons, but does have an effect on the tree-level masses and couplings of the neutralinos and charginos which enter the calculation of the one-loop Higgs boson masses. However, the effects in the one-loop Higgs boson masses due to the changing neutralino and chargino tree-level masses and couplings are tiny.

In the following, two scenarios displaying CP-violation at tree-level will be investigated. In the first scenario we start from a real parameter point and then vary the phase ϕ_λ and discuss the dependence of the Higgs boson masses on this phase. For the second scenario we pick a different real starting point and then allow nonzero values for ϕ_u .

Variation of ϕ_λ

To investigate the dependence of the Higgs boson masses on the phase ϕ_λ we fix the other parameters to

$$\begin{aligned} \tan\beta = 8, \quad |\lambda| = 0.1, \quad |\kappa| = 0.05, \quad |T_\lambda| = 10 \text{ GeV}, \quad |T_\kappa| = 0.5 \text{ GeV}, \quad |\mu| = 100 \text{ GeV}, \\ \text{sgn } R_\lambda = +1, \quad \text{sgn } R_\kappa = -1, \quad M_{\text{SUSY}} = 1.1 \text{ TeV}, \quad M_0 = 600 \text{ GeV}, \quad A_0 = 1000 \text{ GeV}, \\ Q = 300 \text{ GeV}, \quad \phi_u = \phi_s = \phi_\kappa = \phi_{A_i} = \phi_{M_j} = 0 \quad \text{for } i = u, d, e \text{ and } j = 1, 2, 3. \end{aligned}$$

To be able to explain the resulting Higgs boson masses, it is helpful to consider two more quantities. By setting the phase ϕ_λ to a non-zero value we introduce CP-violation. Therefore we cannot distinguish between CP-even and CP-odd Higgs mass eigenstates anymore. A measure for the CP-violation, however is provided by the quantity

$$\mathcal{R}_{i3}^2 + \mathcal{R}_{i4}^2 + \mathcal{R}_{i5}^2. \quad (5.19)$$

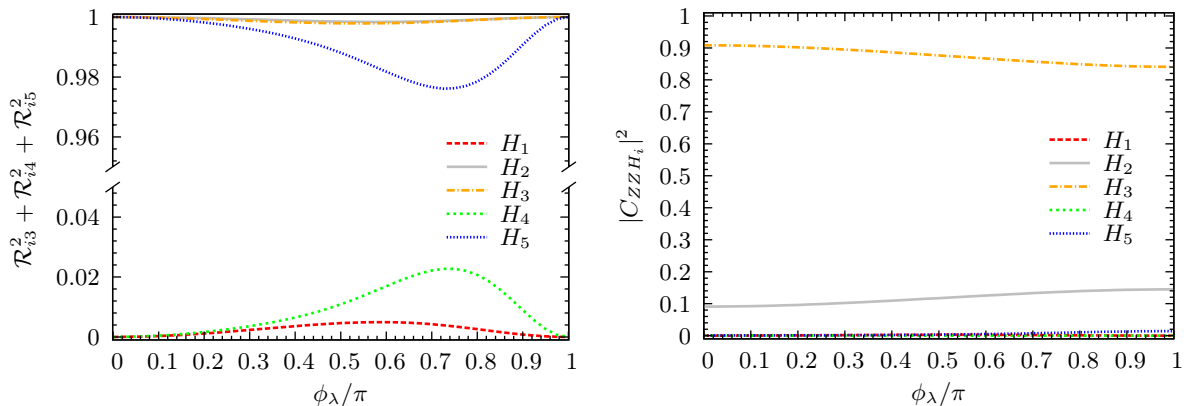


Figure 5.11: The CP-even component of the Higgs bosons at one-loop (left) and the squared coupling ZZH_i normalized to the corresponding SM coupling at one-loop (right) in dependence on ϕ_λ .

Where \mathcal{R}_{ij} is the (i, j) element of the mixing matrix. One can either consider the tree-level quantities, in which case the mixing matrix is defined as the matrix that diagonalizes the Higgs mass matrix (see Eq. (3.28)). Or one can consider the one-loop mixing matrix as defined in Section 4.8. The matrix element squared \mathcal{R}_{i3}^2 is a measure for the strength of the h_d component. Correspondingly, \mathcal{R}_{i4}^2 and \mathcal{R}_{i5}^2 are a measure for the strength of the h_u and h_s component. Without CP-violation the sum of the squares of these three matrix elements is either 0 or 1, depending on whether the Higgs mass eigenstate is CP-odd or CP-even. So if the ‘‘CP-even component’’ $\mathcal{R}_{i3}^2 + \mathcal{R}_{i4}^2 + \mathcal{R}_{i5}^2$ deviates from 0 and 1 this is a sign for CP-violation. In the special case of the real NMSSM we used the singlet component of the Higgs fields to make a statement about their coupling strength to other particles. Here we will make use of the coupling of the i -th Higgs boson to two Z -bosons normalized to the SM value. The square of this normalized coupling will be denoted as $|C_{ZZH_i}|^2$ in the following. It is given by

$$|C_{ZZH_i}|^2 = \left[\cos\beta \mathcal{R}_{i3} + \sin\beta \mathcal{R}_{i4} \right]^2. \quad (5.20)$$

When we refer to the one-loop ZZH_i coupling, we actually mean the coupling as given above but with the one-loop mixing matrix elements instead of the tree-level mixing matrix elements. We did not calculate the loop corrections to this vertex. If $|C_{ZZH_i}|^2 = 1$ the Higgs boson H_i couples to the Z -boson with the same strength as the SM-Higgs, if $|C_{ZZH_i}|^2 < 1$ H_i has a reduced coupling. The CP-even component and $|C_{ZZH_i}|^2$ are plotted in Fig. 5.11 and will be discussed in the following.

The obtained Higgs boson masses at tree-level and at one-loop for this parameter choice are shown in Fig. 5.12 and Fig. 5.13. Note that M_{H_5} is not depicted explicitly, since it displays the same behavior as M_{H_4} and has always almost the same mass as M_{H_4} (the biggest difference in the two masses is less than 2 GeV). In this scenario all Higgs bosons are comparatively light. The mass of the lightest one ranges between ~ 40 GeV and ~ 34 GeV both at tree-level and at one-loop and decreases with increasing ϕ_λ . At the borders of the ϕ_λ range, i.e. for $\phi_\lambda = 0$ and $\phi_\lambda = \pi$ the mass M_{H_1} receives hardly any corrections. Its CP-even component vanishes at these points, i.e. it is CP-odd, whereas for the ϕ_λ values in between CP-violation⁵

⁵By CP-violation we mean the deviation of the CP-even component from zero in this case.

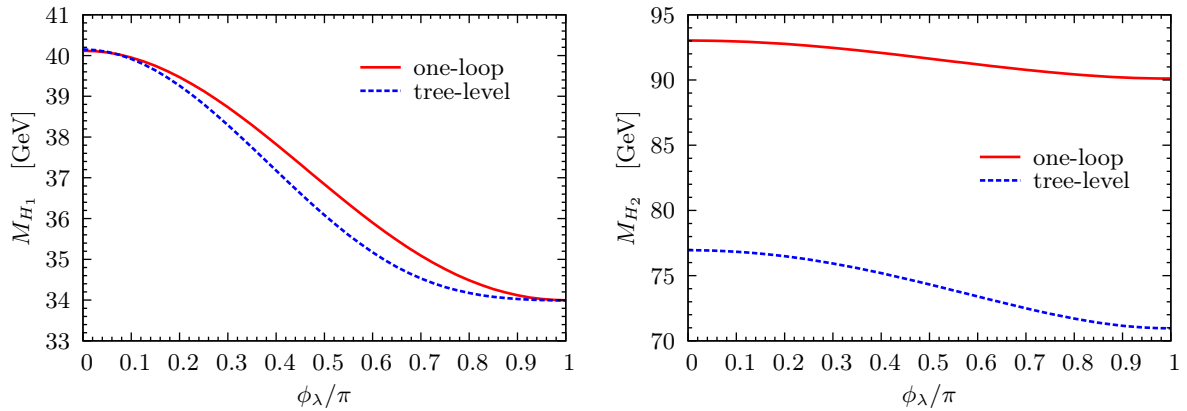


Figure 5.12: The masses of the lightest and next-to-lightest Higgs boson, M_{H_1} (left) and M_{H_2} (right) at tree-level (blue/dashed) and one-loop (red/solid) as a function of ϕ_λ .

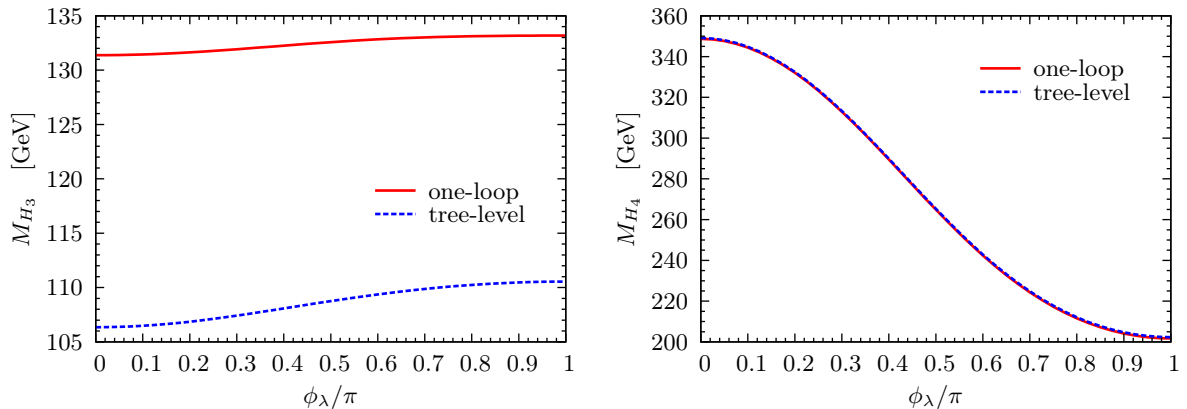


Figure 5.13: The masses M_{H_3} (left) and M_{H_4} (right) at tree-level (blue/dashed) and one-loop (red/solid) as a function of ϕ_λ .

of maximally 0.5% occurs (see Fig. 5.11 on the left) and the mass corrections amount to 2% of the tree-level value. Since H_1 is mostly CP-odd its coupling to the Z -boson all but vanishes (see Fig. 5.11 on the right). The mass of the next-to-lightest Higgs boson M_{H_2} receives corrections of up to 27% of its tree-level mass, so that its one-loop mass ranges from 90 – 93 GeV. H_2 is mostly CP-even (its CP-odd component is always less than 0.2%), but nevertheless its coupling to the Z -boson is drastically reduced to only 9% – 15% of the SM coupling. This is essential if one considers exclusion limits, since such a light Higgs boson can only escape LEP exclusion if its Z -coupling is reduced. The Higgs boson H_3 which is mostly CP-even, however, couples with 84% – 91% of the strength of the SM coupling to the Z -boson and is therefore the most interesting one for phenomenology, since it is the likeliest to be discovered at the LHC. Its one-loop mass ranges from 131 GeV to 133 GeV and the mass corrections are maximally 25 GeV.

The heaviest and next-to-heaviest Higgs bosons H_4 and H_5 cover a broader mass range from 200 GeV to 350 GeV. The mass corrections are tiny and are less than 2% of the tree-level

mass. H_4 and H_5 display the maximal CP-violation occurring in this scenario, which is up to 2.3%. H_4 is mainly CP-odd and H_5 is mainly CP-even. Both have a tiny Z -coupling.

For the complex NMSSM the exclusion limits cannot yet be applied since the decays for the Higgs bosons in the complex NMSSM are not yet implemented in the respective programs. Nevertheless, the scenario discussed here seems plausible as the mass of the SM-like Higgs boson is around 132 GeV. It is surely interesting since it exhibits a mass spectrum which offers the possibility of the SM-like Higgs boson H_3 decaying into the lightest one H_1 . In phenomenological discussions this additional decay channel has to be taken into account.

Variation of ϕ_u

In the following scenario we choose the parameter set

$$\begin{aligned} \tan\beta = 3, \quad |\lambda| = 0.14, \quad |\kappa| = 0.07, \quad |T_\lambda| = 70 \text{ GeV}, \quad |T_\kappa| = 14 \text{ GeV}, \quad |\mu| = 275 \text{ GeV}, \\ \text{sgn } R_\lambda = +1, \quad \text{sgn } R_\kappa = -1, \quad M_{\text{SUSY}} = 1.1 \text{ TeV}, \quad M_0 = 600 \text{ GeV}, \quad A_0 = -900 \text{ GeV}, \\ Q = 300 \text{ GeV}, \quad \phi_s = \phi_\lambda = \phi_\kappa = \phi_{A_i} = \phi_{M_j} = 0 \text{ for } i = u, d, e \text{ and } j = 1, 2, 3, \end{aligned}$$

and vary the phase ϕ_u .

In Fig. 5.14 the CP-even components of the Higgs fields and the normalized Z -coupling squared for this scenario are plotted. For this parameter choice there is only one Higgs boson with noteworthy Z -coupling, namely H_1 . The Higgs bosons H_1 , H_2 and H_5 are mainly CP-even whereas H_4 and H_5 are mainly CP-odd. At $\phi_u = 0$ there is no CP-violation and H_1 is CP-even. With increasing ϕ_u , however, H_1 obtains a small CP-odd component and at the same time its coupling to the Z -boson decreases slightly. At $\phi_u \approx 0.54\pi$ the CP-odd component of H_1 is approximately 0.8%.

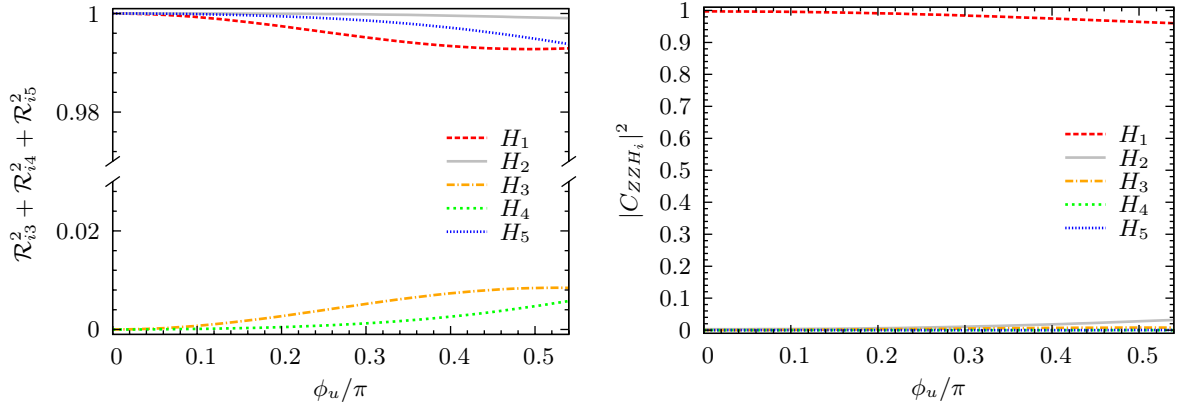


Figure 5.14: The CP-even component of the Higgs bosons at one-loop (left) and the squared coupling ZZH_i normalized to the corresponding SM coupling at one-loop (right) in dependence on ϕ_u .

The Higgs boson masses M_{H_1} and M_{H_2} are shown in Fig. 5.15, while M_{H_3} and M_{H_4} are depicted in Fig. 5.16. Once again M_{H_5} is not plotted, because it displays the same behavior as M_{H_4} . First of all, it is notable that the only Higgs boson that receives any major corrections from tree-level to one-loop is the SM-like H_1 . For M_{H_1} the mass corrections are positive and

can be up to 48 GeV and maximally 55% of the tree-level mass. For all the other Higgs boson masses the corrections are always rather small. The absolute value of the mass corrections is well under 1 GeV and thus less than 0.3% of the respective tree-level masses. The mass of the lightest, i.e. the SM-like Higgs boson, decreases with increasing ϕ_u . At one-loop it ranges between 110 GeV and 120 GeV. Therefore it seems likely that at least part of this parameter space might already be excluded by the experiments. But at the same time this emphasizes the importance of the one-loop corrections, as the tree-level mass of H_1 is surely below the exclusion bounds. The mass of the next-to-lightest Higgs boson M_{H_2} is around 221 GeV and displays only a slight dependence on ϕ_u . The same holds for M_{H_3} , which is around 287 GeV. The masses of the two heaviest Higgs bosons exhibit a stronger dependence on ϕ_u and range between 655 GeV and 766 GeV. Qualitatively the dependence of the masses on the phase ϕ_λ is nearly the same at tree-level as at one-loop. Hence, the main dependence on ϕ_λ already enters in the tree-level mass, whereas varying ϕ_λ does not have such a big effect on the size of the loop corrections.

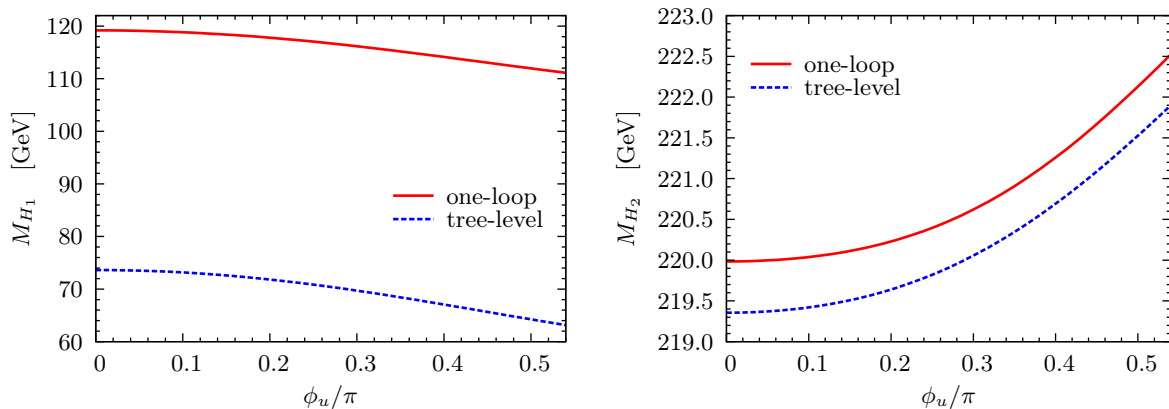


Figure 5.15: The masses of the lightest and next-to-lightest Higgs boson, M_{H_1} (left) and M_{H_2} (right) at tree-level (blue/dashed) and one-loop (red/solid) as a function of ϕ_u .

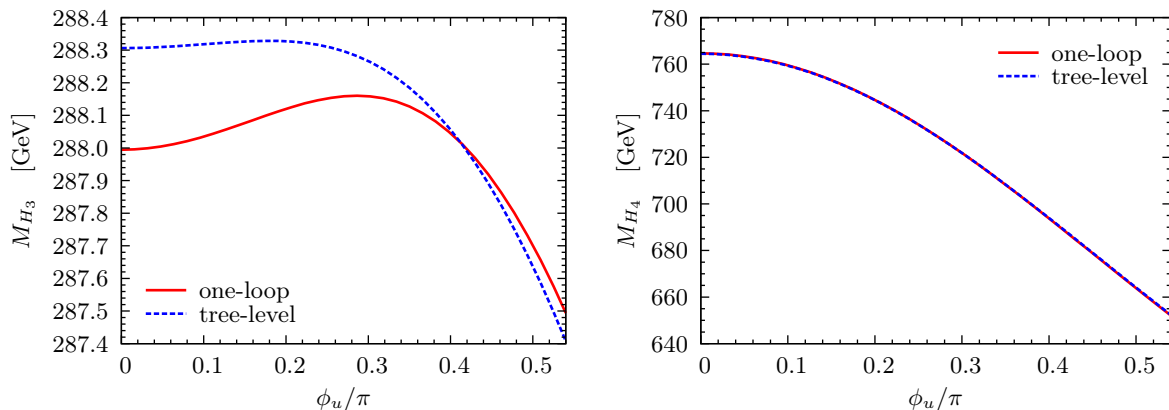


Figure 5.16: The masses M_{H_3} (left) and M_{H_4} (right) at tree-level (blue/dashed) and one-loop (red/solid) as a function of ϕ_u .

5.3.2 CP-Violation Induced at One-Loop Level

To investigate CP-violation induced at one-loop level, we choose a scenario in which the phase of the trilinear soft SUSY breaking parameter for the up-type squarks ϕ_{A_u} is varied. Instead we could also have varied ϕ_{M_i} ($i = 1, 2$) or ϕ_{A_j} ($j = e, d$). But in the example scenarios we considered for those, the effects achieved by varying the phases were marginal. Therefore they will not be presented here.

Variation of ϕ_{A_u}

We vary ϕ_{A_u} and fix all other parameters to

$$\begin{aligned} \tan\beta = 10, \quad |\lambda| = 0.1, \quad |\kappa| = 0.05, \quad |T_\lambda| = 49.8 \text{ GeV}, \quad |T_\kappa| = 2.5 \text{ GeV}, \quad |\mu| = 1000 \text{ GeV}, \\ \text{sgn } R_\lambda = -1, \quad \text{sgn } R_\kappa = -1, \quad M_{\text{SUSY}} = 1.1 \text{ TeV}, \quad M_0 = 600 \text{ GeV}, \quad A_0 = 2000 \text{ GeV}, \\ Q = 300 \text{ GeV}, \quad \phi_u = \phi_s = \phi_\lambda = \phi_\kappa = \phi_{A_i} = \phi_{M_j} = 0 \quad \text{for } i = d, e \text{ and } j = 1, 2, 3. \end{aligned}$$

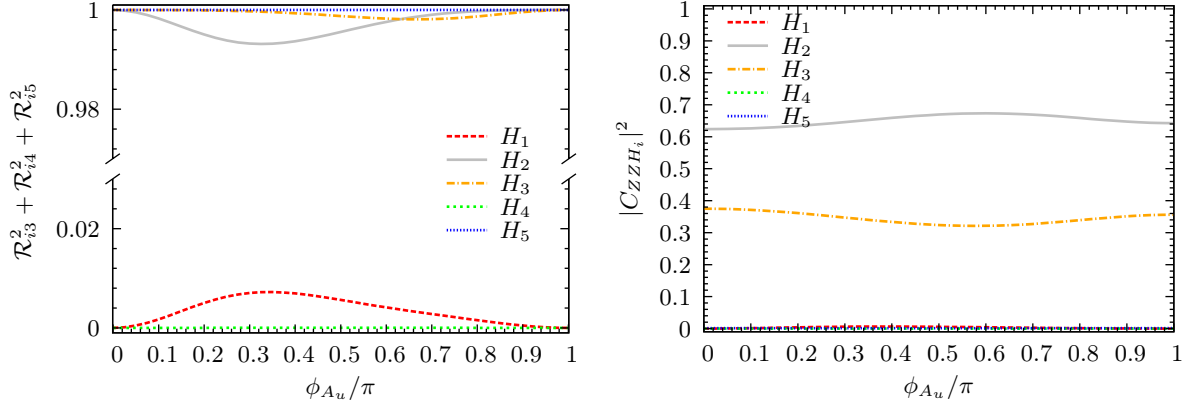


Figure 5.17: The CP-even component of the Higgs bosons at one-loop (left) and the squared coupling ZZH_i normalized to the corresponding SM coupling at one-loop (right) in dependence on ϕ_{A_u} .

In this scenario there are two Higgs bosons with a sizeable coupling to the Z -boson. H_2 couples to the Z -boson with $\sim 65\%$ of the strength of the SM coupling squared and H_3 couples with $\sim 35\%$ of the strength of the SM coupling squared, whereas all other Higgs bosons possess a vanishing Z -coupling (see Fig. 5.17 on the right). Both H_2 and H_3 are mainly CP-even, but the CP-odd component of H_2 can be up to 0.8% , which is - although not very large, the maximal CP-violation occurring in this scenario (see Fig. 5.17 on the left).

Of course the tree-level masses of the Higgs bosons do not depend on ϕ_{A_u} . But they are plotted nevertheless for reference. The masses of the lightest and next-to-lightest Higgs boson M_{H_1} and M_{H_2} are shown in Fig. 5.18. The lightest Higgs boson which is mainly CP-odd and therefore has a vanishing coupling to the Z -boson has a tree-level mass of ~ 82 GeV which receives corrections amounting to maximally 22% of the tree-level mass. This leads to a one-loop mass slightly below 100 GeV. The mass of the next-to-lightest Higgs boson receives corrections of $\sim 34\%$ of the tree-level mass value ($M_{H_2} \approx 99$ GeV). Thus, its one-loop mass ranges from 126 – 132 GeV and the one-loop corrections lift the Higgs mass above the LEP

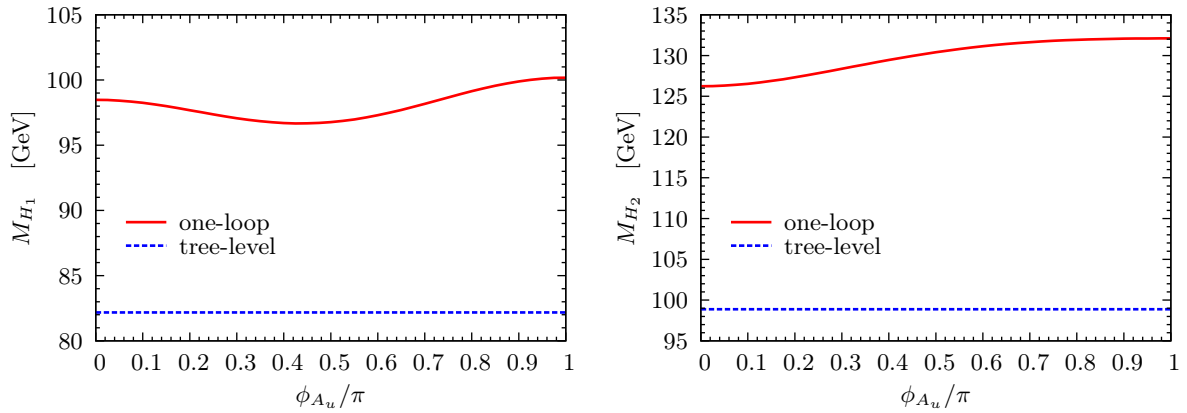


Figure 5.18: The masses of the lightest and next-to-lightest Higgs boson, M_{H_1} (left) and M_{H_2} (right) at tree-level (blue/dashed) and one-loop (red/solid) as a function of ϕ_{A_u} .

exclusion bounds, which of course need to be modified to account for the reduced Z -coupling. Figure 5.19 displays M_{H_3} and M_{H_4} as a function of ϕ_{A_u} . The mass of H_3 receives only small corrections of less than 5%. The tree-level mass of $M_{H_3} \approx 143$ GeV is shifted to 147–150 GeV at one-loop. If H_3 were the SM-Higgs, it would already be excluded by LHC data. But its reduced coupling, both to the vector bosons and the quarks (not explicitly discussed here), might actually save it from exclusion. Of course a thorough investigation of the exclusion limits is inevitable and has to be performed sooner or later. The next-to-heaviest Higgs boson H_4 has a tree-level mass of $M_{H_4} \approx 292$ GeV, which receives corrections of less than 0.5%. The mass of the heaviest Higgs boson is not plotted here. M_{H_5} is approximately 987 GeV, displays quasi no dependence on ϕ_{A_u} and receives tiny corrections of less than 0.05%.

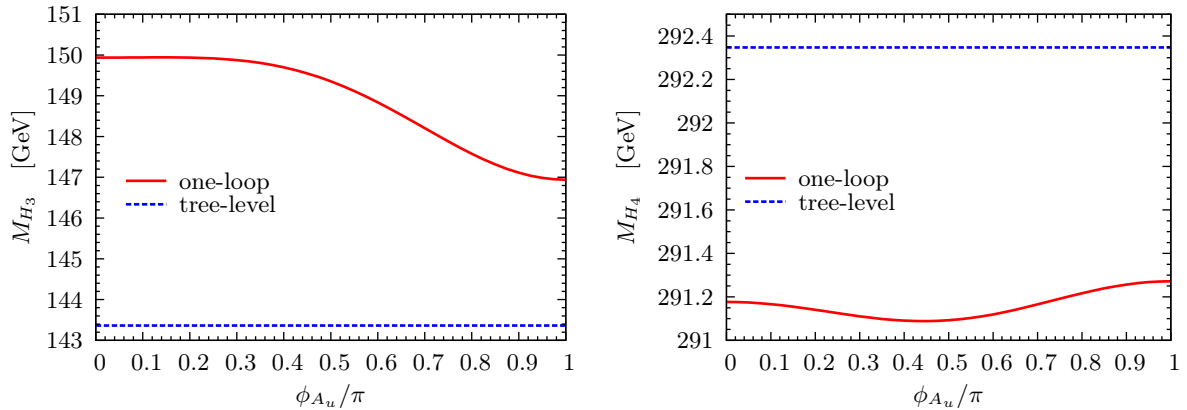


Figure 5.19: The masses M_{H_3} (left) and M_{H_4} (right) at tree-level (blue/dashed) and one-loop (red/solid) as a function of ϕ_{A_u} .

Even though the phase ϕ_{A_u} enters only in the one-loop corrections and not in the tree-level mass, the one-loop masses clearly display a dependence on ϕ_{A_u} . In fact, the one-loop masses can be changed by several GeV by varying ϕ_{A_u} .

Summary and Conclusion

In this thesis the full one-loop calculation of the Higgs boson masses in the complex NMSSM was presented. To this end, the Higgs sector of the NMSSM was firstly discussed at tree-level and later on the full renormalization procedure of the Higgs sector necessary to obtain the one-loop masses was described. This theoretical part was followed by the numerical analysis conducted for some example scenarios.

Although, in contrast to the MSSM, the NMSSM allows for tree-level Higgs boson masses above the mass of the Z -boson, our analysis shows that the inclusion of the one-loop corrections to the Higgs boson masses is nevertheless crucial, since they lift the mass of the light CP-even Higgs boson above the LEP limits. The one-loop corrections can be quite large, especially for Higgs bosons with a small tree-level mass. For some parameter points they can more than triple the tree-level mass. As our discussion of the exclusion limits provided by the collider experiments proves, the NMSSM provides phenomenologically valid scenarios, which should be taken into consideration in the Higgs searches, since they predict Higgs bosons with different properties than those of the MSSM or the SM.

For the special case of the real NMSSM three different renormalization schemes were implemented: a pure $\overline{\text{DR}}$ scheme to make contact to the calculations existing in the literature, a scheme that mixes on-shell and $\overline{\text{DR}}$ renormalization conditions as well as a pure on-shell scheme. For the example scenarios considered here the results obtained employing the different renormalization schemes differed by at most 10%. As an indication for the coupling strength of the Higgs bosons to the other particles we considered the corresponding singlet components. Since the coupling of the Higgs boson to the SM particles decreases with increasing singlet component, a Higgs boson with a large singlet component can escape detection at the collider experiments due to its reduced couplings, even if the SM Higgs boson of the same mass is already excluded. Hence, the singlet component is a useful quantity, which allows to draw conclusions about the properties of the respective Higgs boson. As the investigation of the dependence on the top quark mass revealed, the main part of the corrections for the light CP-even MSSM-like Higgs boson stems from the top sector. The variation of the renormalization scale, which enters the one-loop calculation, provides an estimate for the missing higher order corrections, which are $\mathcal{O}(10\%)$.

For the more general case of the CP-violating NMSSM, i.e. the complex NMSSM, we found that in comparison to the CP-conserving NMSSM only two more counterterms have to be introduced to renormalize the Higgs sector. We showed that setting any of the phases appearing in the Higgs sector at tree-level leads to CP-violation at tree-level. As an indicator for the strength of the CP-violation we used the CP-even component of the respective Higgs boson. If CP is conserved the CP-even component of a Higgs boson can either be zero or one. In the investigated example scenarios the maximal deviation of the CP-even component from these two values was 2.3%. This mixing of the CP-even and CP-odd interaction eigenstates to the one-loop mass eigenstates can reduce the couplings of the mass eigenstates to the SM particles even further. In addition to CP-violation at tree-level, we also discussed CP-violation induced at one-loop level. We found that even though these phases enter only in the one-loop corrections and not in the tree-level Higgs boson masses their variation can have an effect of several GeV on the resulting one-loop masses.

Altogether this thesis contributes to the effort of providing phenomenological predictions for the Higgs sector of the complex NMSSM that might open a new perspective for the ongoing Higgs search at the LHC. Calculating the one-loop masses is only a first step. To obtain the full picture it will, amongst other things, be helpful to calculate the Higgs masses at higher orders. In fact, for the real NMSSM the leading logarithmic $\mathcal{O}(\alpha_t\alpha_s + \alpha_b\alpha_s)$ two-loop corrections to the Higgs boson masses in the effective potential approach are discussed in [44]. For the complex NMSSM the logarithmically enhanced two-loop effects employing the renormalization-group improved approach are presented in [55]. Furthermore, it would be desirable to have the one-loop corrected vertices involving Higgs bosons at our disposal. Once all these different pieces are merged, we will be able to make phenomenological predictions for the NMSSM Higgs bosons that will hopefully enable us to clearly distinguish the NMSSM Higgs sector from the MSSM or SM Higgs sectors.

The Supersymmetric Lagrangian

The Lagrangian of an arbitrary supersymmetric theory can be constructed once the particle content, the gauge structure and the superpotential of the theory are provided. Let us assume a theory which contains chiral supermultiplets formed by a scalar field ϕ_i , its superpartner the Weyl-fermion ψ_i and an auxiliary field F_i . The auxiliary field does not propagate and is therefore no physical field. Its purpose is to close SUSY off-shell. When going on-shell F_i can be eliminated using the equations of motion for F_i . Furthermore there are gauge bosons A_μ^a , the corresponding gaugino λ^a and an auxiliary field \mathcal{D}^a which can be grouped into a gauge supermultiplet. A general scalar superpotential for such a theory would look like this:

$$W = \frac{1}{2}\mu^{ij}\phi_i\phi_j + \frac{1}{6}\lambda^{ijk}\phi_i\phi_j\phi_k. \quad (\text{A.1})$$

The supersymmetric Lagrangian is then given by

$$\mathcal{L}_{\text{SUSY}} = \mathcal{L}_{\text{chiral}} + \mathcal{L}_{\text{chiral,int}} + \mathcal{L}_{\text{gauge}} + \mathcal{L}_{\text{yukawa}}. \quad (\text{A.2})$$

The individual parts of the Lagrangian read

$$\mathcal{L}_{\text{chiral}} = -(\text{D}_\mu\phi_i)^\dagger(\text{D}^\mu\phi_i) - i\psi^{i*}\bar{\sigma}^\mu\text{D}_\mu\psi_i + F^{i*}F_i, \quad (\text{A.3a})$$

$$\mathcal{L}_{\text{chiral,int}} = -\frac{1}{2}W^{ij}\psi_i\psi_j + W^iF_i + c.c., \quad (\text{A.3b})$$

$$\mathcal{L}_{\text{gauge}} = -\frac{1}{4}F_{\mu\nu}^aF^{\mu\nu a} - i\lambda^{a\dagger}\bar{\sigma}^\mu\text{D}_\mu\lambda^a + \frac{1}{2}\mathcal{D}^a\mathcal{D}^a, \quad (\text{A.3c})$$

$$\mathcal{L}_{\text{yukawa}} = -\sqrt{2}g\left((\phi^*T^a\psi)\lambda^a + \lambda^{a\dagger}(\psi^\dagger T^a\phi)\right) + g(\phi^*T^a\phi)\mathcal{D}^a. \quad (\text{A.3d})$$

$\mathcal{L}_{\text{chiral}}$ is of the same form as the free Lagrangian for the supersymmetric theory which is made up of chiral supermultiplets only. However, here we wrote down the gauge invariant form. Hence, the gauge interactions of the chiral supermultiplets have already been incorporated by applying the covariant derivatives

$$\text{D}_\mu\phi_i = \partial_\mu\phi_i + igA_\mu^a(T^a\phi)_i \quad \text{and} \quad \text{D}_\mu\psi_i = \partial_\mu\psi_i + igA_\mu^a(T^a\psi)_i. \quad (\text{A.4})$$

Here g denotes the gauge coupling and T^a are the generators of the gauge group. The index a denotes the adjoint representation. All other renormalizable interactions can be derived from the superpotential and are given by $\mathcal{L}_{\text{chiral,int}}$ with the abbreviations

$$W^i = \frac{\delta W}{\delta \phi_i} \quad \text{and} \quad W^{ij} = \frac{\delta^2 W}{\delta \phi_i \delta \phi_j}. \quad (\text{A.5})$$

Using $\mathcal{L}_{\text{chiral}}$ and $\mathcal{L}_{\text{chiral,int}}$ the equations of motion for F_i can be derived. It turns out that F_i can be replaced by

$$F_i = -W_i^* \quad \text{and} \quad F^{i*} F_i = \left| \frac{\delta W}{\delta \phi_i} \right|^2. \quad (\text{A.6})$$

The gauge field part of the supersymmetric Lagrangian is given by $\mathcal{L}_{\text{gauge}}$. Here $F_{\mu\nu}^a$ is the Yang-Mills field strength tensor

$$F_{\mu\nu}^a = \partial_\mu A_\nu^a - \partial_\nu A_\mu^a - g f^{abc} A_\mu^b A_\nu^c \quad \text{with the structure constants } f^{abc}. \quad (\text{A.7})$$

The covariant derivative of the gaugino fields is

$$D_\mu \lambda^a = \partial_\mu \lambda^a - g f^{abc} A_\mu^b \lambda^c. \quad (\text{A.8})$$

Finally, the only interactions left, which are not forbidden by renormalizability or gauge invariance are summarized in $\mathcal{L}_{\text{yukawa}}$. Using $\mathcal{L}_{\text{gauge}}$ and $\mathcal{L}_{\text{yukawa}}$ we can express the auxiliary field \mathcal{D}^a via

$$\mathcal{D}^a = -g(\phi^* T^a \phi). \quad (\text{A.9})$$

The derivation presented here follows the approach presented in [10].

Loop Functions

When calculating the one-loop self-energies and tadpole diagrams we always come across integrals over the loop momentum. There is a formalism for the treatment of these integrals. These methods were introduced by Passarino and Veltman [56], t'Hooft and Veltman [57] and Melrose [58]. We stick to the conventions as used in `LoopTools` [40] and in [59].

The following loop integrals are encountered when calculation one-loop corrections:

$$A_0(m^2) = 16\pi^2 Q^{4-D} \int \frac{d^D q}{i(2\pi)^D} \frac{1}{q^2 - m^2 + i\varepsilon} \quad (\text{B.1})$$

$$B_0(p^2, m_1^2, m_2^2) = 16\pi^2 Q^{4-D} \int \frac{d^D q}{i(2\pi)^D} \frac{1}{(q^2 - m_1^2 + i\varepsilon)((q-p)^2 - m_2^2 + i\varepsilon)} \quad (\text{B.2})$$

$$\begin{aligned} B_\mu(p^2, m_1^2, m_2^2) &= p_\mu B_1(p^2, m_1^2, m_2^2) = \\ &= 16\pi^2 Q^{4-D} \int \frac{d^D q}{i(2\pi)^D} \frac{q_\mu}{(q^2 - m_1^2 + i\varepsilon)((q-p)^2 - m_2^2 + i\varepsilon)} \end{aligned} \quad (\text{B.3})$$

$$\begin{aligned} B_{\mu\nu}(p^2, m_1^2, m_2^2) &= g_{\mu\nu} B_{00}(p^2, m_1^2, m_2^2) + p_\mu p_\nu B_{11}(p^2, m_1^2, m_2^2) = \\ &= 16\pi^2 Q^{4-D} \int \frac{d^D q}{i(2\pi)^D} \frac{q_\mu q_\nu}{(q^2 - m_1^2 + i\varepsilon)((q-p)^2 - m_2^2 + i\varepsilon)} \end{aligned} \quad (\text{B.4})$$

As mentioned in Section 4.1.1 we use dimensional reduction to regularize the UV-divergences of the loop integrals. Therefore, we calculate the integrals in general D dimensions instead of in four dimensions. Here Q denotes the renormalization scale, which has mass dimension and needs to be introduced to ensure that the overall dimension of the integral remains the same for any D . The infinitesimal imaginary part $i\varepsilon$ is needed to regulate the singularities of the integrand. The loop integrals are classified according to the number of external legs in the corresponding Feynman diagrams. The loop functions with one external leg are denoted by A and those with two external legs are denoted by B . The indices 0, μ and $\mu\nu$ indicate

the Lorentz structure of the integrals. Instead of using B_μ and $B_{\mu\nu}$ one can use the tensor coefficients B_1 , B_{00} and B_{11} . B_1 is the coefficient of p_μ , B_{00} is the coefficient of $g_{\mu\nu}$ and B_{11} is the coefficient of $p_\mu p_\nu$.

By performing the integral one obtains the following analytic expression for the scalar one-point function A_0 :

$$A_0(m^2) = m^2 \left(\Delta - \ln \frac{m^2}{Q^2} + 1 \right) \quad \text{with} \quad \Delta = \frac{2}{4-D} - \gamma_E + \ln 4\pi. \quad (\text{B.5})$$

γ_E denotes the Euler-Mascheroni constant, $\gamma_E \approx 0.5772$. It is apparent that Δ diverges for $D \rightarrow 4$.

The scalar two-point function B_0 can be written as

$$B_0(p^2, m_1^2, m_2^2) = \Delta - \ln \frac{p^2}{Q^2} - f_B(x_+) - f_B(x_-) \quad (\text{B.6})$$

$$\text{with} \quad f_B(x) = \ln(1-x) - x \ln(1-x^{-1}) - 1, \quad x_\pm = \frac{s \pm \sqrt{s^2 - 4p^2(m_1^2 - i\epsilon)}}{2p^2}$$

$$\text{and} \quad s = p^2 - m_2^2 + m_1^2.$$

The tensor coefficients B_1 , B_{00} and B_{11} can be expressed in terms of B_0 and A_0 :

$$B_1(p^2, m_1^2, m_2^2) = \frac{1}{2p^2} \left[A_0(m_1^2) - A_0(m_2^2) - (p^2 - m_2^2 + m_1^2) B_0(p^2, m_1^2, m_2^2) \right], \quad (\text{B.7})$$

$$B_{00}(p^2, m_1^2, m_2^2) = \frac{1}{2(D-1)} \left[A_0(m_2^2) + 2m_1^2 B_0(p^2, m_1^2, m_2^2) + (p^2 - m_2^2 + m_1^2) B_1(p^2, m_1^2, m_2^2) + m_1^2 + m_2^2 - p^2/3 \right], \quad (\text{B.8})$$

$$B_{11}(p^2, m_1^2, m_2^2) = \frac{1}{2p^2(D-1)} \left[(D-2) A_0(m_2^2) - 2m_1^2 B_0(p^2, m_1^2, m_2^2) - D(p^2 - m_2^2 + m_1^2) B_1(p^2, m_1^2, m_2^2) - m_1^2 - m_2^2 + p^2/3 \right]. \quad (\text{B.9})$$

Running Top and Bottom Quark Masses

In the following the formulas needed to convert the input values for the top and bottom quark mass into the running $\overline{\text{DR}}$ masses at the renormalization scale are presented.

Running Top Mass

As input value for the top quark mass we use the pole mass $m_t = 173.3$ GeV.

1. The pole mass is converted into the running pole mass at the scale of the top pole mass (i.e. $Q = m_t$). Therefore the gluon corrections, i.e. the corrections originating from the diagram with a gluon and a top quark in the loop are included. This leads to the running top mass

$$m_t^{\text{run,gluon}}(m_t) = m_t^{\text{pole}} + \Delta m_t^{\text{gluon}} \tag{C.1}$$

$$\text{with } \Delta m_t^{\text{gluon}} = \frac{g_s^2}{6\pi^2} m_t \left[B_1(m_t^2, 0, m_t^2) - B_0(m_t^2, 0, m_t^2) \right].$$

To obtain this correction dimensional reduction was employed. Hence, the running mass is the $\overline{\text{DR}}$ running mass.

2. Now, the running top mass which includes the gluon corrections is evolved from the scale m_t up to the renormalization scale Q by means of the SM renormalization group equation. The renormalization group equation can be found e.g. in [60] and reads

$$m_t^{\text{run,gluon}}(Q) = m_t^{\text{run,gluon}}(m_t) \cdot \left[\frac{\alpha_s(Q)}{\alpha_s(m_t)} \right]^{\frac{1}{\pi\beta_0}} \tag{C.2}$$

$$\text{with } \alpha_s(Q) = \frac{\alpha_s(M_Z)}{1 + \beta_0 \alpha_s(M_Z) \ln\left(\frac{Q^2}{M_Z^2}\right)} \quad \text{and} \quad \beta_0 = \frac{33 - 2n}{12\pi}.$$

Here n is the number of active quark flavors which is taken to be six.

3. Since in the scenario where we actually use the running mass we take the renormalization scale Q to be equal to the SUSY scale, the gluino corrections are added at this scale. By gluino corrections we mean, the corrections due to a gluino and a top squark in the loop. So, finally we obtain the running $\overline{\text{DR}}$ top mass which includes both the gluon and the gluino corrections at the renormalization scale Q :

$$m_t^{\text{run,gluino}}(Q) = m_t^{\text{run,gluon}}(Q) + \Delta m_t^{\text{gluino}}$$

with

$$\Delta m_t^{\text{gluino}} = -\frac{g_s^2}{12\pi^2} \left[m_t \left[B_1(m_t^2, m_{\tilde{g}}^2, m_{\tilde{t}_1}^2) + B_1(m_t^2, m_{\tilde{g}}^2, m_{\tilde{t}_2}^2) \right] + m_{\tilde{g}} \sin(2\theta_{\tilde{t}}) \left[B_0(m_t^2, m_{\tilde{g}}^2, m_{\tilde{t}_1}^2) - B_0(m_t^2, m_{\tilde{g}}^2, m_{\tilde{t}_2}^2) \right] \right].$$

Here $m_{\tilde{g}}$ is the gluino mass, $m_{\tilde{t}_1}$ and $m_{\tilde{t}_2}$ are the top squark masses and $\theta_{\tilde{t}}$ is the rotation angle from the mixing matrix of the squarks defined by:

$$\begin{pmatrix} \tilde{t}_1 \\ \tilde{t}_2 \end{pmatrix} = \begin{pmatrix} \cos \theta_{\tilde{t}} & \sin \theta_{\tilde{t}} \\ -\sin \theta_{\tilde{t}} & \cos \theta_{\tilde{t}} \end{pmatrix} \begin{pmatrix} \tilde{t}_L \\ \tilde{t}_R \end{pmatrix}. \quad (\text{C.3})$$

The formulas for the gluon and gluino corrections were calculated using `FeynArts` and `FormCalc` but can also be found in the literature [59].

Running Bottom Mass

As input value for the bottom mass we take $m_b^{\overline{\text{MS}}}(m_b) = 4.19$ GeV.

1. This $\overline{\text{MS}}$ input value has to be converted into the $\overline{\text{DR}}$ input value. How this is done is described in [61]. The relevant formula is

$$m_b^{\overline{\text{DR}}}(m_b) = m_b^{\overline{\text{MS}}}(m_b) \left(1 - \frac{1}{3\pi} \alpha_s(m_b) - \frac{29}{72\pi} \alpha_s(m_b)^2 \right). \quad (\text{C.4})$$

2. Using the renormalization group equation this can be evolved up to the renormalization scale

$$m_b^{\text{run,gluon}}(Q) = m_b^{\text{run,gluon}}(m_b) \cdot \left[\frac{\alpha_s(Q)}{\alpha_s(m_b)} \right]^{\frac{1}{\pi\beta_0}}, \quad (\text{C.5})$$

where $\alpha_s(Q)$ and β_0 are as given in Eq. C.2.

3. At the renormalization scale Q the gluino corrections are included. They are given by:

$$m_b^{\text{run,gluino}}(Q) = m_b^{\text{run,gluon}}(Q) + \Delta m_b^{\text{gluino}}$$

with

$$\Delta m_b^{\text{gluino}} = -\frac{g_s^2}{12\pi^2} \left[m_b \left[B_1(m_b^2, m_{\tilde{g}}^2, m_{\tilde{b}_1}^2) + B_1(m_b^2, m_{\tilde{g}}^2, m_{\tilde{b}_2}^2) \right] + m_{\tilde{g}} \sin(2\theta_{\tilde{b}}) \left[B_0(m_b^2, m_{\tilde{g}}^2, m_{\tilde{b}_1}^2) - B_0(m_b^2, m_{\tilde{g}}^2, m_{\tilde{b}_2}^2) \right] \right].$$

Here $m_{\tilde{b}_1}$ and $m_{\tilde{b}_2}$ denote the bottom squark masses and $\theta_{\tilde{b}}$ is defined by the mixing of the bottom squarks

$$\begin{pmatrix} \tilde{b}_1 \\ \tilde{b}_2 \end{pmatrix} = \begin{pmatrix} \cos \theta_{\tilde{b}} & \sin \theta_{\tilde{b}} \\ -\sin \theta_{\tilde{b}} & \cos \theta_{\tilde{b}} \end{pmatrix} \begin{pmatrix} \tilde{b}_L \\ \tilde{b}_R \end{pmatrix}. \quad (\text{C.6})$$

Counterterm Mass Matrix of the Higgs Sector

In this appendix the complete counterterm Higgs mass matrix, which one obtains after carrying out the procedure as described in Section 4.2, is presented. The matrix $\delta\mathcal{M}_{\text{Higgs}}$ is given in the basis of the interaction eigenstates after the separation of the Goldstone boson, i.e. the basis is (a, a_s, h_d, h_u, h_s) . Note that the counterterm mass matrix is symmetric

$$\delta\mathcal{M}_{\text{Higgs}}\Big|_{ij} = \delta\mathcal{M}_{\text{Higgs}}\Big|_{ji}. \quad (\text{D.1})$$

Hence, it is sufficient to state 15 elements of the counterterm matrix explicitly and the rest follows from symmetry.

Here the complex parameters were written in terms of their absolute value and their phase. In the NMSSM Higgs mass matrix only three phase combinations appear (see Eq. 3.35)

$$\begin{aligned} \phi_I &= \phi_u - 2\phi_s + \phi_\lambda - \phi_\kappa, \\ \phi_{I_\lambda} &= \phi_u + \phi_s + \phi_{T_\lambda} \quad \text{and} \\ \phi_{I_\kappa} &= 3\phi_s + \phi_{T_\kappa}. \end{aligned} \quad (\text{D.2})$$

Moreover we used the abbreviations $s_x = \sin x$, $c_x = \cos x$ and $t_x = \tan x$. Once again θ_W denotes the Weinberg angle.

$$\begin{aligned} \delta\mathcal{M}_{\text{Higgs}}\Big|_{11} &= \delta M_{H^\pm}^2 + \delta M_Z^2 \frac{2|\lambda|^2 M_W^4}{e^2 M_Z^4} + \delta M_W^2 \left(\frac{2|\lambda|^2 \left(1 - \frac{2M_W^2}{M_Z^2}\right)}{e^2} - 1 \right) + \\ &\quad - \delta Z_e \frac{4|\lambda|^2 M_W^2 s_{\theta_W}^2}{e^2} + \delta\lambda \frac{4|\lambda| M_W^2 s_{\theta_W}^2}{e^2} \end{aligned} \quad (\text{D.3})$$

$$\delta\mathcal{M}_{\text{Higgs}}\Big|_{12} = \delta \tan\beta \frac{2c_{2\beta} c_\beta^2 M_W s_{\theta_W} \left(2|\lambda|^2 M_W^2 s_{\theta_W}^2 + e^2 (M_{H^\pm}^2 - M_W^2) \right)}{e^3 v_s} +$$

$$\begin{aligned}
 & + \delta\lambda \left(\frac{4|\lambda|M_W^3 s_{2\beta} s_{\theta_W}^3}{e^3 v_s} - \frac{3|\kappa|M_W v_s c_{\phi_I} s_{\theta_W}}{e} \right) - \delta\kappa \frac{3|\lambda|M_W v_s c_{\phi_I} s_{\theta_W}}{e} + \\
 & + \frac{\delta M_W^2}{2e^3 M_W M_Z^4 v_s s_{\theta_W}} \left[s_{2\beta} \left(6|\lambda|^2 M_W^2 (-3M_W^2 M_Z^2 + 2M_W^4 + M_Z^4) + \right. \right. \\
 & + e^2 M_Z^2 (-2M_{H^\pm}^2 M_W^2 + M_{H^\pm}^2 M_Z^2 - 3M_W^2 M_Z^2 + 4M_W^4) \left. \right) + \\
 & \left. - 3e^2 |\kappa| |\lambda| M_Z^2 v_s^2 c_{\phi_I} (M_Z^2 - 2M_W^2) \right] + \\
 & + \delta M_Z^2 \frac{M_W^3}{2e^3 M_Z^4 v_s s_{\theta_W}} \left(e^2 (s_{2\beta} (M_{H^\pm}^2 - M_W^2) - 3|\kappa| |\lambda| v_s^2 c_{\phi_I}) + 6|\lambda|^2 M_W^2 s_{2\beta} s_{\theta_W}^2 \right) + \\
 & - \delta v_s \frac{M_W s_{\theta_W}}{e^3 v_s^2} \left(e^2 (3|\kappa| |\lambda| v_s^2 c_{\phi_I} + s_{2\beta} (M_{H^\pm}^2 - M_W^2)) + 2|\lambda|^2 M_W^2 s_{2\beta} s_{\theta_W}^2 \right) + \\
 & + \delta Z_e \frac{M_W s_{\theta_W}}{e^3 v_s} \left(e^2 (3|\kappa| |\lambda| v_s^2 c_{\phi_I} + s_{2\beta} (M_W^2 - M_{H^\pm}^2)) - 6|\lambda|^2 M_W^2 s_{2\beta} s_{\theta_W}^2 \right) + \\
 & + \delta\phi_I \frac{3|\kappa| |\lambda| M_W v_s s_{\theta_W} s_{\phi_I}}{e} - \delta t_{h_u} \frac{c_\beta^3}{v_s} - \delta t_{h_d} \frac{s_\beta^3}{v_s} + \delta M_{H^\pm}^2 \frac{M_W s_{2\beta} s_{\theta_W}}{e v_s} \quad (D.4)
 \end{aligned}$$

$$\begin{aligned}
 \delta\mathcal{M}_{\text{Higgs}} \Big|_{13} & = \delta t_{ad} \frac{e}{2M_W t_\beta s_{\theta_W}} - \delta \tan\beta \frac{c_\beta^3}{2e^2} \left[e^2 \left(\frac{|\kappa| |\lambda| v_s^2 s_{\phi_I - \phi_{I\lambda}}}{t_\beta c_{\phi_{I\lambda}}} + 2c_\beta^2 (M_{H^\pm}^2 - M_W^2) t_{\phi_{I\lambda}} \right) + \right. \\
 & + 4|\lambda|^2 c_\beta^2 M_W^2 s_{\theta_W}^2 t_{\phi_{I\lambda}} \left. \right] + \delta M_Z^2 \frac{c_\beta M_W^2}{4e^2 M_Z^4 s_{\theta_W}^2} \left[-4|\lambda|^2 c_\beta M_W^2 s_\beta s_{\theta_W}^2 t_{\phi_{I\lambda}} + \right. \\
 & + e^2 \left(t_{\phi_{I\lambda}} (|\kappa| |\lambda| v_s^2 c_{\phi_I} + s_{2\beta} (M_W^2 - M_{H^\pm}^2)) - |\kappa| |\lambda| v_s^2 s_{\phi_I} \right) \left. \right] + \\
 & + \delta Z_e \frac{c_\beta}{2e^2} \left[e^2 \left(|\kappa| |\lambda| v_s^2 s_{\phi_I} - t_{\phi_{I\lambda}} (|\kappa| |\lambda| v_s^2 c_{\phi_I} + s_{2\beta} (M_W^2 - M_{H^\pm}^2)) \right) + \right. \\
 & + 4|\lambda|^2 c_\beta M_W^2 s_\beta s_{\theta_W}^2 t_{\phi_{I\lambda}} \left. \right] - \delta M_W^2 \frac{c_\beta (2M_W^2 - M_Z^2)}{4e^2 M_W^2 M_Z^2 s_{\theta_W}^2 c_{\phi_{I\lambda}}} \left[-4|\lambda|^2 c_\beta M_W^2 s_\beta s_{\theta_W}^2 s_{\phi_{I\lambda}} + \right. \\
 & \left. + e^2 \left(s_{\phi_{I\lambda}} (|\kappa| |\lambda| v_s^2 c_{\phi_I} + s_{2\beta} (M_W^2 - M_{H^\pm}^2)) - |\kappa| |\lambda| v_s^2 s_{\phi_I} c_{\phi_{I\lambda}} \right) \right] \quad (D.5)
 \end{aligned}$$

$$\begin{aligned}
 \delta\mathcal{M}_{\text{Higgs}} \Big|_{14} & = \delta t_{ad} \frac{e}{2M_W s_{\theta_W}} - \delta \tan\beta \frac{c_\beta^3}{2e^2} \left[4|\lambda|^2 c_\beta M_W^2 s_\beta s_{\theta_W}^2 t_{\phi_{I\lambda}} + \right. \\
 & + e^2 \left(|\kappa| |\lambda| v_s^2 s_{\phi_I} - t_{\phi_{I\lambda}} (|\kappa| |\lambda| v_s^2 c_{\phi_I} + s_{2\beta} (M_W^2 - M_{H^\pm}^2)) \right) \left. \right] + \\
 & + \delta M_Z^2 \frac{M_W^2 s_\beta}{4e^2 M_Z^4 s_{\theta_W}^2} \left[e^2 \left(t_{\phi_{I\lambda}} (|\kappa| |\lambda| v_s^2 c_{\phi_I} + s_{2\beta} (M_W^2 - M_{H^\pm}^2)) - |\kappa| |\lambda| v_s^2 s_{\phi_I} \right) + \right. \\
 & \left. - 4|\lambda|^2 c_\beta M_W^2 s_\beta s_{\theta_W}^2 t_{\phi_{I\lambda}} \right] + \delta Z_e \frac{s_\beta}{2e^2} \left[4|\lambda|^2 c_\beta M_W^2 s_\beta s_{\theta_W}^2 t_{\phi_{I\lambda}} + \right.
 \end{aligned}$$

$$\begin{aligned}
& + e^2 \left(|\kappa| |\lambda| v_s^2 s_{\phi_I} - t_{\phi_{I\lambda}} (|\kappa| |\lambda| v_s^2 c_{\phi_I} + s_{2\beta} (M_W^2 - M_{H^\pm}^2)) \right) \Big] + \\
& - \delta M_W^2 \frac{s_\beta (2M_W^2 - M_Z^2)}{4e^2 M_W^2 M_Z^2 s_{\theta_W}^2 c_{\phi_{I\lambda}}} \left[-4|\lambda|^2 c_\beta M_W^2 s_\beta s_{\theta_W}^2 s_{\phi_{I\lambda}} + \right. \\
& \left. + e^2 \left(s_{\phi_{I\lambda}} (|\kappa| |\lambda| v_s^2 c_{\phi_I} + s_{2\beta} (M_W^2 - M_{H^\pm}^2)) - |\kappa| |\lambda| v_s^2 s_{\phi_I} c_{\phi_{I\lambda}} \right) \right] \quad (D.6)
\end{aligned}$$

$$\begin{aligned}
\delta \mathcal{M}_{\text{Higgs}} \Big|_{15} & = \delta M_Z^2 \frac{|\kappa| |\lambda| M_W^3 v_s s_{\phi_I}}{2e M_Z^4 s_{\theta_W}} + \delta \tan\beta \frac{c_\beta^2 M_W s_{\theta_W}}{e^3 v_s t_\beta c_{\phi_{I\lambda}}} \left[-4|\lambda|^2 c_\beta M_W^2 s_\beta s_{\theta_W}^2 s_{\phi_{I\lambda}} + \right. \\
& \left. + e^2 \left(s_{\phi_{I\lambda}} (|\kappa| |\lambda| v_s^2 c_{\phi_I} + s_{2\beta} (M_W^2 - M_{H^\pm}^2)) - |\kappa| |\lambda| v_s^2 s_{\phi_I} c_{\phi_{I\lambda}} \right) \right] + \\
& + \delta v_s \frac{M_W s_{\theta_W} t_{\phi_{I\lambda}}}{e^3 v_s^2} \left[e^2 (|\kappa| |\lambda| v_s^2 c_{\phi_I} + s_{2\beta} (M_W^2 - M_{H^\pm}^2)) - 2|\lambda|^2 M_W^2 s_{2\beta} s_{\theta_W}^2 \right] + \\
& + \delta \phi_I \frac{|\kappa| |\lambda| M_W v_s c_{\phi_I} s_{\theta_W}}{e} + \delta \kappa \frac{|\lambda| M_W v_s s_{\theta_W} s_{\phi_I}}{e} + \delta \lambda \frac{|\kappa| M_W v_s s_{\theta_W} s_{\phi_I}}{e} + \\
& + \delta M_W^2 \frac{|\kappa| |\lambda| v_s (M_Z^2 - 2M_W^2) s_{\phi_I}}{2e M_W M_Z^2 s_{\theta_W}} - \delta Z_e \frac{|\kappa| |\lambda| M_W v_s s_{\theta_W} s_{\phi_I}}{e} + \delta t_{ad} \frac{1}{v_s s_\beta} \quad (D.7)
\end{aligned}$$

$$\begin{aligned}
\delta \mathcal{M}_{\text{Higgs}} \Big|_{22} & = -\delta t_{hu} \frac{2M_W s_\beta s_{\theta_W} c_\beta^4}{e v_s^2} + \delta t_{ad} \frac{6M_W s_{\theta_W} t_{\phi_{I\kappa}} c_\beta}{e v_s^2} - \delta t_{hd} \frac{2M_W s_\beta^4 s_{\theta_W} c_\beta}{e v_s^2} + \\
& + \delta \tan\beta \frac{M_W^2 s_{\theta_W}^2 c_\beta^2}{2e^4 v_s^2} \left\{ \left[4 (s_\beta c_\beta^3 - s_\beta^3 c_\beta) (M_{H^\pm}^2 - M_W^2) (3t_{\phi_{I\kappa}} t_{\phi_{I\lambda}} + 4) + \right. \right. \\
& - 6|\kappa| |\lambda| v_s^2 c_\beta^2 (5s_{\phi_I} t_{\phi_{I\kappa}} + c_{\phi_I} (t_{\phi_{I\kappa}} t_{\phi_{I\lambda}} - 2)) + \\
& + 3 \left(2|\kappa| |\lambda| c_{\phi_I} v_s^2 ((t_{\phi_{I\kappa}} t_{\phi_{I\lambda}} - 2) s_\beta^2 + t_{\phi_{I\kappa}} t_{\phi_{I\lambda}}) + \right. \\
& \left. \left. + t_{\phi_{I\kappa}} (2 (M_W^2 - M_{H^\pm}^2) s_{2\beta} t_{\phi_{I\lambda}} - |\kappa| |\lambda| (5c_{2\beta} - 3) s_{\phi_I} v_s^2) \right) \right] e^2 + \\
& + 4|\lambda|^2 M_W^2 s_{\theta_W}^2 (2 (s_\beta c_\beta^3 - s_\beta^3 c_\beta) (3t_{\phi_{I\kappa}} t_{\phi_{I\lambda}} + 4) - 3s_{2\beta} t_{\phi_{I\kappa}} t_{\phi_{I\lambda}}) \Big\} + \\
& + \delta M_Z^2 \frac{M_W^4 s_\beta c_\beta}{e^4 M_Z^4 v_s^2} \left[\left(-15|\kappa| |\lambda| s_{\phi_I} t_{\phi_{I\kappa}} v_s^2 - 3|\kappa| |\lambda| c_{\phi_I} v_s^2 (t_{\phi_{I\kappa}} t_{\phi_{I\lambda}} - 2) + \right. \right. \\
& \left. \left. + 2c_\beta s_\beta (M_{H^\pm}^2 - M_W^2) (3t_{\phi_{I\kappa}} t_{\phi_{I\lambda}} + 2) \right) e^2 + 2|\lambda|^2 M_W^2 s_{2\beta} s_{\theta_W}^2 (3t_{\phi_{I\kappa}} t_{\phi_{I\lambda}} + 4) \right] + \\
& - \delta \phi_I \frac{6|\kappa| |\lambda| M_W^2 s_\beta s_{\theta_W}^2 c_\beta (c_{\phi_{I\kappa}} s_{\phi_I} + 3c_{\phi_I} s_{\phi_{I\kappa}})}{e^2 c_{\phi_{I\kappa}}} + \delta M_{H^\pm}^2 \frac{M_W^2 s_{2\beta}^2 s_{\theta_W}^2}{e^2 v_s^2} + \\
& + \delta M_W^2 \frac{s_{2\beta}}{4e^4 M_Z^4 v_s^2} \left\{ 6 (2M_W^2 - M_Z^2) M_Z^2 \frac{t_{\phi_{I\kappa}}}{c_{\phi_{I\lambda}}} \left[5e^2 |\kappa| |\lambda| c_{\phi_{I\lambda}} s_{\phi_I} v_s^2 + \right. \right.
\end{aligned}$$

$$\begin{aligned}
 & + s_{\phi_{I\lambda}} \left(e^2 (|\kappa||\lambda|c_{\phi_I}v_s^2 + (M_W^2 - M_{H^\pm}^2) s_{2\beta}) - 2|\lambda|^2 M_W^2 s_{2\beta} s_{\theta_W}^2 \right) \Big] + \\
 & + 4 \left[3e^2 |\kappa||\lambda|c_{\phi_I} M_Z^2 (M_Z^2 - 2M_W^2) v_s^2 + \left(4|\lambda|^2 (2M_W^4 - 3M_Z^2 M_W^2 + M_Z^4) M_W^2 + \right. \right. \\
 & \left. \left. + e^2 M_Z^2 (3M_W^4 - 2M_{H^\pm}^2 M_W^2 - 2M_Z^2 M_W^2 + M_{H^\pm}^2 M_Z^2) \right) s_{2\beta} \right] \Big\} + \\
 & + \delta\kappa \frac{3|\lambda| M_W^2 s_{2\beta} s_{\theta_W}^2 (c_{\phi_I} c_{\phi_{I\kappa}} - 3s_{\phi_I} s_{\phi_{I\kappa}})}{e^2 c_{\phi_{I\kappa}}} + \delta\lambda \frac{M_W^2 s_{2\beta} s_{\theta_W}^2}{e^4 v_s^2} \left[4|\lambda| M_W^2 s_{2\beta} s_{\theta_W}^2 + \right. \\
 & \left. + 3e^2 |\kappa| (c_{\phi_I} - 3s_{\phi_I} t_{\phi_{I\kappa}}) v_s^2 \right] - \delta t_{as} \frac{3t_{\phi_{I\kappa}}}{v_s} + \frac{\delta t_{hs}}{v_s} - \delta T_\kappa \frac{3v_s}{\sqrt{2}c_{\phi_{I\kappa}}} + \\
 & + \frac{\delta v_s}{2e^4 v_s^3} \left[2M_W^2 s_{\theta_W}^2 e^2 \left(12c_\beta^2 t_{\phi_{I\kappa}} t_{\phi_{I\lambda}} s_\beta^2 (M_W^2 - M_{H^\pm}^2) - 2s_{2\beta}^2 (M_{H^\pm}^2 - M_W^2) + \right. \right. \\
 & \left. \left. + 3|\kappa||\lambda|s_{2\beta} t_{\phi_{I\kappa}} (c_{\phi_I} t_{\phi_{I\lambda}} - 4s_{\phi_I}) v_s^2 \right) + \frac{3}{\sqrt{2}c_{\phi_{I\kappa}}} |T_\kappa| (c_{\phi_{I\kappa}} - 3) v_s^3 e^4 + \right. \\
 & \left. - 8|\lambda|^2 M_W^4 s_{\theta_W}^4 (6c_\beta^2 t_{\phi_{I\kappa}} t_{\phi_{I\lambda}} s_\beta^2 + s_{2\beta}^2) \right] + \delta Z_e \frac{M_W^2 s_{2\beta} s_{\theta_W}^2}{e^4 v_s^2} \left[e^2 \left(15|\kappa||\lambda|s_{\phi_I} t_{\phi_{I\kappa}} v_s^2 + \right. \right. \\
 & \left. \left. + 3|\kappa||\lambda|c_{\phi_I} v_s^2 (t_{\phi_{I\kappa}} t_{\phi_{I\lambda}} - 2) - 2c_\beta s_\beta (M_{H^\pm}^2 - M_W^2) (3t_{\phi_{I\kappa}} t_{\phi_{I\lambda}} + 2) \right) + \right. \\
 & \left. - 2|\lambda|^2 M_W^2 s_{2\beta} s_{\theta_W}^2 (3t_{\phi_{I\kappa}} t_{\phi_{I\lambda}} + 4) \right] \tag{D.8}
 \end{aligned}$$

$$\begin{aligned}
 \delta\mathcal{M}_{\text{Higgs}} \Big|_{23} &= \frac{\delta t_{ad}}{v_s} - \delta \tan\beta \frac{3|\kappa||\lambda|c_\beta^3 M_W v_s s_{\theta_W} s_{\phi_I}}{e} - \delta\phi_I \frac{3|\kappa||\lambda| M_W v_s s_\beta s_{\theta_W} c_{\phi_I}}{e} + \\
 & + \delta v_s \frac{M_W s_\beta s_{\theta_W}}{e^3 v_s^2 c_{\phi_{I\lambda}}} \left[e^2 \left(s_{\phi_{I\lambda}} (|\kappa||\lambda|v_s^2 c_{\phi_I} + s_{2\beta} (M_W^2 - M_{H^\pm}^2)) + \right. \right. \\
 & \left. \left. - 4|\kappa||\lambda|v_s^2 s_{\phi_I} c_{\phi_{I\lambda}} \right) - 4|\lambda|^2 c_\beta M_W^2 s_\beta s_{\theta_W}^2 s_{\phi_{I\lambda}} \right] - \delta M_Z^2 \frac{3|\kappa||\lambda| M_W^3 v_s s_\beta s_{\phi_I}}{2e M_Z^4 s_{\theta_W}} + \\
 & - \delta M_W^2 \frac{3|\kappa||\lambda| v_s s_\beta s_{\phi_I} (M_Z^2 - 2M_W^2)}{2e M_W M_Z^2 s_{\theta_W}} + \delta Z_e \frac{3|\kappa||\lambda| M_W v_s s_\beta s_{\theta_W} s_{\phi_I}}{e} + \\
 & - \delta\kappa \frac{3|\lambda| M_W v_s s_\beta s_{\theta_W} s_{\phi_I}}{e} - \delta\lambda \frac{3|\kappa| M_W v_s s_\beta s_{\theta_W} s_{\phi_I}}{e} \tag{D.9}
 \end{aligned}$$

$$\begin{aligned}
 \delta\mathcal{M}_{\text{Higgs}} \Big|_{24} &= \frac{\delta t_{ad}}{v_s t_\beta} + \delta \tan\beta \frac{c_\beta M_W s_{\theta_W}}{2e^3 v_s t_\beta c_{\phi_{I\lambda}}} \left[- 8|\lambda|^2 c_\beta M_W^2 s_\beta s_{\theta_W}^2 s_{\phi_{I\lambda}} + \right. \\
 & \left. + e^2 \left(2s_{\phi_{I\lambda}} (|\kappa||\lambda|v_s^2 c_{\phi_I} + s_{2\beta} (M_W^2 - M_{H^\pm}^2)) - |\kappa||\lambda| (3c_{2\beta} - 1) v_s^2 s_{\phi_I} c_{\phi_{I\lambda}} \right) \right] + \\
 & + \delta v_s \frac{c_\beta M_W s_{\theta_W}}{e^3 v_s^2 c_{\phi_{I\lambda}}} \left[e^2 \left(s_{\phi_{I\lambda}} (|\kappa||\lambda|v_s^2 c_{\phi_I} + s_{2\beta} (M_W^2 - M_{H^\pm}^2)) - 4|\kappa||\lambda|v_s^2 s_{\phi_I} c_{\phi_{I\lambda}} \right) + \right.
 \end{aligned}$$

$$\begin{aligned}
& - 4|\lambda|^2 c_\beta M_W^2 s_\beta s_{\theta_W}^2 s_{\phi_{I\lambda}} \left] - \delta M_Z^2 \frac{3|\kappa||\lambda| c_\beta M_W^3 v_s s_{\phi_I}}{2e M_Z^4 s_{\theta_W}} + \delta Z_e \frac{3|\kappa||\lambda| c_\beta M_W v_s s_{\theta_W} s_{\phi_I}}{e} + \right. \\
& - \delta M_W^2 \frac{3|\kappa||\lambda| c_\beta v_s (M_Z^2 - 2M_W^2) s_{\phi_I}}{2e M_W M_Z^2 s_{\theta_W}} - \delta \kappa \frac{3|\lambda| c_\beta M_W v_s s_{\theta_W} s_{\phi_I}}{e} + \\
& \left. - \delta \lambda \frac{3|\kappa| c_\beta M_W v_s s_{\theta_W} s_{\phi_I}}{e} - \delta \phi_I \frac{3|\kappa||\lambda| c_\beta M_W v_s c_{\phi_I} s_{\theta_W}}{e} \right. \quad (D.10)
\end{aligned}$$

$$\begin{aligned}
\delta \mathcal{M}_{\text{Higgs}} \Big|_{25} &= \delta M_Z^2 \frac{2c_\beta s_\beta M_W^4}{e^4 M_Z^4 v_s^2} \left[e^2 \left(3|\kappa||\lambda| s_{\phi_I} v_s^2 + t_{\phi_{I\lambda}} (|\kappa||\lambda| c_{\phi_I} v_s^2 + (M_W^2 - M_{H^\pm}^2) s_{2\beta}) \right) + \right. \\
& - 4|\lambda|^2 c_\beta M_W^2 s_\beta s_{\theta_W}^2 t_{\phi_{I\lambda}} \left] + \delta \lambda \frac{4|\kappa| s_{2\beta} s_{\theta_W}^2 s_{\phi_I} M_W^2}{e^2} + \delta \kappa \frac{4|\lambda| s_{2\beta} s_{\theta_W}^2 s_{\phi_I} M_W^2}{e^2} + \right. \\
& + \delta \tan \beta \frac{2c_\beta^2 s_{\theta_W}^2 M_W^2}{e^4 c_{\phi_{I\lambda}} v_s^2} \left[8|\lambda|^2 c_\beta M_W^2 s_{\theta_W}^2 s_{\phi_{I\lambda}} s_\beta^3 + e^2 \left(|\kappa||\lambda| c_{\phi_{I\lambda}} s_{\phi_I} v_s^2 (3c_{2\beta} + 1) + \right. \right. \\
& \left. \left. - 2s_\beta^2 s_{\phi_{I\lambda}} (|\kappa||\lambda| c_{\phi_I} v_s^2 + (M_W^2 - M_{H^\pm}^2) s_{2\beta}) \right) \right] - \delta t_{a_d} \frac{4c_\beta s_{\theta_W} M_W}{e v_s^2} + \\
& + \delta Z_e \frac{2s_{\theta_W}^2 M_W^2}{e^4 v_s^2} \left[8|\lambda|^2 c_\beta^2 M_W^2 s_\beta^2 s_{\theta_W}^2 t_{\phi_{I\lambda}} - e^2 \left(-4c_\beta^2 (M_{H^\pm}^2 - M_W^2) t_{\phi_{I\lambda}} s_\beta^2 + \right. \right. \\
& \left. \left. + 6|\kappa||\lambda| c_\beta s_{\phi_I} v_s^2 s_\beta + |\kappa||\lambda| c_{\phi_I} s_{2\beta} t_{\phi_{I\lambda}} v_s^2 \right) \right] + \delta \phi_I \frac{8|\kappa||\lambda| c_\beta c_{\phi_I} s_\beta s_{\theta_W}^2 M_W^2}{e^2} + \\
& + \delta M_W^2 \frac{(M_Z^2 - 2M_W^2) s_{2\beta}}{e^4 M_Z^2 v_s^2} \left[-4|\lambda|^2 c_\beta M_W^2 s_\beta s_{\theta_W}^2 t_{\phi_{I\lambda}} + \right. \\
& \left. + e^2 \left(3|\kappa||\lambda| s_{\phi_I} v_s^2 + t_{\phi_{I\lambda}} (|\kappa||\lambda| c_{\phi_I} v_s^2 + (M_W^2 - M_{H^\pm}^2) s_{2\beta}) \right) \right] + \frac{2\delta t_{a_s}}{v_s} + \\
& + \frac{\delta v_s}{e^4 v_s^3} \left[\sqrt{2} |T_\kappa| s_{\phi_{I\kappa}} v_s^3 e^4 + 4|\lambda|^2 M_W^4 s_{2\beta}^2 s_{\theta_W}^4 t_{\phi_{I\lambda}} + \right. \\
& \left. + 2M_W^2 s_{2\beta} s_{\theta_W}^2 e^2 \left(4|\kappa||\lambda| s_{\phi_I} v_s^2 - t_{\phi_{I\lambda}} (|\kappa||\lambda| c_{\phi_I} v_s^2 + (M_W^2 - M_{H^\pm}^2) s_{2\beta}) \right) \right] \quad (D.11)
\end{aligned}$$

$$\begin{aligned}
\delta \mathcal{M}_{\text{Higgs}} \Big|_{33} &= \delta \tan \beta \frac{2c_\beta^3 s_\beta}{e^2} \left[2|\lambda|^2 M_W^2 s_{\theta_W}^2 + e^2 (M_{H^\pm}^2 - M_W^2 - M_Z^2) \right] + \\
& + \frac{\delta M_Z^2}{2} \left[c_{2\beta} \left(1 - \frac{2|\lambda|^2 M_W^4}{e^2 M_Z^4} \right) + \frac{2|\lambda|^2 M_W^4}{e^2 M_Z^4} + 1 \right] + \\
& - \delta M_W^2 \frac{s_\beta^2}{e^2 M_Z^2} \left[|\lambda|^2 (4M_W^2 - 2M_Z^2) + e^2 M_Z^2 \right] - \delta Z_e \frac{4|\lambda|^2 M_W^2 s_\beta^2 s_{\theta_W}^2}{e^2} + \\
& + \delta \lambda \frac{4|\lambda| M_W^2 s_\beta^2 s_{\theta_W}^2}{e^2} - \delta t_{h_d} \frac{e (c_{3\beta} - 5c_\beta)}{8M_W s_{\theta_W}} - \delta t_{h_u} \frac{e c_\beta^2 s_\beta}{2M_W s_{\theta_W}} + \delta M_{H^\pm}^2 s_\beta^2 \quad (D.12)
\end{aligned}$$

$$\begin{aligned}
 \delta\mathcal{M}_{\text{Higgs}}\Big|_{34} = & -\delta\tan\beta\frac{c_{2\beta}c_\beta^2}{e^2}\left[s_{\theta_W}^2(e^2M_Z^2-2|\lambda|^2M_W^2)+e^2M_{H^\pm}^2\right]-\delta M_{H^\pm}^2c_\beta s_\beta+ \\
 & +\delta M_W^2\frac{c_\beta s_\beta}{e^2M_Z^2}\left[|\lambda|^2(2M_Z^2-4M_W^2)+e^2M_Z^2\right]+\delta t_{h_u}\frac{ec_\beta^3}{2M_Ws_{\theta_W}}+\delta t_{h_d}\frac{es_\beta^3}{2M_Ws_{\theta_W}}+ \\
 & +\delta\lambda\frac{2|\lambda|M_W^2s_{2\beta}s_{\theta_W}^2}{e^2}+\delta M_Z^2c_\beta s_\beta\left[\frac{2|\lambda|^2M_W^4}{e^2M_Z^4}-1\right]-\delta Z_e\frac{2|\lambda|^2M_W^2s_{2\beta}s_{\theta_W}^2}{e^2} \quad (\text{D.13})
 \end{aligned}$$

$$\begin{aligned}
 \delta\mathcal{M}_{\text{Higgs}}\Big|_{35} = & \frac{\delta M_W^2}{4e^3M_WM_Z^4s_{\theta_W}v_s}\left[c_{3\beta}\left(6|\lambda|^2(2M_W^4-3M_Z^2M_W^2+M_Z^4)M_W^2+\right.\right. \\
 & \left.+e^2M_Z^2(4M_W^4-2M_{H^\pm}^2M_W^2-3M_Z^2M_W^2+M_{H^\pm}^2M_Z^2)\right)+ \\
 & -c_\beta\left(2(2M_W^2-M_Z^2)(3M_W^4-3M_Z^2M_W^2+2e^2M_Z^2v_s^2)|\lambda|^2+\right. \\
 & \left.+e^2M_Z^2(4M_W^4-2M_{H^\pm}^2M_W^2-3M_Z^2M_W^2+M_{H^\pm}^2M_Z^2)\right)+ \\
 & \left.-2e^2|\kappa||\lambda|c_{\phi_I}M_Z^2s_\beta v_s^2(M_Z^2-2M_W^2)\right]-\delta M_{H^\pm}^2\frac{2c_\beta M_Ws_{\theta_W}s_\beta^2}{ev_s}+ \\
 & +\delta M_Z^2\frac{M_W^3}{4e^3M_Z^6s_{\theta_W}v_s}\left[e^2(c_{3\beta}(M_{H^\pm}^2-M_W^2)-2|\kappa||\lambda|c_{\phi_I}s_\beta v_s^2)M_Z^2+\right. \\
 & \left.+c_\beta\left((6M_W^4-6M_Z^2M_W^2+4e^2M_Z^2v_s^2)|\lambda|^2+e^2(M_W^2-M_{H^\pm}^2)M_Z^2\right)\right]+ \\
 & +6|\lambda|^2c_{3\beta}M_W^2s_{\theta_W}^2M_Z^2\left]-\delta\kappa\frac{|\lambda|c_{\phi_I}M_Ws_{\theta_W}v_s s_\beta}{e}+\delta\phi_I\frac{|\kappa||\lambda|M_Ws_{\theta_W}s_{\phi_I}v_s s_\beta}{e}+ \\
 & +\delta\lambda\frac{M_Ws_{\theta_W}}{e^3v_s}\left[e^2(4|\lambda|c_\beta-|\kappa|c_{\phi_I}s_\beta)v_s^2-8|\lambda|c_\beta M_W^2s_\beta^2s_{\theta_W}^2\right]+\delta t_{h_u}\frac{c_\beta^3s_\beta}{v_s}+ \\
 & -\delta\tan\beta\frac{c_\beta^2M_Ws_{\theta_W}}{2e^3v_s}\left[e^2\left(2s_\beta(M_{H^\pm}^2-M_W^2+2|\lambda|^2v_s^2+3c_{2\beta}(M_{H^\pm}^2-M_W^2))\right)+\right. \\
 & \left.+|\kappa||\lambda|c_{\beta-\phi_I}v_s^2+|\kappa||\lambda|c_{\beta+\phi_I}v_s^2\right)-2|\lambda|^2M_W^2(s_\beta-3s_{3\beta})s_{\theta_W}^2\left]+\delta t_{h_d}\frac{s_\beta^4}{v_s}+ \\
 & +\delta v_s\frac{M_Ws_{\theta_W}}{2e^3v_s^2}\left[e^2\left(c_{3\beta}(M_W^2-M_{H^\pm}^2)+c_\beta(M_{H^\pm}^2-M_W^2+4|\lambda|^2v_s^2)+\right.\right. \\
 & \left.-2|\kappa||\lambda|c_{\phi_I}s_\beta v_s^2\right)+8|\lambda|^2c_\beta M_W^2s_\beta^2s_{\theta_W}^2\left]-\delta Z_e\frac{M_Ws_{\theta_W}}{2e^3M_Z^2v_s}\left[6|\lambda|^2c_{3\beta}M_W^2s_{\theta_W}^2M_Z^2+\right.\right. \\
 & \left.\left.+c_\beta\left((6M_W^4-6M_Z^2M_W^2+4e^2M_Z^2v_s^2)|\lambda|^2+e^2(M_W^2-M_{H^\pm}^2)M_Z^2\right)\right]+
 \end{aligned}$$

$$+ e^2 \left(c_{3\beta} (M_{H^\pm}^2 - M_W^2) - 2|\kappa||\lambda|c_{\phi_I}s_\beta v_s^2 \right) M_Z^2 \Big] \quad (\text{D.14})$$

$$\begin{aligned} \delta\mathcal{M}_{\text{Higgs}} \Big|_{44} &= -\delta\tan\beta \frac{2c_\beta^3 s_\beta}{e^2} \left[2|\lambda|^2 M_W^2 s_{\theta_W}^2 + e^2 (M_{H^\pm}^2 - M_W^2 - M_Z^2) \right] + c_\beta^2 \delta M_{H^\pm}^2 + \\ &- \delta Z_e \frac{4|\lambda|^2 c_\beta^2 M_W^2 s_{\theta_W}^2}{e^2} - \delta M_W^2 \frac{c_\beta^2}{e^2 M_Z^2} \left[|\lambda|^2 (4M_W^2 - 2M_Z^2) + e^2 M_Z^2 \right] + \\ &+ \delta M_Z^2 \left[c_{2\beta} \left(\frac{|\lambda|^2 M_W^4}{e^2 M_Z^4} - \frac{1}{2} \right) + \frac{|\lambda|^2 M_W^4}{e^2 M_Z^4} + \frac{1}{2} \right] + \delta\lambda \frac{4|\lambda|c_\beta^2 M_W^2 s_{\theta_W}^2}{e^2} + \\ &- \frac{ec_\beta s_\beta^2 \delta t_{h_d}}{2M_W s_{\theta_W}} + \frac{e(5s_\beta + s_{3\beta}) \delta t_{h_u}}{8M_W s_{\theta_W}} \end{aligned} \quad (\text{D.15})$$

$$\begin{aligned} \delta\mathcal{M}_{\text{Higgs}} \Big|_{45} &= \delta t_{h_u} \frac{c_\beta^4}{v_s} - \delta M_{H^\pm}^2 \frac{2M_W s_\beta s_{\theta_W} c_\beta^2}{e v_s} + \delta\tan\beta \frac{M_W s_{\theta_W} c_\beta^2}{2e^3 v_s} \left[e^2 \left(2|\kappa||\lambda|c_{\phi_I}s_\beta v_s^2 + \right. \right. \\ &- 3c_{3\beta} (M_{H^\pm}^2 - M_W^2) + c_\beta (-M_{H^\pm}^2 + M_W^2 + 4|\lambda|^2 v_s^2) \Big) + \\ &- 2|\lambda|^2 (c_\beta + 3c_{3\beta}) M_W^2 s_{\theta_W}^2 \Big] - \delta\kappa \frac{|\lambda|c_{\phi_I} M_W s_{\theta_W} v_s c_\beta}{e} + \delta t_{h_d} \frac{s_\beta^3 c_\beta}{v_s} + \\ &- \frac{\delta M_W^2}{4e^3 M_W M_Z^4 s_{\theta_W} v_s} \left[e^2 |\kappa||\lambda|(c_{\beta-\phi_I} + c_{\beta+\phi_I}) M_Z^2 (M_Z^2 - 2M_W^2) v_s^2 + \right. \\ &+ 2s_\beta \left(2(2M_W^2 - M_Z^2) (3M_W^4 - 3M_Z^2 M_W^2 + e^2 M_Z^2 v_s^2) |\lambda|^2 + \right. \\ &+ e^2 M_Z^2 (4M_W^4 - 2M_{H^\pm}^2 M_W^2 - 3M_Z^2 M_W^2 + M_{H^\pm}^2 M_Z^2) + \\ &+ c_{2\beta} \left(6|\lambda|^2 (2M_W^4 - 3M_Z^2 M_W^2 + M_Z^4) M_W^2 + \right. \\ &+ e^2 M_Z^2 (4M_W^4 - 2M_{H^\pm}^2 M_W^2 - 3M_Z^2 M_W^2 + M_{H^\pm}^2 M_Z^2) \Big) \Big] + \\ &+ \delta M_Z^2 \frac{M_W^3}{4e^3 M_Z^6 s_{\theta_W} v_s} \left[-e^2 |\kappa||\lambda|c_{\beta-\phi_I} M_Z^2 v_s^2 - e^2 |\kappa||\lambda|c_{\beta+\phi_I} M_Z^2 v_s^2 + \right. \\ &+ 2s_\beta \left(2(3M_W^4 - 3M_Z^2 M_W^2 + e^2 M_Z^2 v_s^2) |\lambda|^2 + e^2 (M_W^2 - M_{H^\pm}^2) M_Z^2 + \right. \\ &- c_{2\beta} M_Z^2 \left((M_{H^\pm}^2 - M_W^2) e^2 + 6|\lambda|^2 M_W^2 s_{\theta_W}^2 \right) \Big] + \delta\phi_I \frac{|\kappa||\lambda| M_W s_{\theta_W} s_{\phi_I} v_s c_\beta}{e} + \\ &- \delta\lambda \frac{M_W s_{\theta_W}}{e^3 v_s} \left[8|\lambda|c_\beta^2 M_W^2 s_\beta s_{\theta_W}^2 + e^2 (|\kappa|c_\beta c_{\phi_I} - 4|\lambda|s_\beta) v_s^2 \right] + \\ &+ \delta v_s \frac{M_W s_{\theta_W}}{2e^3 v_s^2} \left[-e^2 \left(|\kappa||\lambda|(c_{\beta-\phi_I} + c_{\beta+\phi_I}) v_s^2 - 2s_\beta (M_{H^\pm}^2 - M_W^2 + 2|\lambda|^2 v_s^2 + \right. \right. \end{aligned}$$

$$\begin{aligned}
 & + c_{2\beta} (M_{H^\pm}^2 - M_W^2) \Big) + 8|\lambda|^2 c_\beta^2 M_W^2 s_\beta s_{\theta_W}^2 \Big] + \\
 & - \delta Z_e \frac{M_W s_{\theta_W}}{2e^3 M_Z^2 v_s} \left[2s_\beta \left(-c_{2\beta} M_Z^2 ((M_{H^\pm}^2 - M_W^2) e^2 + 6|\lambda|^2 M_W^2 s_{\theta_W}^2) + \right. \right. \\
 & + 2(3M_W^4 - 3M_Z^2 M_W^2 + e^2 M_Z^2 v_s^2) |\lambda|^2 + e^2 (M_W^2 - M_{H^\pm}^2) M_Z^2 \Big) + \\
 & \left. \left. - e^2 |\kappa| |\lambda| (c_{\beta-\phi_I} + c_{\beta+\phi_I}) M_Z^2 v_s^2 \right] \right. \tag{D.16}
 \end{aligned}$$

$$\begin{aligned}
 \delta \mathcal{M}_{\text{Higgs}} \Big|_{55} = & -\tan\beta \frac{M_W^2 s_{\theta_W}^2 c_\beta^2}{2e^4 v_s^2} \left[\left(|\kappa| |\lambda| (c_{\phi_I} (4 - 2t_{\phi_{I\kappa}} t_{\phi_{I\lambda}}) - 15s_{\phi_I} t_{\phi_{I\kappa}}) v_s^2 c_\beta^2 + \right. \right. \\
 & + 4(M_{H^\pm}^2 - M_W^2) s_\beta (t_{\phi_{I\kappa}} t_{\phi_{I\lambda}} - 4) c_\beta^3 - 4((M_{H^\pm}^2 - M_W^2) s_\beta^3 (t_{\phi_{I\kappa}} t_{\phi_{I\lambda}} - 4) + \\
 & - M_W^2 s_\beta t_{\phi_{I\kappa}} t_{\phi_{I\lambda}}) c_\beta + 2|\kappa| |\lambda| c_{\phi_I} ((t_{\phi_{I\kappa}} t_{\phi_{I\lambda}} - 2) s_\beta^2 + t_{\phi_{I\kappa}} t_{\phi_{I\lambda}}) v_s^2 + \\
 & \left. \left. - \frac{1}{2} t_{\phi_{I\kappa}} (4s_{2\beta} t_{\phi_{I\lambda}} M_{H^\pm}^2 + |\kappa| |\lambda| (5c_{2\beta} - 11) s_{\phi_I} v_s^2) \right) e^2 + \right. \\
 & \left. + 8|\lambda|^2 c_\beta M_W^2 s_\beta s_{\theta_W}^2 \left((t_{\phi_{I\kappa}} t_{\phi_{I\lambda}} - 4) c_\beta^2 - t_{\phi_{I\kappa}} t_{\phi_{I\lambda}} + s_\beta^2 (4 - t_{\phi_{I\kappa}} t_{\phi_{I\lambda}}) \right) \right] + \\
 & + \delta M_Z^2 \frac{M_W^4 s_\beta c_\beta}{e^4 M_Z^4 v_s^2} \left[e^2 \left(-2c_\beta s_\beta (t_{\phi_{I\kappa}} t_{\phi_{I\lambda}} M_{H^\pm}^2 - 2M_{H^\pm}^2 + 2M_W^2) + \right. \right. \\
 & + |\kappa| |\lambda| c_{\phi_I} (t_{\phi_{I\kappa}} t_{\phi_{I\lambda}} - 2) v_s^2 + t_{\phi_{I\kappa}} (s_{2\beta} t_{\phi_{I\lambda}} M_W^2 + 5|\kappa| |\lambda| s_{\phi_I} v_s^2) \Big) + \\
 & \left. - 2|\lambda|^2 M_W^2 s_{2\beta} s_{\theta_W}^2 (t_{\phi_{I\kappa}} t_{\phi_{I\lambda}} - 4) \right] - \delta t_{ad} \frac{2M_W s_{\theta_W} t_{\phi_{I\kappa}} c_\beta}{e v_s^2} + \\
 & - \delta t_{hd} \frac{2M_W s_\beta^4 s_{\theta_W} c_\beta}{e v_s^2} - \delta t_{hu} \frac{2M_W s_\beta s_{\theta_W} c_\beta^4}{e v_s^2} + \delta M_{H^\pm}^2 \frac{M_W^2 s_{2\beta}^2 s_{\theta_W}^2}{e^2 v_s^2} + \\
 & + \delta \phi_I \frac{2|\kappa| |\lambda| M_W^2 s_\beta s_{\theta_W}^2 (c_{\phi_{I\kappa}} s_{\phi_I} + 3c_{\phi_I} s_{\phi_{I\kappa}}) c_\beta}{e^2 c_{\phi_{I\kappa}}} + \\
 & + \delta M_W^2 \frac{s_{2\beta}}{4e^4 M_Z^4 v_s^2} \left[4 \left((e^2 M_Z^2 (3M_W^4 - 2M_{H^\pm}^2 M_W^2 - 2M_Z^2 M_W^2 + M_{H^\pm}^2 M_Z^2) + \right. \right. \\
 & + 4|\lambda|^2 (2M_W^4 - 3M_Z^2 M_W^2 + M_Z^4) M_W^2) s_{2\beta} - e^2 |\kappa| |\lambda| c_{\phi_I} M_Z^2 (M_Z^2 - 2M_W^2) v_s^2 \Big) + \\
 & - 2M_Z^2 (2M_W^2 - M_Z^2) \frac{t_{\phi_{I\kappa}}}{c_{\phi_{I\lambda}}} \left(s_{\phi_{I\lambda}} (e^2 (|\kappa| |\lambda| c_{\phi_I} v_s^2 + (M_W^2 - M_{H^\pm}^2) s_{2\beta}) + \right. \\
 & \left. \left. - 2|\lambda|^2 M_W^2 s_{2\beta} s_{\theta_W}^2) + 5e^2 |\kappa| |\lambda| c_{\phi_{I\lambda}} s_{\phi_I} v_s^2 \right) \right] +
 \end{aligned}$$

$$\begin{aligned}
& + \delta\kappa \frac{\left(4e^2|\kappa|v_s^2 - 2|\lambda|c_\beta M_W^2 s_\beta s_{\theta_W}^2 (c_{\phi_I} - 3s_{\phi_I} t_{\phi_{I\kappa}})\right)}{e^2} + \delta t_{a_s} \frac{t_{\phi_{I\kappa}}}{v_s} + \frac{\delta t_{h_s}}{v_s} + \\
& + \delta\lambda \frac{M_W^2 s_{2\beta} s_{\theta_W}^2 \left(4|\lambda| M_W^2 s_{2\beta} s_{\theta_W}^2 - e^2 |\kappa| (c_{\phi_I} - 3s_{\phi_I} t_{\phi_{I\kappa}}) v_s^2\right)}{e^4 v_s^2} + \delta T_\kappa \frac{v_s}{\sqrt{2} c_{\phi_{I\kappa}}} + \\
& + \frac{\delta v_s}{4e^4 M_Z^4 v_s^3} \left\{ M_W^2 \left[e^2 M_Z^4 s_{\theta_W}^2 \left(\frac{|\kappa| |\lambda| v_s^2 t_{\phi_{I\kappa}} \left(3c_{2\beta - \phi_{I\lambda} - \phi_I} - 5c_{2\beta - \phi_{I\lambda} + \phi_I}\right)}{c_{\phi_{I\lambda}}} \right) + \right. \right. \\
& + 4c_{4\beta} (M_{H^\pm}^2 - M_W^2) \left. \right] - 2M_Z^2 s_{\theta_W}^2 t_{\phi_{I\kappa}} \left(2s_{2\beta}^2 t_{\phi_{I\lambda}} \left(-2|\lambda|^2 M_W^2 M_Z^2 s_{\theta_W}^2 + \right. \right. \\
& + e^2 M_Z^2 (M_W^2 - M_{H^\pm}^2) \left. \left. - e^2 |\kappa| |\lambda| M_Z^2 v_s^2 \frac{c_{\phi_I} c_{2\beta + \phi_{I\lambda}} + 4s_{\phi_I} s_{2\beta + \phi_{I\lambda}}}{c_{\phi_{I\lambda}}} \right) \right] + \\
& + 8|\lambda|^2 (c_{4\beta} - 1) M_W^2 M_Z^4 s_{\theta_W}^4 \left. \right] + 16e^4 |\kappa|^2 M_Z^4 v_s^4 - 4e^2 M_W^2 M_Z^4 s_{\theta_W} (M_{H^\pm}^2 - M_W^2) + \\
& - \sqrt{2} e^4 M_Z^4 v_s^3 |T_\kappa| \frac{c_{2\phi_{I\kappa}} - 3}{c_{\phi_{I\kappa}}} \left. \right\} + \delta Z_e \frac{M_W^2 s_{2\beta} s_{\theta_W}^2}{e^4 v_s^2} \left[2|\lambda|^2 M_W^2 s_{2\beta} s_{\theta_W}^2 (t_{\phi_{I\kappa}} t_{\phi_{I\lambda}} - 4) + \right. \\
& - e^2 \left(|\kappa| |\lambda| c_{\phi_I} (t_{\phi_{I\kappa}} t_{\phi_{I\lambda}} - 2) v_s^2 - 2c_\beta s_\beta (t_{\phi_{I\kappa}} t_{\phi_{I\lambda}} M_{H^\pm}^2 - 2M_{H^\pm}^2 + 2M_W^2) + \right. \\
& \left. \left. + t_{\phi_{I\kappa}} (s_{2\beta} t_{\phi_{I\lambda}} M_W^2 + 5|\kappa| |\lambda| s_{\phi_I} v_s^2) \right) \right] \tag{D.17}
\end{aligned}$$

Chargino and Neutralino Counterterm Mass Matrices

In this appendix the counterterm mass matrices for the charginos and neutralinos are given. The chargino mass matrix (see Eq. (3.46)) can be written in terms of the following parameters: $|M_2|$, M_W , $\tan\beta$, $|\lambda|$, v_s , ϕ_{M_2} , ϕ_λ , ϕ_u and ϕ_s . If one now introduces counterterms for these parameters and expands the mass matrix around the counterterms, one obtains the counterterm chargino mass matrix:

$$\delta\mathcal{M}_{\chi^\pm}\Big|_{11} = \delta M_2 e^{i\phi_{M_2}} + i \delta\phi_{M_2} |M_2| e^{i\phi_{M_2}}, \quad (\text{E.1})$$

$$\delta\mathcal{M}_{\chi^\pm}\Big|_{12} = \left[\delta M_W^2 \frac{s_\beta}{\sqrt{2}M_W} + \delta\tan\beta \sqrt{2}c_\beta^3 M_W \right] e^{-i\phi_u} - i \delta\phi_u (\mathcal{M}_{\chi^\pm})_{12}, \quad (\text{E.2})$$

$$\delta\mathcal{M}_{\chi^\pm}\Big|_{21} = \delta M_W^2 \frac{c_\beta}{\sqrt{2}M_W} - \delta\tan\beta \sqrt{2}c_\beta^2 M_W s_\beta, \quad (\text{E.3})$$

$$\delta\mathcal{M}_{\chi^\pm}\Big|_{22} = \left[\delta\lambda \frac{v_s}{\sqrt{2}} + \delta v_s \frac{\lambda}{\sqrt{2}} \right] e^{i\phi_s} + i (\delta\phi_s + \delta\phi_\lambda) (\mathcal{M}_{\chi^\pm})_{22}. \quad (\text{E.4})$$

Here $(\mathcal{M}_{\chi^\pm})_{ij}$ denotes the respective element of the chargino mass matrix. Also keep in mind that $\delta\lambda$ and δM_2 denote the counterterms to the absolute values $|\lambda|$ and $|M_2|$, whereas λ and M_2 are complex ($\lambda = |\lambda| e^{i\phi_\lambda}$ and $M_2 = |M_2| e^{i\phi_{M_2}}$).

The neutralino mass matrix (see Eq. (3.42)) can be written in terms of the parameters $|M_1|$, $|M_2|$, M_W , M_Z , $\tan\beta$, e , $|\lambda|$, $|\kappa|$, v_s , ϕ_{M_1} , ϕ_{M_2} , ϕ_λ , ϕ_κ , ϕ_u and ϕ_s . After introducing counterterms for these parameters and expanding around these, we obtain the following counterterm mass matrix:

$$\delta\mathcal{M}_{\chi^0}\Big|_{11} = \delta M_1 e^{i\phi_{M_1}} + i |M_1| e^{i\phi_{M_1}}, \quad (\text{E.5})$$

$$\delta\mathcal{M}_{\chi^0}\Big|_{13} = (\delta M_W^2 - \delta M_Z^2) \frac{c_\beta}{2M_Z s_{\theta_W}} + \delta\tan\beta \frac{c_\beta M_Z s_{\theta_W} s_{2\beta}}{2}, \quad (\text{E.6})$$

$$\delta\mathcal{M}_{\chi^0}\Big|_{14} = \left[(\delta M_Z^2 - \delta M_W^2) \frac{s_\beta}{2M_Z s_{\theta_W}} + \delta\tan\beta \frac{c_\beta^3 M_W s_{\theta_W}}{c_W} \right] e^{-i\phi_u} - i \delta\phi_u (\mathcal{M}_{\chi^0})_{14}, \quad (\text{E.7})$$

$$\delta\mathcal{M}_{\chi^0}\Big|_{22} = \delta M_2 e^{i\phi_{M_2}} + i |M_2| e^{i\phi_{M_2}}, \quad (\text{E.8})$$

$$\delta\mathcal{M}_{\chi^0}\Big|_{23} = \delta M_W^2 \frac{c_\beta}{2M_W} - \delta \tan\beta c_\beta^2 M_W s_\beta, \quad (\text{E.9})$$

$$\delta\mathcal{M}_{\chi^0}\Big|_{24} = \left[-\delta M_W^2 \frac{s_\beta}{2M_W} - \delta \tan\beta c_\beta^3 M_W \right] e^{-i\phi_u} - i \delta\phi_u (\mathcal{M}_{\chi^0})_{24}, \quad (\text{E.10})$$

$$\delta\mathcal{M}_{\chi^0}\Big|_{34} = \left[-\delta\lambda \frac{v_s}{\sqrt{2}} - \delta v_s \frac{\lambda}{\sqrt{2}} \right] e^{i\phi_s} + i (\delta\phi_s + \delta\phi_\lambda) (\mathcal{M}_{\chi^0})_{34}, \quad (\text{E.11})$$

$$\begin{aligned} \delta\mathcal{M}_{\chi^0}\Big|_{35} = & \left[- (c_W^4 \delta M_Z^2 - 2c_W^2 \delta M_W^2 + \delta M_W^2) \frac{\lambda s_\beta}{\sqrt{2}e M_W s_{\theta_W}} - \delta \tan\beta \frac{\sqrt{2}\lambda c_\beta^3 M_W s_{\theta_W}}{e} + \right. \\ & \left. + (\lambda \delta Z_e - \delta\lambda) \frac{\sqrt{2}M_W s_{\theta_W} s_\beta}{e} \right] e^{i\phi_u} + i (\delta\phi_u + \delta\phi_\lambda) (\mathcal{M}_{\chi^0})_{34}, \end{aligned} \quad (\text{E.12})$$

$$\begin{aligned} \delta\mathcal{M}_{\chi^0}\Big|_{45} = & - (c_W^4 \delta M_Z^2 - 2c_W^2 \delta M_W^2 + \delta M_W^2) \frac{\lambda c_\beta}{\sqrt{2}e M_W s_{\theta_W}} + \delta \tan\beta \frac{\lambda c_\beta M_W s_{\theta_W} s_{2\beta}}{\sqrt{2}e} + \\ & + (\lambda \delta Z_e - \delta\lambda) \frac{\sqrt{2}c_\beta M_W s_{\theta_W}}{e} + i \delta\phi_\lambda (\mathcal{M}_{\chi^0})_{45}, \end{aligned} \quad (\text{E.13})$$

$$\delta\mathcal{M}_{\chi^0}\Big|_{55} = \left[\sqrt{2}\delta\kappa v_s + \sqrt{2}\kappa\delta v_s \right] e^{i\phi_s} + i (\delta\phi_s + \delta\phi_\kappa) (\mathcal{M}_{\chi^0})_{55}, \quad (\text{E.14})$$

$$\delta\mathcal{M}_{\chi^0}\Big|_{12} = \delta\mathcal{M}_{\chi^0}\Big|_{15} = \delta\mathcal{M}_{\chi^0}\Big|_{25} = \delta\mathcal{M}_{\chi^0}\Big|_{33} = \delta\mathcal{M}_{\chi^0}\Big|_{44} = 0. \quad (\text{E.15})$$

All other elements follow from the symmetry

$$\delta\mathcal{M}_{\chi^0}\Big|_{ij} = \delta\mathcal{M}_{\chi^0}\Big|_{ji}. \quad (\text{E.16})$$

$(\mathcal{M}_{\chi^0})_{ij}$ denotes the respective matrix element of the neutralino mass matrix.

Acknowledgments

First of all I would like to thank Prof. Dr. Margarete Mühlleitner, who gave me the chance to work on this interesting topic of current research. She always found time to discuss my problems and was very supportive. Her comments and suggestions were especially helpful in the process of writing this thesis.

Thanks also to Prof. Dr. Dieter Zeppenfeld, who agreed to act as second reviewer for this thesis.

I am certainly much obliged to Dr. Heidi Rzehak for the patience with which she answered my thousand questions and always came up with helpful ideas.

Special thanks also to Thorben Graf and Ramona Gröber, with whom I worked together closely. Thorben helped me getting started here and the fruitful discussion with Ramona towards the end of this thesis were indispensable.

Furthermore, I would like to thank everybody who was willing to lend me some of their time for proofreading parts of this thesis. In particular I should mention Yasmin Ansruther, Johannes Bellm, Anastasiya Bierweiler, Ramona Gröber, Matthias Kerner, Sophy Palmer, Juraj Streicher and Michael Walz.

I am also in debt to my family and Michi, who supported me during my course of studies. For their love and care I am grateful.

Last but not least, I should thank everybody here at the institute for this last year, which I enjoyed very much. I am already looking forward to the next few years.

References

- [1] S. Glashow, *Partial Symmetries of Weak Interactions*. Nucl.Phys. **22** (1961) 579–588.
S. Weinberg, *A Model of Leptons*. Phys.Rev.Lett. **19** (1967) 1264–1266.
A. Salam, *Weak and Electromagnetic Interactions*. Originally printed in *Svartholm: Elementary Particle Theory, Proceedings Of The Nobel Symposium Held 1968 At Lerum, Sweden*, Stockholm 1968, 367–377.
- [2] S. Glashow, J. Iliopoulos, and L. Maiani, *Weak Interactions with Lepton-Hadron Symmetry*. Phys.Rev. **D2** (1970) 1285–1292.
- [3] N. Cabibbo, *Unitary Symmetry and Leptonic Decays*. Phys.Rev.Lett. **10** (1963) 531–533.
M. Kobayashi and T. Maskawa, *CP Violation in the Renormalizable Theory of Weak Interaction*. Prog.Theor.Phys. **49** (1973) 652–657.
- [4] P. W. Higgs, *Broken symmetries, massless particles and gauge fields*. Phys.Lett. **12** (1964) 132–133.
P. W. Higgs, *Broken Symmetries and the Masses of Gauge Bosons*. Phys.Rev.Lett. **13** (1964) 508–509.
P. W. Higgs, *Spontaneous Symmetry Breakdown without Massless Bosons*. Phys.Rev. **145** (1966) 1156–1163.
F. Englert and R. Brout, *Broken Symmetry and the Mass of Gauge Vector Mesons*. Phys.Rev.Lett. **13** (1964) 321–322.
T. Kibble, *Symmetry breaking in nonAbelian gauge theories*. Phys.Rev. **155** (1967) 1554–1561.
- [5] D. Volkov and V. Akulov, *Is the Neutrino a Goldstone Particle?* Phys.Lett. **B46** (1973) 109–110.
J. Wess and B. Zumino, *Supergauge Transformations in Four-Dimensions*. Nucl.Phys. **B70** (1974) 39–50.

- P. Fayet, *Supersymmetry and Weak, Electromagnetic and Strong Interactions*. Phys.Lett. **B64** (1976) 159.
- P. Fayet, *Spontaneously Broken Supersymmetric Theories of Weak, Electromagnetic and Strong Interactions*. Phys.Lett. **B69** (1977) 489.
- P. Fayet, *Relations Between the Masses of the Superpartners of Leptons and Quarks, the Goldstino Couplings and the Neutral Currents*. Phys.Lett. **B84** (1979) 416.
- G. R. Farrar and P. Fayet, *Phenomenology of the Production, Decay, and Detection of New Hadronic States Associated with Supersymmetry*. Phys.Lett. **B76** (1978) 575–579.
- E. Witten, *Dynamical Breaking of Supersymmetry*. Nucl.Phys. **B188** (1981) 513.
- H. P. Nilles, *Supersymmetry, Supergravity and Particle Physics*. Phys.Rept. **110** (1984) 1–162.
- H. E. Haber and G. L. Kane, *The Search for Supersymmetry: Probing Physics Beyond the Standard Model*. Phys.Rept. **117** (1985) 75–263.
- M. Sohnius, *Introducing Supersymmetry*. Phys.Rept. **128** (1985) 39–204.
- J. Gunion and H. E. Haber, *Higgs Bosons in Supersymmetric Models. 1*. Nucl.Phys. **B272** (1986) 1.
- J. Gunion and H. E. Haber, *Higgs Bosons in Supersymmetric Models. 2. Implications for Phenomenology*. Nucl.Phys. **B278** (1986) 449.
- A. Lahanas and D. V. Nanopoulos, *The Road to No Scale Supergravity*. Phys.Rept. **145** (1987) 1.
- [6] P. Fayet, *Supergauge Invariant Extension of the Higgs Mechanism and a Model for the electron and Its Neutrino*. Nucl.Phys. **B90** (1975) 104–124.
- R. Barbieri, S. Ferrara, and C. A. Savoy, *Gauge Models with Spontaneously Broken Local Supersymmetry*. Phys.Lett. **B119** (1982) 343.
- M. Dine, W. Fischler, and M. Srednicki, *A Simple Solution to the Strong CP Problem with a Harmless Axion*. Phys.Lett. **B104** (1981) 199.
- H. P. Nilles, M. Srednicki, and D. Wyler, *Weak Interaction Breakdown Induced by Supergravity*. Phys.Lett. **B120** (1983) 346.
- J. Frere, D. Jones, and S. Raby, *Fermion Masses and Induction of the Weak Scale by Supergravity*. Nucl.Phys. **B222** (1983) 11.
- J. Derendinger and C. A. Savoy, *Quantum Effects and $SU(2) \times U(1)$ Breaking in Supergravity Gauge Theories*. Nucl.Phys. **B237** (1984) 307.
- [7] J. R. Ellis, J. Gunion, H. E. Haber, L. Roszkowski, and F. Zwirner, *Higgs Bosons in a Nonminimal Supersymmetric Model*. Phys.Rev. **D39** (1989) 844.
- M. Drees, *Supersymmetric Models with Extended Higgs Sector*. Int.J.Mod.Phys. **A4** (1989) 3635.
- U. Ellwanger, M. Rausch de Traubenberg, and C. A. Savoy, *Particle spectrum in supersymmetric models with a gauge singlet*. Phys.Lett. **B315** (1993) 331–337, [arXiv:hep-ph/9307322](https://arxiv.org/abs/hep-ph/9307322) [hep-ph].

- U. Ellwanger, M. Rausch de Traubenberg, and C. A. Savoy, *Higgs phenomenology of the supersymmetric model with a gauge singlet*. Z.Phys. **C67** (1995) 665–670, [arXiv:hep-ph/9502206](#) [hep-ph].
- U. Ellwanger, M. Rausch de Traubenberg, and C. A. Savoy, *Phenomenology of supersymmetric models with a singlet*. Nucl.Phys. **B492** (1997) 21–50, [arXiv:hep-ph/9611251](#) [hep-ph].
- T. Elliott, S. King, and P. White, *Unification constraints in the next-to-minimal supersymmetric standard model*. Phys.Lett. **B351** (1995) 213–219, [arXiv:hep-ph/9406303](#) [hep-ph].
- S. King and P. White, *Resolving the constrained minimal and next-to-minimal supersymmetric standard models*. Phys.Rev. **D52** (1995) 4183–4216, [arXiv:hep-ph/9505326](#) [hep-ph].
- F. Franke and H. Fraas, *Neutralinos and Higgs bosons in the next-to-minimal supersymmetric standard model*. Int.J.Mod.Phys. **A12** (1997) 479–534, [arXiv:hep-ph/9512366](#) [hep-ph].
- [8] K. Nakamura et al. (Particle Data Group), *Review of Particle Physics*. J.Phys.G **37** (2010) 075021. <http://pdg.lbl.gov>.
- [9] E. Witten, *Mass Hierarchies in Supersymmetric Theories*. Phys.Lett. **B105** (1981) 267.
- J. Polchinski and L. Susskind, *Breaking of Supersymmetry at Intermediate-Energy*. Phys.Rev. **D26** (1982) 3661.
- S. Dimopoulos and H. Georgi, *Softly Broken Supersymmetry and SU(5)*. Nucl.Phys. **B193** (1981) 150.
- N. Sakai, *Naturalness in Supersymmetric Guts*. Z.Phys. **C11** (1981) 153.
- [10] S. P. Martin, *A Supersymmetry primer*. [arXiv:hep-ph/9709356](#) [hep-ph].
- [11] H. Baer and X. Tata, *Weak scale supersymmetry: From superfields to scattering events*.
- [12] H. Kalka and G. Soff, *Supersymmetry. (In German)*.
- [13] S. R. Coleman and J. Mandula, *All Possible Symmetries of the S Matrix*. Phys.Rev. **159** (1967) 1251–1256.
- [14] R. Haag, J. T. Lopuszanski, and M. Sohnius, *All Possible Generators of Supersymmetries of the s Matrix*. Nucl.Phys. **B88** (1975) 257.
- [15] J. R. Ellis, S. Kelley, and D. V. Nanopoulos, *Probing the desert using gauge coupling unification*. Phys.Lett. **B260** (1991) 131–137.
- C. Giunti, C. Kim, and U. Lee, *Running coupling constants and grand unification models*. Mod.Phys.Lett. **A6** (1991) 1745–1755.
- [16] M. Maniatis, *The Next-to-Minimal Supersymmetric extension of the Standard Model reviewed*. Int.J.Mod.Phys. **A25** (2010) 3505–3602, [arXiv:0906.0777](#) [hep-ph].
- [17] U. Ellwanger, C. Hugonie, and A. M. Teixeira, *The Next-to-Minimal Supersymmetric Standard Model*. Phys.Rept. **496** (2010) 1–77, [arXiv:0910.1785](#) [hep-ph].

-
- [18] L. Girardello and M. T. Grisaru, *Soft Breaking of Supersymmetry*. Nucl.Phys. **B194** (1982) 65.
- [19] L. Faddeev and V. Popov, *Feynman Diagrams for the Yang-Mills Field*. Phys.Lett. **B25** (1967) 29–30.
- [20] T. Graf, *One-Loop-Corrections to the NMSSM Higgs Boson Masses*. diploma thesis **KIT** (2011) .
- [21] J. E. Kim and H. P. Nilles, *The mu Problem and the Strong CP Problem*. Phys.Lett. **B138** (1984) 150.
- [22] R. Peccei and H. R. Quinn, *Constraints Imposed by CP Conservation in the Presence of Instantons*. Phys.Rev. **D16** (1977) 1791–1797.
- R. Peccei and H. R. Quinn, *CP Conservation in the Presence of Instantons*. Phys.Rev.Lett. **38** (1977) 1440–1443.
- [23] S. Weinberg, *A New Light Boson?* Phys.Rev.Lett. **40** (1978) 223–226.
- J. Callan, Curtis G., R. F. Dashen, D. J. Gross, F. Wilczek, and A. Zee, *The Effect of Instantons on the heavy quark potential*. Phys.Rev. **D18** (1978) 4684.
- [24] D. J. Miller, R. Nevzorov, and P. M. Zerwas, *The Higgs sector of the next-to-minimal supersymmetric standard model*. Nucl.Phys. **B681** (2004) 3–30, [arXiv:hep-ph/0304049](#) [hep-ph].
- [25] W. Pauli and F. Villars, *On the Invariant regularization in relativistic quantum theory*. Rev.Mod.Phys. **21** (1949) 434–444.
- [26] G. 't Hooft and M. Veltman, *Regularization and Renormalization of Gauge Fields*. Nucl.Phys. **B44** (1972) 189–213.
- C. Bollini and J. Giambiagi, *Dimensional Renormalization: The Number of Dimensions as a Regularizing Parameter*. Nuovo Cim. **B12** (1972) 20–25.
- [27] W. Siegel, *Supersymmetric Dimensional Regularization via Dimensional Reduction*. Phys.Lett. **B84** (1979) 193.
- [28] A. Denner, *Techniques for calculation of electroweak radiative corrections at the one loop level and results for W physics at LEP-200*. Fortsch.Phys. **41** (1993) 307–420, [arXiv:0709.1075](#) [hep-ph].
- [29] T. Hahn and M. Perez-Victoria, *Automatized one loop calculations in four-dimensions and D-dimensions*. Comput.Phys.Commun. **118** (1999) 153–165, [arXiv:hep-ph/9807565](#) [hep-ph].
- [30] M. Frank, T. Hahn, S. Heinemeyer, W. Hollik, H. Rzehak, *et al.*, *The Higgs Boson Masses and Mixings of the Complex MSSM in the Feynman-Diagrammatic Approach*. JHEP **0702** (2007) 047, [arXiv:hep-ph/0611326](#) [hep-ph].
- [31] K. E. Williams, *The Higgs Sector of the Complex Minimal Supersymmetric Standard Model*. Doctoral thesis **Durham University** (2008) .
- [32] H. A. Rzehak, *Zwei-Schleifen-Beiträge im supersymmetrischen Higgs-Sektor*. Doktorarbeit **Technische Universität München** (2005) .
-

- [33] T. Fritzsche, *Untersuchungen zum Massenspektrum von Neutralinos und Charginos im Minimalen Supersymmetrischen Standardmodell*. Diplomarbeit **Universität Karlsruhe** (2000) .
- [34] M. Frank, S. Heinemeyer, W. Hollik, and G. Weiglein, *FeynHiggs1.2: Hybrid \overline{MS} -bar / on-shell renormalization for the CP even Higgs boson sector in the MSSM*. arXiv:hep-ph/0202166 [hep-ph].
- [35] P. H. Chankowski, S. Pokorski, and J. Rosiek, *One loop corrections to the supersymmetric Higgs boson couplings and LEP phenomenology*. Phys.Lett. **B286** (1992) 307–314.
- P. H. Chankowski, S. Pokorski, and J. Rosiek, *Complete on-shell renormalization scheme for the minimal supersymmetric Higgs sector*. Nucl.Phys. **B423** (1994) 437–496, arXiv:hep-ph/9303309 [hep-ph].
- [36] A. Dabelstein, *The One loop renormalization of the MSSM Higgs sector and its application to the neutral scalar Higgs masses*. Z.Phys. **C67** (1995) 495–512, arXiv:hep-ph/9409375 [hep-ph].
- A. Dabelstein, *Fermionic decays of neutral MSSM Higgs bosons at the one loop level*. Nucl.Phys. **B456** (1995) 25–56, arXiv:hep-ph/9503443 [hep-ph].
- [37] A. C. Fowler, *Higher order and CP-violating effects in the neutralino and Higgs boson sectors of the MSSM*. Doctoral thesis **Durham University** (2010) .
- [38] F. Staub, *SARAH*. arXiv:0806.0538 [hep-ph].
- [39] T. Hahn, *Generating Feynman diagrams and amplitudes with FeynArts 3*. Comput.Phys.Comm. **140** (2001) 418–431, arXiv:hep-ph/0012260 [hep-ph].
- [40] T. Hahn and M. Perez-Victoria, *Automatized one loop calculations in four-dimensions and D-dimensions*. Comput.Phys.Comm. **118** (1999) 153–165, arXiv:hep-ph/9807565 [hep-ph].
- T. Hahn, *A Mathematica interface for FormCalc-generated code*. Comput.Phys.Comm. **178** (2008) 217–221, arXiv:hep-ph/0611273 [hep-ph].
- [41] P. Z. Skands, B. Allanach, H. Baer, C. Balazs, G. Belanger, *et al.*, *SUSY Les Houches accord: Interfacing SUSY spectrum calculators, decay packages, and event generators*. JHEP **0407** (2004) 036, arXiv:hep-ph/0311123 [hep-ph].
- B. Allanach, C. Balazs, G. Belanger, M. Bernhardt, F. Boudjema, *et al.*, *SUSY Les Houches Accord 2*. Comput.Phys.Comm. **180** (2009) 8–25, arXiv:0801.0045 [hep-ph].
- F. Mahmoudi, S. Heinemeyer, A. Arbey, A. Bharucha, T. Goto, *et al.*, *Flavour Les Houches Accord: Interfacing Flavour related Codes*. arXiv:1008.0762 [hep-ph].
- [42] K. Nakamura *et al.* (Particle Data Group), *Review of Particle Physics*. J.Phys.G **37** (2010) 075021. <http://pdg.lbl.gov>.
- [43] A. Djouadi, M. Mühlleitner, and M. Spira, *Decays of supersymmetric particles: The Program SUSY-HIT (SUSpect-SdecaY-Hdecay-InTerface)*. Acta Phys.Polon. **B38** (2007) 635–644, arXiv:hep-ph/0609292 [hep-ph].

-
- [44] G. Degrandi and P. Slavich, *On the radiative corrections to the neutral Higgs boson masses in the NMSSM*. Nucl.Phys. **B825** (2010) 119–150, arXiv:0907.4682 [hep-ph].
- [45] K. Ender, T. Graf, M. Mühlleitner, and H. Rzehak, *Analysis of the NMSSM Higgs Boson Masses at One-Loop Level*. arXiv:1111.4952 [hep-ph].
- [46] **CMS** Collaboration, S. Chatrchyan *et al.*, *Search for Supersymmetry at the LHC in Events with Jets and Missing Transverse Energy*. arXiv:1109.2352 [hep-ex].
ATLAS Collaboration, G. Aad *et al.*, *Search for squarks and gluinos using final states with jets and missing transverse momentum with the ATLAS detector in $\sqrt{s} = 7$ TeV proton-proton collisions*. arXiv:1109.6572 [hep-ex].
- [47] M. Spira, *HIGLU: A program for the calculation of the total Higgs production cross-section at hadron colliders via gluon fusion including QCD corrections*. arXiv:hep-ph/9510347 [hep-ph].
- [48] A. Djouadi, J. Kalinowski, and M. Spira, *HDECAY: A Program for Higgs boson decays in the standard model and its supersymmetric extension*. Comput.Phys.Commun. **108** (1998) 56–74, arXiv:hep-ph/9704448 [hep-ph].
- [49] M. Mühlleitner *et al.*, *HDECAY for the NMSSM*. (to be published) .
- [50] **ALEPH, DELPHI, L3, OPAL, LEP Working Group for Higgs Boson Searches** Collaboration, S. Schael *et al.*, *Search for neutral MSSM Higgs bosons at LEP*. Eur.Phys.J. **C47** (2006) 547–587, arXiv:hep-ex/0602042 [hep-ex].
- [51] **LEP Higgs Working Group** Collaboration, *Searches for Higgs bosons decaying into Photons: Combined Results from the LEP Experiments*. LHWG Note (2002-02) .
- [52] **D0** Collaboration. Note 5980 (2009) .
CDF Collaboration. Note 9888 (2009) .
- [53] **ATLAS** Collaboration, *Combined Standard Model Higgs boson searches with up to 2.3 fb⁻¹ of pp collisions at $\sqrt{s}=7$ TeV at the LHC* Tech. Rep. ATLAS-CONF-2011-157, CERN, Geneva, Nov, 2011.
CMS Collaboration, *Combined Standard Model Higgs boson searches with up to 2.3 inverse femtobarns of pp collision data at $\sqrt{s}=7$ TeV at the LHC* Tech. Rep. CMS-PAS-HIG-11-023, CERN, Nov, 2011.
- [54] P. Bechtle, O. Brein, S. Heinemeyer, G. Weiglein, and K. E. Williams, *HiggsBounds: Confronting Arbitrary Higgs Sectors with Exclusion Bounds from LEP and the Tevatron*. Comput.Phys.Commun. **181** (2010) 138–167, arXiv:0811.4169 [hep-ph].
P. Bechtle, O. Brein, S. Heinemeyer, G. Weiglein, and K. E. Williams, *HiggsBounds 2.0.0: Confronting Neutral and Charged Higgs Sector Predictions with Exclusion Bounds from LEP and the Tevatron*. Comput.Phys.Commun. **182** (2011) 2605–2631, arXiv:1102.1898 [hep-ph].
- [55] K. Cheung, T.-J. Hou, J. S. Lee, and E. Senaha, *The Higgs Boson Sector of the Next-to-MSSM with CP Violation*. Phys.Rev. **D82** (2010) 075007, arXiv:1006.1458 [hep-ph].
- [56] G. Passarino and M. Veltman, *One Loop Corrections for $e^+ e^-$ Annihilation Into $\mu^+ \mu^-$ in the Weinberg Model*. Nucl.Phys. **B160** (1979) 151.
-

- [57] G. 't Hooft and M. Veltman, *Scalar One Loop Integrals*. Nucl.Phys. **B153** (1979) 365–401.
- [58] D. Melrose, *Reduction of Feynman diagrams*. Nuovo Cim. **40** (1965) 181–213.
- [59] D. M. Pierce, J. A. Bagger, K. T. Matchev, and R.-j. Zhang, *Precision corrections in the minimal supersymmetric standard model*. Nucl.Phys. **B491** (1997) 3–67, [arXiv:hep-ph/9606211](#) [hep-ph].
- [60] G. Dissertori, I. Knowles, and M. Schmelling, *Quantum Chromodynamics:High Energy Experiments and Theory*. Oxford University Press (2003) .
- [61] H. Baer, J. Ferrandis, K. Melnikov, and X. Tata, *Relating bottom quark mass in DR-BAR and MS-BAR regularization schemes*. Phys.Rev. **D66** (2002) 074007, [arXiv:hep-ph/0207126](#) [hep-ph].